

UNIVERSITY OF TWENTE.

Mechanical Engineering
Faculty Engineering Technology

Removal of Volatile Organic Compounds and other odourous compounds using ozone generated by UV-C light in aerobic digestion installations

Casper van Boggelen

Chairman: prof.dr.ir. G. Brem (Gerrit)

External member: dr.ir. A.G.J. van der Ham (Louis)

Internal supervisor: ir. E.A. Bramer (Eddy)

Company supervisor: ir. J. ten Hove (Sander)



A thesis submitted in partial fulfilment of the University's requirements for the
Master of Science-degree

December 28, 2020

Acknowledgements

I would like to take a moment to thank the following persons, who either made it possible to do this research or made a contribution in any kind of manner.

First of all, a big thanks to Sander ten Hove from WTT. You have been my daily (external) supervisor, guiding me through the whole process of this thesis, arguing about the results and thinking about the upcoming moves. Also I feel obligated to thank several other WTT colleagues: among which Imko Vroom has been an amazing guidance before, during and after the experimental part of this thesis. The discussions about the results and comparison with biofilters I had with Elian Baan were valuable. Thijs Zanderink helped me a lot with reaction mechanisms, and probably I forget multiple other colleagues: thank you as well.

Furthermore Jack Delin and Per Kaijser from the UV-reactor supplier, Centriair, helped me greatly with the experimental setup and shared a lot of their knowledge. Thank you for this and the related scientific papers you shared. Thanks to the personnel of Orgaworld Lelystad as well, especially Tido Giesen and Laurens Welles, for the thoughts and learning process concerning these experiments as well.

Following are Eddy Bramer -my internal supervisor- and Gerrit Brem -my supervising professor- from the University of Twente. Thank you for the supervision and evaluation.

Last, but definitely not least, thanks to my friends and most certainly my family for the support during this process. It would not have been possible without it.

Samenvatting

Luchtbehandeling en geurbestrijding is van groot belang in composteerinstallaties. De lucht bevat vaak zeer hoge geurwaardes, vervelend voor de omgeving. Die geur bestaat voor een groot deel uit ammoniak, maar er zijn ook veel vluchtige organische componenten aanwezig, een verzamelnaam voor allerlei (vaak stinkende) lange ketens van koolwaterstoffen. Sinds het eind van vorige eeuw wordt de luchtbehandeling in composteerinstallaties vaak gedaan met behulp van een zure wasser en een biofilter. Een zure wasser wast vrijwel alle ammoniak uit de lucht met behulp van een zwavelzuuroplossing in een grote kolom waar lucht en zuur tegen elkaar in stromen. Een biofilter bevat een organisch pakkingsmateriaal, vaak bestaande uit verschillende houtsoorten. Hierop groeien miljarden micro-organismen, die de vluchtige organische componenten opknippen in kleinere koolwaterstoffen die minder stinken onder invloed van zuurstof. Met voldoende verblijftijd kan dit zelfs resulteren in de eindproducten CO_2 en H_2O . Deze combinatie levert met goede omstandigheden vaak een hoog verwijderingsrendement op, in combinatie met lage kosten. Toch heeft deze combinatie zijn nadelen, er is namelijk een groot grondoppervlak nodig en de “goede omstandigheden” zijn soms lastig te behalen of te behouden. Denk hierbij aan een optimale temperatuur, luchtvochtigheid, drukval en de kwaliteit van het hout.

De UV-reactor gebruikt een compleet andere techniek om een vergelijkbaar resultaat te behalen. Deze techniek wordt nog niet gebruikt in composteerinstallaties, maar al wel regelmatig in bijvoorbeeld de slachtindustrie, visverwerkingsindustrie en bandenfabricage industrie. Vanwege de hoge ammoniakconcentraties in composteerinstallaties is het echter wel van belang om een zure wasser voor de UV-reactor te schakelen. Lagedruk ultraviolet lampen hebben twee pieken in hun lightspectrum: op 185 en 254 nm om precies te zijn. De piek op 185 nm zorgt voor de ozongeneratie, waarbij zuurstof omgezet wordt in onder andere ozon en andere radicalen met behulp van de UV-straling. Deze radicalen reageren met de dubbele bindingen die veelal aanwezig zijn in vluchtige organische componenten. De piek op 254 nm heeft echter een andere invloed, die breekt rechtstreeks lange koolwaterstoffen (waaronder vluchtige organische componenten) in stukken. Allebei deze effecten werken geurverminderend.

Als de zure wasser in combinatie met een UV-reactor en een actief koolfilter vergeleken wordt met de zure wasser en een biofilter samen, valt op dat de verwijderingsrendementen zeer dicht bij elkaar liggen. Het grote voordeel van de UV-installatie is dat deze erg goed om kan gaan met fluctuerende ingaande lucht, zoals de temperatuur en het debiet. Daarnaast heeft deze combinatie slechts één vijfde van het grondoppervlak nodig ten opzichte van een biofilter.

Om de bevindingen van voorgaande onderzoeken te bevestigen, zijn meerdere experimenten uitgevoerd in bestaande composteerinstallaties. Hierbij was het doel om in verwijderingsrendementen te bepalen van zowel de geurvracht als ammoniak en vluchtige organische componenten. Ook de vergelijking tussen de vaakgebruikte biofilters is interessant om in deze experimenten mee te nemen. Typische composteerinstallaties van WTT hebben een luchtdebiet van 100,000 m³ per uur. Eerst zijn er in Lelystad kleinschalige testen uitgevoerd met een luchtdebiet van 700 m³ per uur. Om te verifiëren dat dit ook werkt voor een grotere hoeveelheid lucht, zijn deze experimenten herhaald. In Erembodegem is dit opnieuw gedaan met een luchtdebiet van 10,000 m³ per uur, één tiende van een volledige installatie.

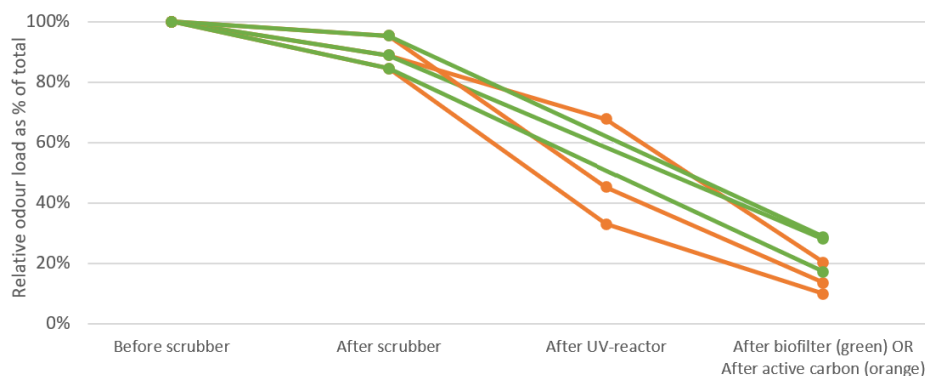


Figure 1: Experimentele resultaten: vergelijking biofilter (groen) en UV-installatie (oranje) voor drie scenario's.

De resultaten van de geurverwijderingsrendementen van de experimenten in Erembodegem zijn te zien in Figuur 1. Zoals gezegd liggen de verwijderingsrendementen van de drie scenario's erg dicht bij elkaar. De groene lijnen zijn de zure wasser met biofilters, als functie van relatieve geurbelasting. Daartegen uitgezet zijn de oranje lijnen: de UV-installatie.

Ook financieel verschillen de twee technieken nauwelijks. Er is een berekening gemaakt voor een casus van 53.000 m³ per uur, met een geurbelasting van 10.000 OU/m³. Gefundeerde aannames op basis van literatuur en eerder verzamelde informatie zijn gemaakt om tot een eindresultaat te komen. De kosten zijn opgesplitst in investeringskosten, onderhoudskosten en operationele kosten. De totale jaarlijkse kosten, waarin de investeringskosten zijn opgenomen als rentepercentage, komen voor beide technieken vrijwel gelijk uit. Deze casus van 53.000 m³ per uur is te behandelen voor rond de €150.000 per jaar.

Samenvattend is de UV-techniek met een actief koolfilter een zeer goede kandidaat om biofilters te vervangen. De kosten en verwijderingsrendementen zijn vergelijkbaar. Over het algemeen is er geen betere, maar onder bepaalde specifieke eisen van installaties, kan de UV-installatie een voordeel bieden. Bijvoorbeeld een ernstig fluctuerende luchtstroom of weinig beschikbaar grondoppervlak, bijvoorbeeld doordat een installatie vlakbij stedelijk gebied staat. Ook is het mogelijk om dit achteraf in te bouwen bij een installatie waarbij de luchtbehandeling aan vervanging toe is, bijvoorbeeld bij een slecht functionerend biofilter.

Abstract

Odour abatement is critical in composting facilities. The air contains extremely high odour values, mainly consisting of ammonia and so called Volatile Organic Compounds (VOCs), an umbrella term for a series of usually long-chain hydrocarbons. During the 20th and 21st century, odour abatement is usually done using an acid scrubber in combination with a biofilter. An acid scrubber washes out ammonia with high efficiencies, using sulphuric acid in counter-current with the air flow. A biofilter uses an organic packing material, usually several kinds of wood chips. Microorganisms present on this material convert VOCs to smaller less-smelling strings of hydrocarbons (possibly to the end products CO_2 and H_2O), while consuming oxygen. Although this combination combines relatively low costs with a great removal efficiency under optimal conditions, it also has its drawbacks. Mainly its required ground surface area and obtaining these optimal conditions mentioned: temperature, humidity, pressure drop and wood-quality.

The UV-reactor technique uses a totally different technique to achieve a similar result. Although this technique is not yet applied in the composting industry, it is often applied in other industrial-scale markets such as the slaughter-, fish processing- and tyre manufacturing-industry. For the composting industry it must be combined with an acid scrubber, because of the high ammonia concentrations. Low pressure ultraviolet lights, mainly consisting of 185 nm and 254 nm wavelengths, destroy VOCs as well. The 185 nm wavelength converts oxygen into ozone and other radicals. These react with VOCs to transform them into other less-smelling molecules. Furthermore, the 254 nm wavelength directly attacks the double bonds present in lots of VOCs, reducing odours as well. Both the costs and removal efficiency of the UV-installation (with acid scrubber and active carbon filter) are similar to these of the acid scrubber with biofilter. Main advantages are its capacity to cope with fluctuating inlet conditions, such as temperature and the fact that only a fifth of the ground surface area is required.

To confirm the online-findings, experiments have been conducted in existing composting facilities. The main goal of these experiments was to find removal efficiencies of both odour concentrations, as well as ammonia and VOCs. Furthermore the comparison with biofilters is interesting to take into account with these experiments. Typical composting installations have to cope with an air flow of approx. $100,000 \text{ m}^3/\text{h}$. Small-scale experiments of $700 \text{ m}^3/\text{h}$ have been conducted in Lelystad. To verify scalability and achieve more accurate results, similar experiments have been conducted on a medium-scale of $10,000 \text{ m}^3/\text{h}$ in Erembodegem, a tenth of the full-scale installation.

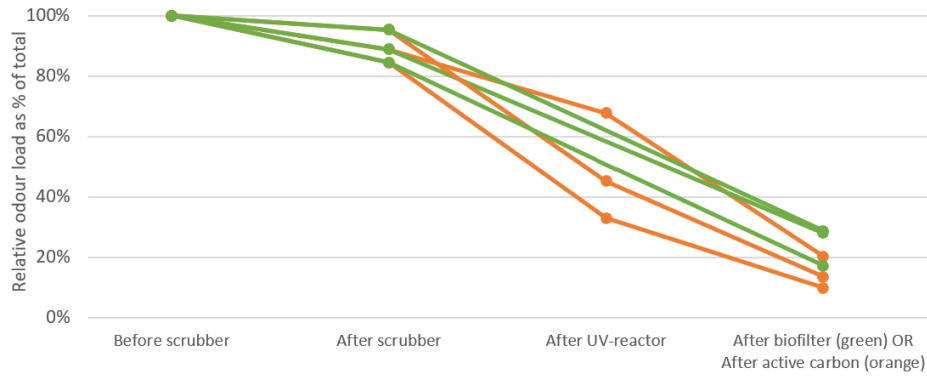


Figure 2: *Experimental results: comparison of biofilter (green) and UV-installation (orange) for three scenarios.*

As can be seen in Figure 2, removal efficiencies are very comparable. Generally in favour of the combination of acid scrubber, UV-reactor and active carbon filter, shown in orange lines. Financially, the two are very similar as well. The comparison is based on a case with an air flow of $53,000 \text{ m}^3/\text{h}$ and an odour load of $10,000 \text{ OU}/\text{m}^3$. Several assumptions have been combined with known data from existing installations. A separation between investment costs, maintenance costs and operational costs has been made. Annual costs turn out to be in the same order of magnitude, both around $\text{€}150,000$ per year to treat the complete air flow.

Concluding, the UV-technique with an active carbon filter is a significant competitor to use in stead of a biofilter. Both the costs and removal are similar. Depending on the requirements of a specific installation, such as limited ground surface area available, it might even be the better case. Also retrofitting is an option for older installations, for instance in case of a malfunctioning biofilter.

Contents

1	Introduction	1
1.1	Scope and Objectives of this Research	2
1.2	Method	2
1.3	Report Structure	3
2	Literature Survey	4
2.1	The Unit to Measure Amounts of Odour in Air	4
2.1.1	Measuring Method of Odour Units	4
2.1.2	Odour Threshold Value	5
2.2	Pollutants in Composting Air	5
2.2.1	Volatile Organic Compounds and Their Subgroups	5
2.3	Working Principle of Several Treatment Techniques	7
2.3.1	Ammonia Removal by Wet Acid Scrubber	7
2.3.2	Biological Treatment by a Biofilter	8
2.3.3	Ultraviolet-light technology	9
2.3.4	Activated Carbon Filter	13
2.3.5	Alternative Treatment Methods	14
2.4	Literature Study: Summarised	16
3	Experimental Setup and Methodology	17
3.1	Requirements and Research Questions for a Testing Setup	17
3.2	Implementation: Orgaworld Lelystad	18
3.2.1	Day-, Week- and Month-dynamics On-Site	18
3.3	Design of a Small-Scale UV-Testing-Setup	19
3.4	Measurement Devices Used	20
3.5	External Analysis: Odour Testing and GC-MS	21
3.6	Extensive Testing Schemes	22
4	Experimental Results	23
4.1	Odour Testing Results: Lelystad and Erembodegem	23
4.1.1	Small-Scale: Lelystad	23
4.1.2	Medium-Scale: Erembodegem	25
4.1.3	Comparison: UV-installation and biofilter	27
4.2	GC-MS Analysis Results	28
4.2.1	Small-Scale: Lelystad	29
4.2.2	Medium-Scale: Erembodegem	30
4.3	Ozone Generation and Depletion	31
4.4	Treatability of Composting Air Pollutants	32

5	Mathematical Reactor Modelling	34
5.1	Plug Flow Reactor	36
5.2	Modelling the UV-technique	37
5.2.1	Ozone Generation Modelling	38
5.2.2	VOC and Ozone Depletion Modelling	39
5.3	Modelling Examples: Several Scenarios	40
5.3.1	Erembodegem Case	40
5.3.2	High Initial Concentrations Case	41
5.3.3	Higher Air Flow Case	43
6	Discussion	45
6.1	General Remarks on the Experimental Results	45
6.2	Mismatch in Measured VOCs: FID and GC-MS	45
6.3	Increase of Odour Level in Ammonia Scrubber	46
6.4	VOC loss in condensate disposal	47
6.5	Scalability Issues to a Full-Scale Installation	48
6.6	Extension of the Mathematical Model	48
7	Financial Feasibility Analysis	49
7.1	Biofilter Compared To UV-Technique	49
7.2	Catalytic Combustion Compared To UV with AC-filter	51
8	Conclusion	53
8.1	Recommendations	54
	Appendices	60
A	Measurement Devices Used	61
A.1	Kitagawa Pump Explanation of Working Principle	61
A.2	Measuring VOCs: Photoionisation-/Flame Ionisation Detector	62
B	Testing Conditions Separated Per Day	63
C	Extensive Experimental Results	65
C.1	Odour Perception of Regularly Found Compounds	66
C.2	Odour Testing Results: Lelystad and Erembodegem	66
C.3	GC-MS Results: Lelystad and Erembodegem	70
D	FID Development Over Time	73
E	Photos of experiments	74
F	Modelling: Derivation CSTR	76
G	Modelling and MatLab files	77
H	Financial Analysis	82
H.1	General Assumptions and Explanation	82

List of Figures

1	Experimentele resultaten: vergelijking biofilter en UV-installatie.	iv
2	Experimental results: comparison of biofilter and UV-installation	vi
2.1	Benzene ring.	6
2.2	Schematic view of a typical counter-current wet spray scrubber	7
2.3	Layout of a typical biofilter (schematically).	9
2.4	The electromagnetic spectrum, detailed focus on UV-light.	9
2.5	Spectral energy distribution of mercury discharge lamps.	10
2.6	The formation of ozone from oxygen molecules using UV-lights.	11
2.7	Oxidation reaction mechanism for DMS and DMDS using ozone.	12
2.8	Reaction rate influence of several physical parameters.	12
2.9	Visual representation of a catalyst reaction.	15
3.1	Plant layout of Orgaworld's location: ZAW in Lelystad.	18
3.2	Schematic flowchart of desired experimental setup.	20
3.3	Drawing of experimental setup, components drawn to scale.	20
4.1	Summarised results of Small-Scale odour scenario experiments in Lelystad.	24
4.2	Summarised results of Medium-Scale odour testing in Erembodegem.	26
4.3	Odour removal efficiency comparison: complete UV-installation and biofilter.	27
4.4	Odour removal efficiency comparison with "after scrubber" as index number.	28
4.5	Components found while conducting GC-MS analysis on untreated air.	29
4.6	The problematic compounds found in the four GC-MS analysis conducted.	30
4.7	Major compounds found in GC-MS analysis conducted in Erembodegem.	31
5.1	Schematically shown CSTR.	35
5.2	Schematically shown Plug Flow Reactor.	35
5.3	A combination of two PFR's to simulate the UV-installation.	38
5.4	Concentrations of multiple compounds for the first case.	41
5.5	Conversion rates for the first case.	41
5.6	All plots of Figure 5.4 into one figure.	41
5.7	Concentrations of multiple compounds for the high load case.	42
5.8	Conversion rates for the high load case.	42
5.9	All plots of Figure 5.7 into one figure.	42
5.10	Concentrations of multiple compounds for the high air flow case.	43
5.11	Conversion rates for high air flow case.	44
5.12	All plots of Figure 5.10 into one figure.	44
6.1	Visual representation of the difference between VOCs and odour strength.	46
C.1	More extensive testing data of Lelystad experiments day 1, 2 and 3.	67

C.2	More extensive testing data of Erembodegem experiments, day "4". . . .	70
C.3	GC-MS data Lelystad: OTVs, OAVs & measured concentrations.	71
C.4	GC-MS data Erembodegem: OTVs, OAVs & measurements.	72
D.1	The continuous development of the FID signal in Lelystad (90 min). . . .	73

List of Tables

2.1	Several forms of reactive oxygen with their oxidation potentials.	11
3.1	Average waste age (in days) in a regular week. The colours represent the odours, where red is the worst and green is the cleanest.	19
4.1	Sensory odour development for all scenarios in Erembodegem.	26
4.2	Ozone generation levels with clean inlet air	32
4.3	Ozone depletion through the afterburner	32
4.4	Treatability of airborne components with highest concentrations.	32
5.1	Continuous Stirred Tank Reactor versus Plug Flow Reactor.	36
5.2	Results of PFR and CSTR derivations for several reaction orders.	37
5.3	Model input of the "standard" case, dimensions refer to Figure 5.3.	40
5.4	Model characteristics of the high inlet concentration case.	41
5.5	Model characteristics of the high air flow case.	43
6.1	Results of condensate test to map VOC losses.	47
7.1	UV-technique compared to the traditional biofilter technique.	50
7.2	Comparison of catalytic combustion, UV-technique an active carbon.	52
C.1	Odour perception, OTVs and solubility in water of the most prominent compounds found in composting air.	66
G.1	Ozone measurements in Lelystad, using fresh air.	77
G.2	Calculated ozone generation for a number of known cases, used as calibration.	77

Glossary: Acronyms & Abbreviations

Symbol	Unit	Meaning
AC	n.a.	Active Carbon, filter used for odour abatement
AP	n.a.	Alpha-Pinene, a specific VOC compound
C_A	mol/m ³	Concentration of component A
CSTR	n.a.	Continuous Stirred Tank Reactor
DM(D)S	n.a.	Dimethyl (di)Sulfide
E_A	J/mol	Activation Energy
FID	n.a.	Flame Ionization Detector, measures VOC using H ₂
GC-MS	n.a.	Gas Chromatography–Mass Spectrometry, Measures VOC
k	n.a.	Rate constant in Arrhenius equation
MSW	n.a.	Type of waste: Municipal Solid Waste
OAV	n.a.	Odour Activity Value (concentration divided by OTV)
ODE	n.a.	Ordinary Differential Equation
OTV	ppm	Odour Threshold Value(s)
OUe	n.a.	European Odour Unit, dilution factor to quantify odour
PFR	n.a.	Plug Flow Reactor
PID	n.a.	Photoionisation Detector, measures VOC using UV-light
ppm	n.a.	Parts per million (by volume), concentration
Φ_V	m ³ /s	Volume Flow through CSTR
Q	m ³ /s	Volume Flow through PFR
R	$\frac{J}{\text{mol}\cdot\text{K}}$	Universal gas constant
r_A	n.a.	Reaction Rate of component A
TOC	ppm	Total organic carbon
T	K	Temperature
τ	s	Residence Time
UV	n.a.	Ultraviolet (light), referring to a wavelength region
V	m ³	Reactor volume of CSTR/PFR
VFG	n.a.	Type of waste: Fruit, Vegetable and Garden
VOC	ppm	Volatile Organic Compound(s)
VSC	ppm	Volatile Sulphuric Compound(s)
WTT	n.a.	Waste Treatment Technologies, graduation company
ζ_A	n.a.	Conversion rate of component A

Chapter 1

Introduction

Waste Treatment Technologies (WTT) is a member of the Convertus group. WTT designs, builds, operates and services household waste treatment facilities all around the globe. More specifically MSW (Municipal Solid Waste) and VFG (Fruit, Vegetable and Garden) waste is processed by both aerobic digestion, better known as composting, as well as anaerobic digestion, better known as fermentation where biogas is produced.

Composting is an exothermic process existing of a mechanical and biological component. The mechanical part gets rid of metals, paper, glass and all kinds of plastic. Large tunnels of 6 x 6 x 30 meters are then filled with organic material, these tunnels have a special aeration floor, also called a "spigot floor". The air fed through these channels is a combination of recycled air and fresh hall air. With this ratio temperature and oxygen concentration are regulated. Aerobic microorganisms convert organic waste into a high-grade compost. During the process, humidity is controlled via a percolation system, which could be compared to a sprinkler system inside a building. This percolate is actually process water, and therefore contains high loads of valuable microorganisms. This water cannot be used over and over again, due to accumulation of dissolved particles, therefore it has to be discharged regularly.

Fermentation is very similar to composting, as it uses the same mechanical treatment and containers for biological conversion. The major difference is the absence of oxygen, which can be assured due to airtight tunnels. Anaerobic bacteria convert organic waste to biogas with an approximate composition of 40% CO₂ and 60% CH₄. When the optimal fermentation temperature of around 38°C is reached, supply of fresh air is stopped. Recirculating the air makes the bacteria consume all remaining oxygen. Similar to the composting technique, anaerobic digestion uses an even larger percolate tank. Microorganisms in the water ensure even higher biogas conversion. After anaerobic digestion, the remaining waste can still be used to produce a lower-grade compost.

For this research the scope is limited to aerobic digestion or composting, which is the process occurring in presence of oxygen. Composting processes typically are accompanied by high odour concentrations in the exhaust, requiring odour abatement techniques. There are many treatment techniques, all with their own advantages and disadvantages, the most used technique at composting facilities is a biofilter [21, 36]. From time to time, new technologies emerge to the market, requiring extensive testing and verifying before it can be implemented on large scale.

One of the techniques is treatment of composting air by ozone generated by UV-light, more specifically UV-C light, which is a specific part of the UV-spectrum. This is currently already implemented in many households, as well as some other markets on industrial scale. Examples are the fish processing industry, frying industry, tyre manufacturing industry, slaughter industry, sewage treatment and biogas processing plants [17].

1.1 Scope and Objectives of this Research

The objective of this research is to investigate whether ozone generated by UV-lamps, a relatively new treatment method for composting air, could replace the traditional biofilter with comparable or better efficiencies, costs and implementation? Several research questions have been made to answer this matter.

- What influence has ozone generated by UV-light on odour removal? How does this odour removal compare to air pollutant removal?
- What are the efficiencies at which odour can be removed by UV-C and ozone? By which circumstances are these efficiencies influenced? How do these efficiencies compare to a scrubber with biofilter?
- Does this air purification technique function properly stand-alone, or does it require additional purification techniques?
- How can a mathematical model be implemented to estimate VOC removal efficiencies by ozone and UV-C light, based on residence time, air composition and UV-power?
- Could it be financially feasible to remove VOCs using ozone and UV-C on both investment costs as well as recurring costs? How does the UV-technique compare to a biofilter, often used in composting facilities?

1.2 Method

To present an answer to all research questions above, a certain method has been used. First an extensive literature survey is executed to gain insight in the current state of the art odour abatement techniques, critical pollutants, typical air composition and gaps in the literature. These gaps mainly consist of experimental verification of the UV-technique for composting air specifically. There is much literature available about composting air treatment, but usually using other techniques. Furthermore, much literature is available describing cases for the UV-technique as well, but this generally concerns low concentrations or lab-scale pilots.

To fill in this literature gap, relatively large-scale experiments have been executed. During these experiments, a series of techniques is combined to be able to calculate odour removal efficiencies. An acid scrubber, the UV-technique and an active carbon filter are combined to gain insight in total removal possibilities. The comparison with the already installed biofilter is useful as well. Furthermore a mathematical model has been made to predict concentrations over time with multiple plug flow reactors. The experimental results can be supported by this model. To verify validity, additional experiments have to be executed.

1.3 Report Structure

To gain better navigation through this report, the structure is explained in this section. Already introduced is the topic of air treatment, which is further investigated fundamentally in the literature survey. Starting with the actual pollutants and several techniques to remove them, followed by an explanation of new emerging techniques such as ozone generated by UV-C light and plasma with their (dis)advantages.

The chapter thereafter describes the actual testing setup and methodology. This also describes the measuring techniques and devices, the testing location and the characteristics of experiments conducted. This all in order to increase repeatability of the experiments, increase the quality of the results and provide background information and recall the outcomes. This means all aspects will be handled to understand the underlying thoughts of the experiments.

The results of the experiments are treated in Chapter 4. This will be objectively reporting the results without much discussion. In the following chapter, a mathematical model has been made trying to link data and results of the conducted experiments with reactor models found in literature. Such a model could be helpful in the future, to predict possible treatment solutions and their corresponding efficiencies.

The experimental results are questioned and discussed in Chapter 6. Also the interpretation of the results is given here. A financial feasibility study has been done to compare the UV-technique to existing and commonly used techniques, such as the biofilter. This study can be found in Chapter 7. Finally, both partial and overall conclusions are presented at the end in Chapter 8. In this chapter, every aspect is ticked to give an overview of this thesis.

Chapter 2

Literature Survey

The process of composting requires millions of microorganisms to convert organic waste into compost under specific circumstances. A mixture of recycled air and fresh hall air is fed through spigot floors in large 6 x 6 x 30 meter tunnels. The ratio of this mixture regulates the oxygen concentration and air temperature, two of the major environmental conditions for the microorganisms. The result of this composting process is usually lots of odours at the exhaust and a Rottegrad V compost, which is a measure for compost maturity, quality and stability [16]. The scientific relevance of this literature survey lies especially in the upscaling of the UV-photocatalysis technique to remove pollutants from air. Currently much research has been done to use photocatalysis for effective purification of indoor air [25, 36, 49, 50]. One of the questions is whether this technique is suitable for larger industrial scale applications as well. A sub question to start with is how to quantify the amount of odours released, then typical pollutants are discussed for composting air and several other air treatment techniques are discussed. The working principle of this photocatalysis by UV-light is examined in depth to get a better understanding for its upscaling potential.

2.1 The Unit to Measure Amounts of Odour in Air

Various industries pollute a certain amount of odours into the air or water as a result of the outlet air through their chimneys or waste dumping in open water. Earlier it was difficult to objectively define the amount of odour, as there is no SI-unit to measure the rate of odour in air or water, such as meters, ppm, seconds or grams. In 2003, a European standard has been developed to overcome this problem, being the "European Odour Units" according to NEN-EN-13725, it is expressed in ou_E/m^3 [12] and is used to give certain permits. The previous Dutch odour units sometimes still found "geureenheden (ge)" is replaced as $2 \text{ ge} = 1 \text{ ou}_E/m^3$. The standardised unit is better, but still far from perfect, as it does not take into account the type of odour, i.e. if it smells rotten, burned, acidic, corpse, excremental, etc.

2.1.1 Measuring Method of Odour Units

To get a better understanding of the odour results, it is important to understand the procedure to determine the amount of European Odour Units. A certified panel with an odd amount of persons is gathered. The air to be analysed is evaporated into exactly one cubic meter of neutral gas under normalised conditions. This concentration is doubled every repetition (anti-dilution) until at least half of the panel has a physiological response,

this is the detection limit. In other words, the amount of European Odour Units per cubic meter is equal to the amount of dilutions required not to stink anymore [32]. Due to this measuring method, there will always be an uncertainty factor of two, which is often taken into account in the permits.

2.1.2 Odour Threshold Value

All odourous compounds have their own Odour Threshold Value (OTV), this is the lower detection limit of odourous smell and is determined empirically for a large amount of often-occurring compounds. A certain compound with a concentration of 40 ppm and an OTV of 60 ppm will not be smelled, while another compound with a concentration of 8 ppm and an OTV of 1 ppm will smell relatively strong. The ratio of concentration divided by OTV indicates the smell strongness of a compound. The OTV is determined by various factors, such as shape, polarity, partial charges and molecular mass of certain components [8].

2.2 Pollutants in Composting Air

It is important to understand what types of pollutants are present in the air to be treated. This gives insight in treatability by certain treatment techniques and removal efficiencies. Many studies have been conducted on the topic of air components in composting installations [45]. The pollutant with the highest concentration is usually ammonia in composting installations, although ammonia is relatively easy and cheap to successfully remove using an acid ammonia scrubber, as will be thoroughly explained in Section 2.3.1. Next to ammonia, it is expected that Volatile Organic Compounds (or VOCs) will have a large contribution to the odour concentrations, possibly even the largest. Therefore this is the group of interest for this research. Several VOC subgroups will be explained below.

2.2.1 Volatile Organic Compounds and Their Subgroups

”Volatile Organic Compounds” is an umbrella term for many different kinds of carbohydrates and hydrocarbons. Hydrocarbons are long molecule strings only consisting carbon and hydrogen atoms, possibly with multiple double bindings or more complex structures. Hydrocarbon are not to be confused with carbohydrates, as carbohydrates also contain oxygen atoms. These VOCs actually occur naturally in the atmospheric troposphere, they are a significant precursor of secondary organic aerosols and ozone [52]. As mentioned earlier, the VOCs exist of thousands of molecules, which can be placed in several subgroups. One important example of these subgroups are for instance Volatile Sulphuric Compounds (VSCs) [51]. Several others exist as well, one subgroup causing less odour concentrations in composting air than others. The ten for composting air considered to be important groups will be described below: first ethers, alcohols, ketones, aldehydes and aromatic-, cyclic- and aliphatic-carbohydrates, as these are often found in composting air, but less important to the overall odour concentration. Then the more odour-carrying VOCs are discussed: VSCs, terpenes and mercaptanes.

Aromatic carbohydrates contain at least of a ring of atoms joined by two types of covalent bonds with a unique molecular stability [48]. Since these rings occur in multiple groups, an example of the structure of such a ring is shown in Figure 2.1. This is the simplest and most well-known example, the benzene ring. The most occurring aromatic carbohydrate

in composting air is toluene. These VOCs have a relative high concentration, but a high OTV as well, making their presence less relevant.

Cyclic carbohydrates also consist of an atom ring, since this ensures the lowest energy state and is more thermodynamically stable. The main difference is that aromatic carbohydrates only have bonds with itself and aromatic ones are more stable [48]. This instability makes them less relevant.

Aliphatic carbohydrates are the final group of carbohydrates, no such ring is incorporated in the molecular structure. These are also known as alkanes, often with a structure with the form C_XH_{2X+2} [48]. These molecules are often found in composting air, especially pentane, but due to their high OTV they do not contribute much to the overall odour strength.

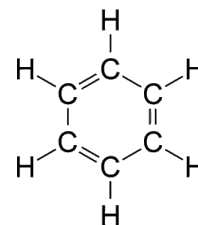


Figure 2.1:
Benzene ring.

Ethers, alcohols and ketones are respectively a molecule with an oxygen atom connected to two alkyl (i.e. CH_3) groups, a molecule connected to at least one hydroxyl ($-OH$) group and a carbon atom double bounded to an oxygen atom and two rest-groups [8]. All of these three groups frequently occur in composting air. Although often in either components with low concentrations or components with a high OTV, making them not contributing much to the overall odour strength.

Aldehydes are organic compounds containing a $-CHO$ group. They are the result of oxidising alcohols. Since alcohols (especially ethanol) are often present in composting air, the reaction with ozone stimulates the formation of aldehydes [13]. Depending on the exact composting air composition, several aldehydes are formed, such as ethanal, decanal and nonanal. They come in high concentrations and low OTVs, therefore being quite smelly. Aldehydes are often used in perfumes, since they smell like lemons, roses, oranges and other depending on the type of aldehyde.

These were VOC subgroups commonly occurring in composting air, but not contributing that much to the overall odour. More problematic subgroups are VSCs, terpenes and mercaptanes. Organic Sulphuric Compounds (VSCs) are -as the name suggests- organic components with one or multiple sulphur atoms connected to them. VSCs are one of the main threats concerning odour load. Especially dimethylsulfide typically has a high concentration in composting air and has a relatively low OTV [14].

Terpenes are harder to describe, as they do not have an exact definition. However, they are highly aromatic organic compounds which often appear in plants as natural defence against infectious germs, certain insect species or to heal from damage. They determine the majority of the smell of lavender, rosemary and pine. The other side of terpenes is that they might destroy mechanical properties of plastic piping and cover the smell of natural gas [41]. Terpenes often occurring in composting air are limonene and α -pinene.

Mercaptanes, sometimes referred to as thiols as well, is an organic sulphurous component with a sulfanyl ($-SH$) group attached. They are known for their extremely low OTV's, possibly even below the measurement threshold of a GC-MS analysis, making them an unacceptable group of VOCs, possibly creating enormous odour loads. Research done by Centriair shows extremely high removal efficiencies of UV-lamps for mercaptans [31].

2.3 Working Principle of Several Treatment Techniques

Now that the pollutants are clarified, the most-used treatment techniques to remove the majority of these pollutants are presented in the coming section. Their purposes, removal efficiencies, advantages and disadvantages are discussed. Possible combination of techniques are described in a later stage. First the wet acid scrubber is explained, which removes ammonia efficiently. Then three often-used techniques to remove VOCs are presented: a biofilter, the UV-light technology and an active carbon filter. This section is finalised with less-used outdated and futuristic techniques, being catalytic combustion and plasma technology.

2.3.1 Ammonia Removal by Wet Acid Scrubber

Various types of scrubbers exist, such as dry scrubbers and wet scrubbers, both available with either a horizontal or vertical layout. For the most efficient removal of ammonia, often wet (spray) acid scrubbers are used. Its working principle can be explained using Figure 2.2.

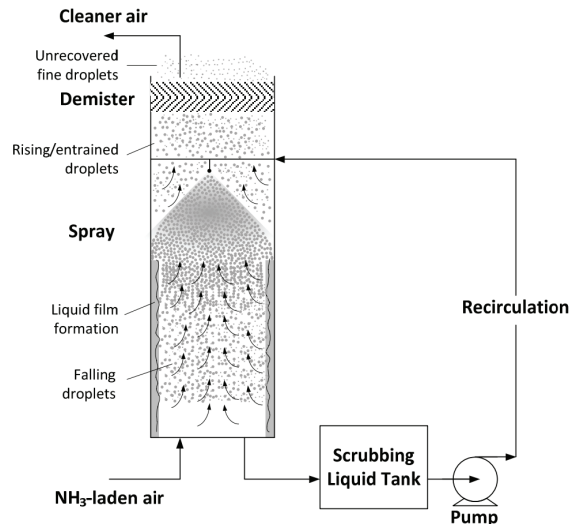
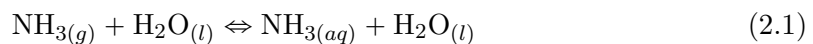


Figure 2.2: Schematic view of a typical counter-current wet spray ammonia scrubber [18].

Air with a large NH₃-load enters from the bottom, where the NH₃ mixes with a diluted acid solution falling as droplets in counter-current direction in the scrubber column. The majority of larger droplets move down counter-currently against the airflow, while some smaller droplets can be potentially entrained by air flowing up [18]. The droplets and liquid film on the scrubbers' sidewalls provide a large reaction surface, improving its efficiency. This acidic liquid can be recirculated and reused using a pump and storage tank several times, making it a closed loop system. First of all, the NH₃ solves in water to its aqueous phase as seen in Equation 2.1. Then it reacts with the H⁺ derived from the acidic liquid to ammonium (NH₄) according to Equation 2.2. After too many ammonium salts are dissolved in the liquid by the process, the electroconductivity (measured in mS/cm) becomes too large and the liquid needs to be substituted.



In practice, this is a proven technology to remove ammonia with efficiencies of at least 95%, but typically as high as 99%, both for horizontal and vertical layouts. Such high efficiencies are reached especially with high inlet concentrations, up to several hundreds of ppm's. These efficiencies are necessary as both a biofilter and the UV-reactor cannot withstand more than around 10 ppm. Typical ammonia inlet concentrations in composting are between 100 and 300 ppm. The major drawback of the acid scrubber system is the high pressure drop, caused by the packing material inside the scrubber column, the air experiences much resistance and therefore pressure drops up to a few thousand Pascal could occur. Especially with large air flows, this massively increases your fan requirement. Although the investment costs for an acid scrubber are relatively low, the operational costs existing of a large fan and the chemicals required for efficient removal are high. This is discussed in more detail in Section 7.

2.3.2 Biological Treatment by a Biofilter

Next to physical and chemical odour abatement techniques stands biological treatment. This system potentially has several advantages, such as low operational costs, a high efficiency and being ecofriendly [42]. Another advantage is the fact that besides VOC removal efficiencies of around 95%, it also achieves ammonia removal efficiencies up to 80%. As mentioned before, the application of microorganisms in biofilters has long been used in the waste treatment industry. Typically hydrogen sulphide (or H_2S) originates from anaerobic parts of the waste treatment process, being a very corroding component. According to previous research and experience, high removal efficiencies also yield for H_2S [21].

The biofilm attached to the (organic) packing material contains many microorganisms which absorb noxious gases in the waste air, which are then broken down into carbon dioxide, water and salts. The energy and nutrients contained in the waste air is used by the microorganisms to grow and duplicate [3]. The operation temperature has an enormous impact, especially since the microorganisms have a specific operating range: either psychrophilic, mesophilic or thermophilic. A typical biofilter uses mesophilic bacteria, with a range between 20 and 35°C. However, the composting air outlet is typically between 40 and 50°C.

To increase efficiencies, very specific packing materials are used with a certain ratio of surface per volume, in order to find an optimum between a large biofilm surface and sufficiently low pressure drop. Too much biofilm surface area causes the air to congest in the material, similar to the acid scrubber. A typical schematic layout of the working principle of a biofilter can be seen in Figure 2.3. First the air is humidified before it enters the biofilters organic packing material, usually specific types of mixed wood chips. The water sprayed from the top drips to the bottom, where it is caught. Depending on the air- and water characteristics, this could either be reused for spraying or treated in a wastewater treatment plant, then a fresher water source is used for spraying. Treated air leaves from the top of the biofilter to a chimney to be released in the air.

In Section 4.4 also the biological treatability of the most severe airborne compounds found in several GC-MS analysis has been investigated, either by a biofilter as described or a bio-trickling filter. The results are promising. Despite, there are some major challenges with and disadvantages of biofilters. The first is the lack of a scientific approach for the

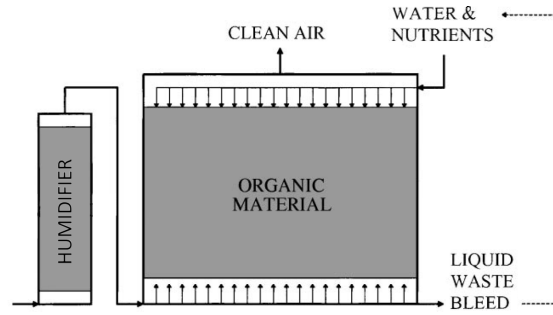


Figure 2.3: Schematic layout of a typical biofilter [30].

operating and optimisation of a biofilter, most of this is done empirically, as the microbiology is understood insufficiently and external factors have a major influence. Also, controlling the performance variables is difficult, the temperature is often too high, therefore the bed is too dry or dusty and the pH of recirculating water could be wrong as well. Non-homogeneous distribution of air is another possibility, causing unused and less efficient zones in the biofilter. Over time, the increasing mass of the biofilters' packing material causes higher pressure drops than anticipated with the installed fan capacity.

Lastly, possibly the most severe disadvantage, is the ground area required for a biofilter. This heavily depends on the specific details of the air to be treated, but a rule of thumb is that between 80 and 100 m² is required for an air flow of 10,000 m³/h.

2.3.3 Ultraviolet-light technology

The UV-lamps that will be used are mercury discharge lamps with two effective wavelengths, being 185 and 254 nm [31]. First the electromagnetic spectrum will be described in the following section to get a better understanding. Furthermore the working of ozone will be explained.

Electromagnetic Spectrum

The electromagnetic spectrum is outlined in Figure 2.4. Ultraviolet light has a wavelength below visible light, but is larger than X-rays. As can be seen in the figure, there are several types of UV-light. Although the UV-lamps used often are called UV-C lamps, this is not completely true. It is a combination of Vacuum-UV and UV-C. The first one is responsible for the ozone creation process [54], while the latter is responsible for the germicidal effect, directly destroying VOCs and double bonds incorporated in them [2].

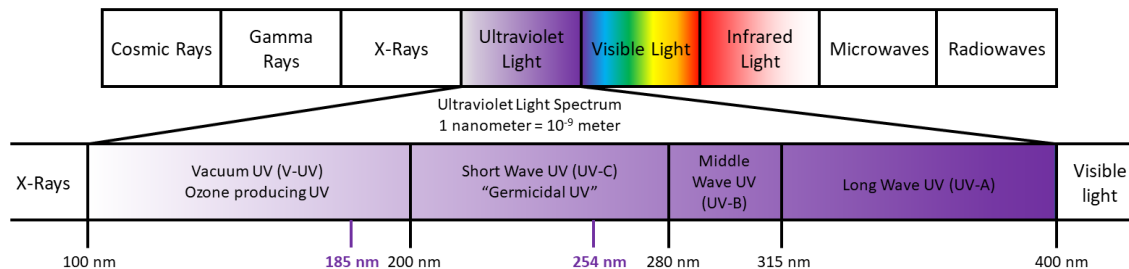


Figure 2.4: The electromagnetic spectrum, detailed focus on UV-light.

Each type of UV-lamp has its own spectral energy distribution plot. The low-pressure Hg-lamp has two wavelengths peaks: 185 and 254 nm. The difference with a high-pressure UV-lamp can easily be seen in Figure 2.5, where many more wavelengths have peak appearances.

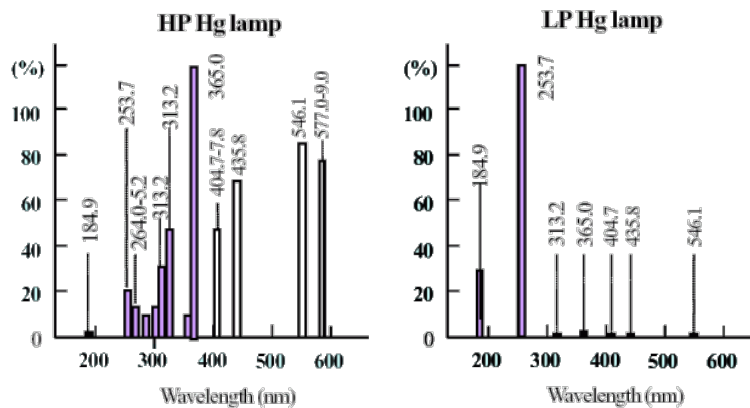


Figure 2.5: Spectral energy distribution of high- and low-pressure mercury discharge lamps.

The 185 nm wavelength produces ozone molecules from oxygen, which will be explained in further detail in Section 2.3.3. On the other hand, the 254 nm wavelength directly destroys VOC molecules and cuts them into smaller molecules, possibly other VOCs. Examples of such reactions can be seen in Equations 2.3 and 2.4 [46], where for example C_2H_6 and H_2S are decomposed into several different radicals using photons ($h\nu$).



Ozone Formation from and Reaction with Oxygen

The process of global ozone formation occurs all the time, in the ozone layer. This ozone layer is found mostly in the stratosphere, between 10 and 16 km above earth's surface. The process is very similar, but the initiation is different. The ozone layer is formed both by extreme high voltages in the form of thunder as well as from sunlight, which amongst many other wavelengths consists of 185 nm UV-light. UV-light bulbs also emit 185 nm.

As can be seen in Figure 2.6, first oxygen molecules (O_2) present in air are split to two unstable atomic oxygen atoms O_1 by the UV-light. These oxygen radicals then connect to other O_2 molecules to form ozone (O_3). Both the unstable O_1 as well as the semi-stable O_3 is able to react with the double bonds of VOCs and other airborne gases in the air flow. Simplified this means the long hydrocarbon molecules are shortened to less smelly shorter molecules [47], possibly even to H_2O , CO_2 and SO_2 .

An example of such a relatively complex reaction mechanism can be seen in Figure 2.7. Dimethyl sulfide (DMS) and dimethyl disulfide (DMDS) react with ozone. Both VOCs are regularly present in composting air, as can be read in Section 4.2.1. In several stages DMS and DMDS are reduced to CO_2 , H_2O , SO_2 , SO_3 and SO_4 respectively with the use of ozone molecules in each reaction. The reaction rate is limited to the ozone concentration present.

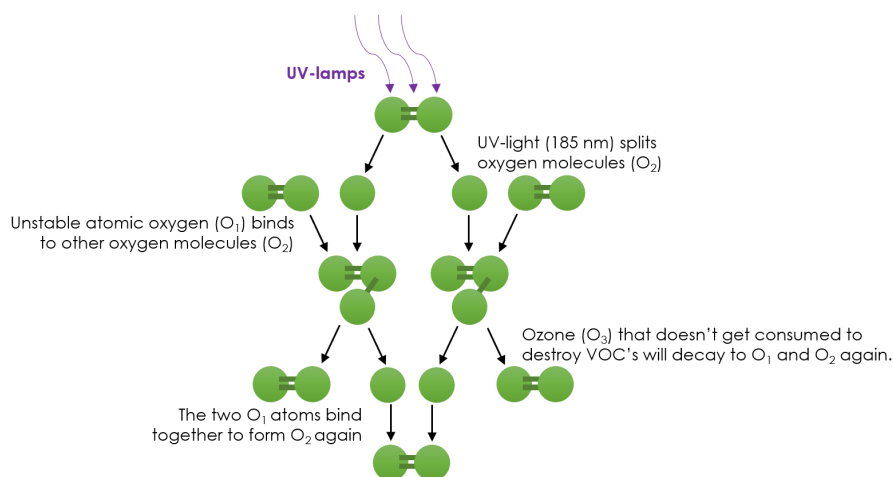


Figure 2.6: *The formation of ozone from oxygen molecules using UV-lights.*

If too much UV-power is installed, there will be non-reacting O_1 or O_3 molecules present in the air. Ozone in too high concentration can be harmful for mankind, as it can damage the lungs, cause chest pain, coughing, shortness of breath and several other breath-related symptoms. After a short period of time these O_1 atoms bind together to reform to the stable oxygen molecule O_2 again [49].

Hydroxyl Groups as Oxidation Mechanism

As already mentioned in Section 2.3.3 and shown in Figure 2.7, reaction mechanisms can be difficult. Previously the focus lied on ozone as oxidant, but the hydroxyl radical is another example of a strong oxidant, together with several other oxygen-containing molecules as seen in Table 2.1, sorted from weakest to strongest oxidants.

Table 2.1: *Several forms of reactive oxygen with their oxidation potentials. Several are present in and after the UV-reactor.*

Substance	Water	Oxygen	Ozone	Oxygen radical	Hydroxyl radical
Redox potential	1.23 V	1.23 V	2.07 V	2.42 V	2.86 V
Structure					

Hydroxyl radicals have the highest redox potential, and therefore are one of the most reactive molecules. Hydroxyls are generated when electronically excited single oxygen molecules, O_1 , react with a water molecule to two OH-radicals. These radicals yield for instance unsubstituted alkanes (such as ethane, propane, etc.) directly by hydrogen transfer according to Equation 2.5. The oxidation or redox potentials have been conducted from previous work of Peter Atkins and A.J. Bard [5, 6]. The oxidation rate constant is strongly dependant on the molecular weight of the VOCs, and increases with increasing organic compound weight: bigger molecules are more reactive [39].



Instead of releasing the hydrogen-atom from the VOC, it is also possible that the hydroxyl

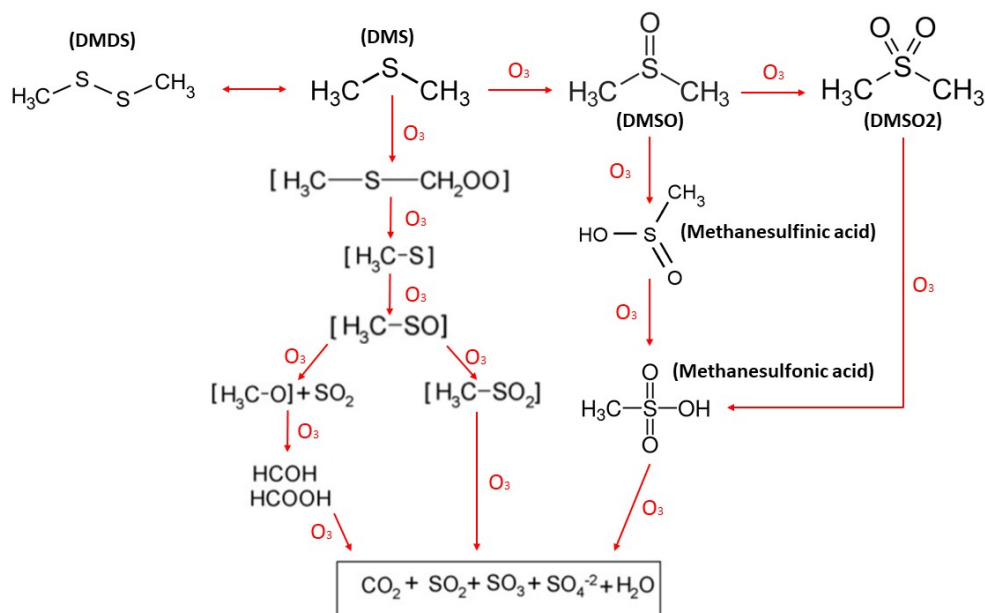


Figure 2.7: Plausible breakdown reaction mechanism for the oxidation of DMS and DMDS with the use of ozone [15]. Rate is limited to ozone concentration.

radical is added to the double bond of an organic compound to decrease odours. This is the case in for instance chloroethylenes. OH^- radical activates the ring of aromatic carbohydrates (often present in composting air) for electrophilic substitution [22] to reduce odour concentrations.

Effect of External Conditions on Reaction Rate of Ozone with VOCs

The external conditions play a significant role in the reaction rate of the system. In Figure 2.8 the effect of several conditions is shown. For instance, Figure 2.8a shows the effect of the wavelength of the UV-light, in which the band gap energy can be seen clearly as threshold value. The wavelengths are assumed to be equal to 185 and 254 nm for the type of UV-lamp chosen in this specific case.

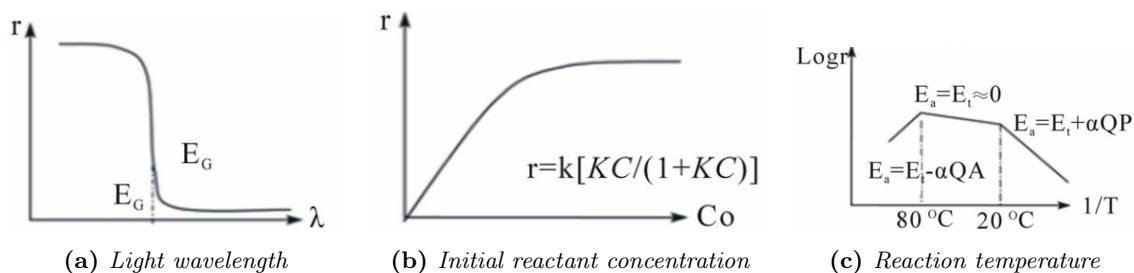


Figure 2.8: Reaction rate influence of several physical parameters [28].

Initial Contaminant Concentrations Several researches show that enhancing the initial contaminant concentration up to a certain level, will increase the reaction rate in the process of VOC removal [9, 24, 33]. Of course, this is limited up to a certain concentration, after which the reaction rate will remain relatively constant. The reaction rate r is varying proportionally to the initial reactant concentration C_0 , as seen in Figure 2.8b as well.

Reaction Temperature The reaction temperature generally is optimal between 20°C and 80°C. Below room temperature the apparent activation energy becomes positive and therefore the activity decreases significantly, as seen in Figure 2.8c. This which will never happen during operation for composting air, as this is typically between 40 and 60°C. Above 80°C is undesirable as well, as the activation energy becomes negative. This means the reaction will evolve spontaneously, energy is released and an exothermic reaction occurs.

Relative Humidity Excessive water vapour will lower the rate of reaction, as water molecules occupy the reactants places on the surface. This hydrophilic effect at the surface will prevail over the oxidising effect of the reactants, especially when high values of relative humidity are present [28]. Although, the truth lies more precise. Certain VOCs do not respond to a change in relative humidity at all, where for other VOCs the reaction rate significantly decreases. One thing is certain, the reaction rate never increases for any VOC with increasing relative humidity [7]. The research of O'Malley shows the reactivity for total oxidation of VOCs with different functional groups varied in the following order: alcohols \geq aromatics \geq ketones \geq carboxylic acids \geq alkanes [35]. This means alcohols are the most prone to relative humidity changes, compared to other VOC groups.

Light Intensity The light intensity, or irradiance, is another important factor next to the wavelength concerning the degradation rate of the VOCs. The reaction rate r is linearly proportional to the irradiance or photon flux on a certain cross-sectional surface area of the reactor tube. This linear behaviour only yields for medium and high irradiance, for low photon fluxes it is proportional as $r \sim \Phi^{1/2}$ [28].

2.3.4 Activated Carbon Filter

Activated Carbon (AC) filters have a bed with a large amount of carbon grains. These are materials with a high carbon-content, such as bamboo, coal or several kinds of wood. These materials are activated using either carbonisation or oxidation. The first uses pyrolysis at temperatures between 600-900°C. In the second scenario, the material is exposed to an oxygen-rich environment at elevated temperatures, at least 250°C but preferably 600°C or more. The oxygen opens up small pores, resulting in a large internal surface area in the carbon grains. The principle of chemical adsorption is used to purify water for instance. Or in this case, air. All kinds of molecules, amongst which VOCs and residual ozone molecules, can be trapped in the pores of the carbon grain. Although many of the molecules with a particle size between 0.5 and 50 μm can be adsorbed, it hardly removes any minerals, salts or dissolved inorganic compounds such as magnesium. These carbon grains have a large specific area, the surface area per unit volume is in the order of magnitude of 3000 m^2 for one gram of carbon grains, ensuring sufficient space to adsorb molecules.

As one could imagine, activated carbon grains have a finite lifetime. At a certain moment, all active surface area is occupied by VOCs and other impurities such as ozone or ammonia. This results in a saturated filter, meaning that either all activated carbon has to be replaced or reactivated using thermal and/or pressure swing [10]. The cost price of a kilogram of activated carbon is relatively high -currently around EUR 3 per kg- which means that it is often not financially feasible to run with a standalone AC-filter due to the high operational expenditures.

Since an AC-filter has such high removal efficiencies for a variety of compounds, this makes it ultimately suitable as final stage to cope with unexpected situations where the UV-power turns out to be insufficient. Such situations can be unforeseen high concentrations of VOC inlet or a sudden increase in air flow. The AC-filter then acts as a so called "Police Filter".

Lifetime Elongation of Active Carbon Filter by UV-C and Ozone

As mentioned in the previous paragraph, the lifetime of an AC-filter is finite, although its lifespan can possibly be extended by the use of the UV-C and ozone techniques (described in Sections 2.3.3 and 2.3.3) in front of the AC-filter. This elongation often results in an increase of lifespan in the order of four times longer [44], but depending on composition this can be shorter or longer. The elongation can be explained by three effects:

The first reason for lifetime elongation is the fact that both the UV-radiation as well as the ozone molecules ensure a complete VOC destruction before the air even encounters the filter, since for instance H_2O and CO_2 just pass the filter without blocking pores. Secondly, the rest-ozone remaining when not all molecules are utilised to destroy VOCs can regenerate certain readily filled pores by decomposition of caught VOCs [44]. This frees up the pores occupied previously. Lastly there is also a conversion of very long VOC strings to (several) shorter VOC strings, which might possibly not be trapped in the AC-filter.

Another possibility to extend the lifespan of an AC-filter is to only utilise the filter during periods with highly concentrated air inlets. During other periods, where the AC-filter is not required to reach the odour limits, the filter can be bypassed automatically and sensor-based.

2.3.5 Alternative Treatment Methods

Catalytic Combustion

Catalytic combustion is another air treatment and odour abatement technique often used, traditionally this has been a high-efficiency and relatively low-costs solution. However, it is extremely important to keep the catalyst in good condition, as replacement is expensive. Possible failure mechanisms are irreversible adsorption with the catalyst surface, fouling the surface area, oxidation of a metallic catalyst or exceeding thermal limits of the catalyst [34]. Also high concentrations of sulphur in the fuel can form a problem, as sulphur accumulation occurs in the catalysts, causing an early maximum deactivation of the catalyst [29, 38].

The working principle of catalytic combustion is to decrease the activation energy required compared to regular combustion of certain reactants. An example is given in Figure 2.9, where the reactant H_2O_2 is reduced to its products, being H_2O and O_2 . Clearly, the activation energy required with catalyst is significantly lower than without catalyst. For carbohydrates with the form C_xH_y , the net reaction is as follows:

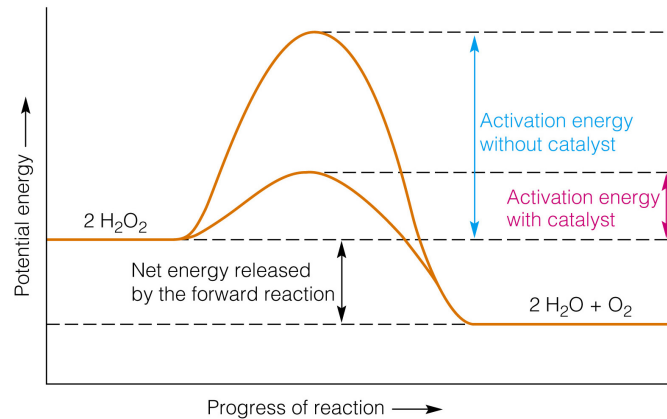
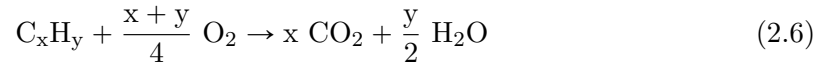
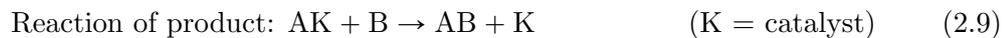


Figure 2.9: Visual representation of the energy released by a reaction and the change in activation energy by a catalyst.

If the catalyst is used and maintained properly, it does not require replacement for up to 20 years. This can be explained by the fact that the catalyst is not consumed and therefore preserved in the chemical reaction. A general form of a catalytic reaction is shown below. In Equation 2.7, the reaction without catalyst (and therefore high activation energy) can be seen. Furthermore, in Equation 2.8, the transient product can be seen, which is used and then preserved in Equation 2.9. The net equation of the middle and bottom equation is the same as the top equation.



Disadvantages of this technique are the low resistance for temperature variations, low mechanical resistance of the catalysts itself, the environmental concerns about the fact of burning all pollutants and a limited temperature range of the catalyst, being high at 800°C , making it very energy consuming. Catalytic combustion is not suitable for large volume flows either [29]. All in all, this makes it unsuitable for application in composting facilities.

Plasma Technology

There are several forms of plasma, which can roughly be subdivided into two categories: thermal plasma and non-thermal plasma. For this case, only non-thermal plasma is considered. This technology is based on an electric field that accelerates free electrons, these electrons heat up to temperatures as high as $200,000^\circ\text{C}$. Since these electrons are far from a thermal equilibrium with surrounding molecules, their collisions cause excited

gas molecules which will emit either heat or photons [34]. In this way, ions and radicals (such as ozone) are generated, similar to the UV-technique described in Section 2.3.3. The biggest drawback compared to the UV-technique however, is that no direct radiation will destroy VOCs directly. Another disadvantage is that there is a high percentage of by-products, apart from the high energy consumption because of the low energy efficiency.

2.4 Literature Study: Summarised

Odour is measured using a certified European method based around the dilution required when the air does not smell anymore. Each individual compound has an own odour threshold value, which is the minimum concentration to be smelled. Apart from ammonia, the majority of smelling compounds can be summarised as volatile organic compounds. These VOCs can be divided into all kinds of subgroups, amongst which some are more important than others. This importance can either be caused by its powerful smell or the fact that they are hard to remove. An acid scrubber is necessary for composting air to remove the (typical) high concentrations of ammonia very efficiently. Traditionally a biofilter is used to remove VOCs biologically using microorganisms, but alternatively the UV-technique can be used to achieve a similar result. The wavelengths of 185 and 254 nm emitted by the UV-bulbs are responsible for ozone generation and directly destroying double bonds respectively, both decreasing VOC concentrations. There are other radicals, such as hydroxyl, which work similarly as ozone and are generated in parallel. External conditions all have their own influence on the UV-reactor, such as initial pollutant concentration, reaction temperature, relative humidity and the UV-power. An active carbon filter is another technique which is highly efficient, but expensive to use for VOC removal. An additional advantage of the UV-technique is that it elongates active carbon lifetime.

The major gap in this literature study is the translation of small-scale UV-experiments to a large-scale composting air case. There is much literature available about large-scale composting odour abatement, but usually using biofilters or bio-trickling systems. Literature about the UV-technique is available as well, but only for other large-scale industries such as the slaughter- or tyre manufacturing industry. Therefore large-scale composting experiments will be executed to fill in this white field.

Chapter 3

Experimental Setup and Methodology

In order to gain a feeling for reachable UV-reactor odour removal efficiencies and to find correspondence with the literature, experiments have been executed. The goal is to find removal efficiencies per component (scrubber, UV-reactor, active carbon and biofilters) and to be able to compare them later financially as well. This chapter describes the methodology used, existing of the requirements for a small-scale test, an explanation of the testing-site and its characteristics, the measuremental devices which have been used in parallel to several professional companies executing measurements and the characteristics and testing scheme for the specific testing sites in Lelystad and Erembodegem. All of this contributes to, amongst other things, improved results quality, background information for the interpretation and a better repeatability for verification purposes.

3.1 Requirements and Research Questions for a Testing Setup

In order to achieve reliable testing results, it is important to setup an extensive list of requirements and questions. Following from this list is the design, implementation, testing schemes and a list of measuremental devices, so all elements of interest are taken care of.

- Is the use of an acid scrubber necessary, to achieve at least a $\geq 95\%$ removal-rate of ammonia? This is, in order to prevent that most of the UV-capacity breaks down NH_3 in stead of the more smelly VOCs.
- What is the relation between the specific power (J/m^3) and the odour reduction. Can this be assumed linearly or could it be a more complex relation?
- How does the retention time nearby a UV lamp influence the VOC and/or odour removal efficiency? Does the orientation of the lamps have any influence?
- What is the effect of time-dynamics on the influent characteristics concerning both VOCs and odour?
- Is it necessary to install an active carbon filter after the UV-reactor to cope with influent fluctuations? What role does the retention time play? Can the lifespan be elongated by bypassing this filter during low-concentration operation? How does the UV-reactor influence the lifespan of an active carbon filter?

3.2 Implementation: Orgaworld Lelystad

A large-scale waste treatment facility owned and operated by Orgaworld (part of Renewi) is located southeast of Lelystad, The Netherlands. Due to a mutual interest in odour removal alternatives, this place will be used to execute the testing. Two separate processes can be divided: twelve open fields where field composting of VFG waste occurs and sludge drying occurs in eight large aerobic composting tunnels, treating 110,000,000 kg of waste each year [37]. Most of the odours are released in the early composting/drying stage. Sludge drying lasts for five to seven days, while the waste lies at the field composting for two to three weeks.

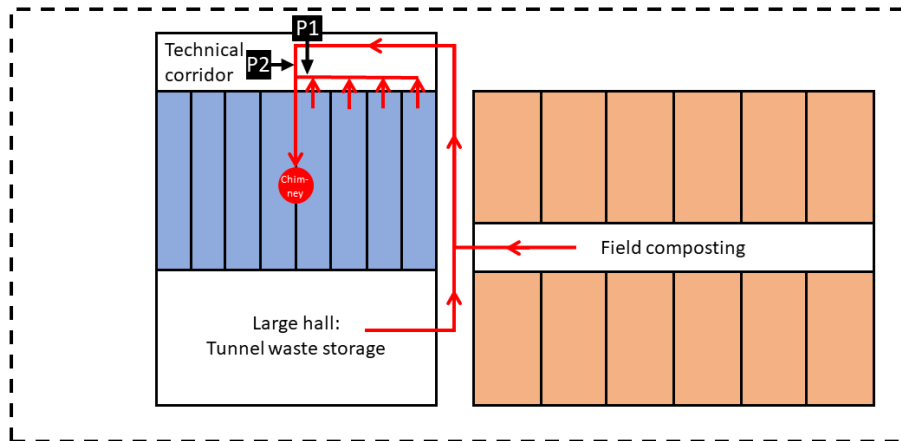


Figure 3.1: Plant layout of eight tunnels (blue) and twelve fields (orange) at Orgaworld ZAW in Lelystad. Air flows are indicated with red arrows, measurement positions P1 and P2 are indicated with black boxes. Air is released in the chimney.

3.2.1 Day-, Week- and Month-dynamics On-Site

To get a better understanding of the testing results, it is important to identify possible dynamics in the odour concentrations. Research has been done in the past by Orgaworld to determine part of these dynamics, and they can be split up in three parts: fluctuations during the day, fluctuations during the week and fluctuations in between months or even seasons. These results are used to determine optimal planning of testing, so as little variation in environmental conditions as possible will be encountered.

The day dynamics are relatively comparable for every day, since there is no fluctuation in the on-site planning per day. Therefore the conditions will be assumed to be similar each day at the same time, as well as throughout the day.

Due to the operational structure throughout the week applied at the Orgaworld testing facility in Lelystad, there is an enormous but recurring fluctuation per week. In a regular week, everyday expect Friday two composting tunnels are emptied and refilled. As there are eight in total, this means on Thursdays you have the youngest and most smelly waste, as can be seen in Table 3.1.

Tunnels	Mon	Tue	Wed	Thu	Fri	Sat	Sun
1&2	0	1	2	3	4	5	6
3&4	6	0	1	2	3	4	5
5&6	5	6	0	1	2	3	4
7&8	4	5	6	0	1	2	3 +
Avg. age	3.8	3.0	2.3	1.5	2.5	3.5	4.5

Table 3.1: Average waste age (in days) in a regular week. The colours represent the odours, where red is the worst and green is the cleanest.

Lastly the month-dynamics, caused by different waste inputs throughout the seasons. For example, during the fall, especially the amount of garden waste increases tremendously, being very wet compared to summer VFG-waste or MSW. The month-dynamics will be neglected for this experiment however, due to the relatively short testing period.

Apart from these day-, week and month-dynamics, there are even smaller time-scale variations in the flow. To give a clear indication, a FID-device has been used to measure the VOCs real-time in the air. The FID-signal has been continuously measured for over 90 minutes, and the results would vary heavily whether a test would have been conducted in either the first 30, the middle 30 or the final 30 minutes of this period. The graph can be found in Figure D.1 in Appendix D.

3.3 Design of a Small-Scale UV-Testing-Setup

The design of the experimental setup can be seen in Figure 3.2, where an air flow of around 700 m³/h will be treated. To give an indication of sizing, the complete air flow is around 105,000 m³/h, so less than 1% of the total air flow is treated in this test. The on-scale drawing is shown in Figure 3.3, all further explanation below will refer to these two figures. The "existing piping" can be either at L1 (sludge drying tunnel air) or L2 (mixed air with field composting air), as is referred to in Figure 3.1 in Section 3.2.

Furthermore a counter-flow ammonia-scrubber will be implemented in order to remove most of the ammonia. Expected influent concentrations are depending on the type of air, but will be between 80 and 300 ppm. The air enters on top of the cylinder, while leaving at the bottom. The acidic water, being 96% sulphuric acid diluted until a pH of 3-4 is reached, is pumped vice versa from an acid storage: from top to bottom. In this cylinder, a high specific area packaging is placed to increase reaction time and surface area, resulting in a higher ammonia removal efficiency. This scrubber is designed for an air flow of 500 m³/h, but can be stretched to 1000 m³/h.

After the ammonia-scrubber the air will be sucked by the fan through the UV-reactor, where a changeable power of UV-lamps is installed. In order to make a fair comparison for scenarios with a different amount of power, the airflow must be adjusted when less lamps are turned on. Although this box usually operates with up to 50 UV lamps, this specific UV-reactor can operate with 2, 4, 6, 8 and 10 lamps of 145 Watt each and is designed for an air flow of 400-2500 m³/h.

The fan, mentioned earlier, is able to cope with a maximum air flow of around $1500 \text{ m}^3/\text{h}$ in the complete setup with a scrubber, UV-reactor and active carbon. The active carbon boxes are filled with 160 kg of activated carbon grains. There is actually a possibility to bypass the active carbon boxes, in order to tweak the retention time in the afterburner, which is a 720 mm diameter pipe of 12 meters with several measurement points, being the first part of the outlet. In here, possible reaction effects of the ozone after a certain amount of time can be found.

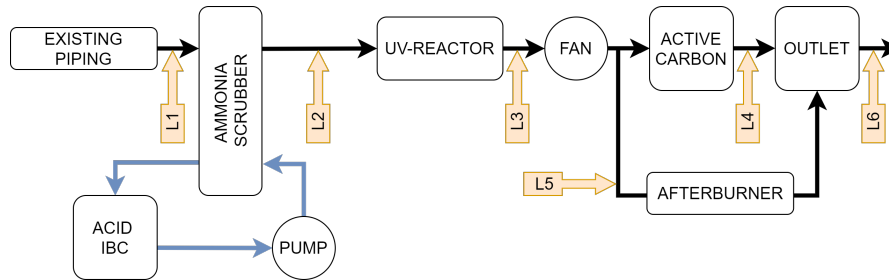


Figure 3.2: Schematic flowchart of desired experimental setup. Measurement locations are indicated with orange L1 until L6.

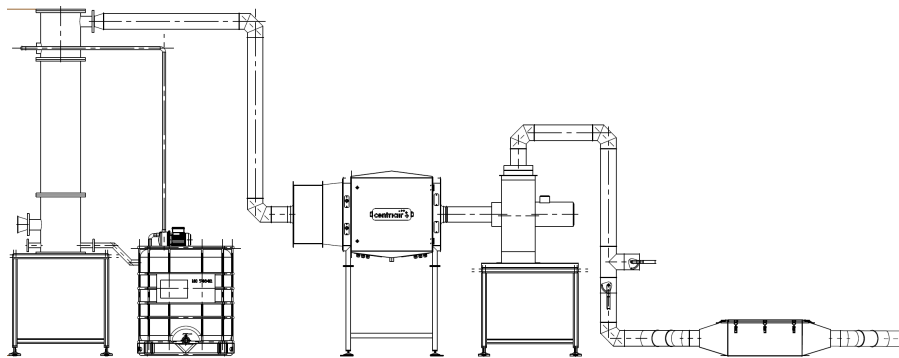


Figure 3.3: Actual drawing of of desired experimental setup with components drawn to scale. Fltr: scrubber, IBC storage, UV-reactor, fan on an increase, active carbon (afterburner not shown behind AC).

3.4 Measurement Devices Used

In order to determine efficiency of the system and its individual parts, a series of measurement instruments is required, which is described shortly in this section. A way more extensive description is given in Appendix A.

Multiple thermocouple temperature probes with an expected range between 20°C and 60°C to indicate characteristics of influent air, functioning status of the ammonia-scrubber and possible leakages/false air suction are used with an accuracy of $\pm 0.5^\circ\text{C}$. To determine over- and underpressure caused by the fan, a digital differential pressure device is required, the Extech HD750 with an accuracy of $\pm 30 \text{ Pa}$. The expected range is between -1000 Pa and $+1000 \text{ Pa}$. This might indicate a congestion in the scrubber or incorrect settings or installation elsewhere. Air velocity devices are necessary to map air flows through the installation, which can be calculated in combination with the inner diameter

of the section, for instance the Testo 440 kit. Such devices require the most laminar flow as possible, so a straight section of pipe before the measurement location is advised. The velocity range is between 0 and 15 m/s. To overcome the turbulence-problem, a pitot-tube could replace the air velocity device. Such a tube measures the stagnation and static pressures and calculates the air speed using the dynamic pressure. However, because of financial considerations, this is outside the scope of this project. Electrical conductivity (EC) and pH devices are required to control the IBC functioning as acid storage for the ammonia-scrubber, the device used is the Hanna Hi 9813 combination meter. The electrical conductivity may not exceed 200 mS/cm, indicating that the water is too saturated with salts, mostly caused by the high ammonia concentration. At the same time, the pH must be kept between 3 and 5 for optimum ammonium removal performance. Furthermore, a Kitagawa pump is required in combination with ozone and ammonia Kitagawa-tubes to determine their concentrations. Their working principle is similar to the better-known Dräger-tubes. Ozone concentrations indicate the functioning of the UV-lamps and active carbon filter, where concentrations are expected between 0 and 5 ppm. Ammonia concentrations are an indication of the ammonia-scrubber's functioning, the required range of untreated air is as high as 300 ppm, although a more precise tube might be necessary to determine concentrations after the scrubber. Alternatively, a Dräger-pump and corresponding tubes function perfectly as well. Data acquisition is done by myself and several colleagues simultaneously, all devices are mobile devices, so can be taken to several measurement points.

So far the devices are all straightforward and often used measurement devices, it becomes more complex when determining the amount of VOCs, being one of the most important objective measurements to indicate odourous compounds. A Flame Ionization Detector (FID)-device has been chosen to execute this task, although a comparison with the Photoionisation Detector (PID) as well as a more extensive explanation can be found in Appendix A. The FID-device produces a signal in ppm's, caused by ionization due to burning organic compounds with H₂ gas. The result is a ppm-equivalent to propane, as this is the calibration gas, therefore all hydrocarbons will be measured. The expected range is between 0 and 150 ppm.

3.5 External Analysis: Odour Testing and GC-MS

Some measurements are beyond the scope of WTT and will be outsourced because of enormous investment/training costs. The first external analysis is the odour testing. As thoroughly explained earlier in Section 2.1.1, the amount of odour units are determined on several locations (L1 until L6, as mentioned in Section 3.3), during several scenarios.

Another analysis is gas chromatography, mass spectrometry (GC-MS), which gives an analytical indication of prominent components present in the air flows on locations L1 until L6. This is done using the combination of both gas chromatography as well as mass spectrometry techniques, as the name suggests. Without diving into the working principles, the result of this is a chromatogram and an intensity-mass spectrum, combined this gives a great representation of present components. The only limitation of this technique is the fact that volatile organic compounds with less than 5 carbon atoms are hard to capture using GC-MS (for instance methane, ethane, methanol and formaldehyde cannot be detected). This minimum number of C-atoms decreases in case oxygen, nitrogen or another atom is present (for instance dichloromethane or acetone can be detected).

3.6 Extensive Testing Schemes

While making a testing scheme, the most important characteristic is the amount of air. All components described in Section 3.3 are able to cope with air flows between 500 and 1000 m³/h in Lelystad, and around 10,000 m³/h for Erembodegem. The functioning of the ammonia scrubber can easily be tested using ammonia Kitagawa tubes. Influent VOC levels can be determined using the FID device. Furthermore, the effect of different UV-powers must be investigated, all possibilities will be tested and ozone levels will be measured. After getting a better understanding of pollution concentrations and ozone concentrations, a more detailed scheme can be made, where air flows can be matched to the amount of UV-lamps.

In the testing scheme for Lelystad, also an active carbon (AC) filter is integrated. In order to guarantee well functioning of the active carbon, it is important to tweak the AC-bypass such that the manufacturers advised retention time is being reached. Lastly, in order to check whether an active carbon filter is necessary at all, the AC-bypass can be tweaked as well: in full-scale installations the ozone has a retention time of around 20 seconds before exiting through the chimney. This can be simulated using the afterburner. By regulating the air flow through the afterburner with the AC-bypass, the retention time mentioned earlier can be achieved, to check whether only ozone could be sufficient to treat the air successfully.

Chapter 4

Experimental Results

As already mentioned in the previous section, tests have been conducted to get insight in the real removal efficiency of both individual components as well as the system as a whole. First, a small-scale experiment with air flow rates up to 1000 m³/h has been done at the Orgaworld ZAW facility in Lelystad, Netherlands. Furthermore, a medium-scale experiment up to 10,000 m³/h has been executed in Erembodegem, Belgium.

In both experiments, the measured odour unit concentrations are the leading measurement when determining efficiencies. Although this is a subjective unit, and more objective units such as total Volatile Organic Compounds (VOCs) are available by GC-MS and FID-devices, it still gives the best indication of the functioning of individual components as well as the system. This is because a very small percentage of the VOCs, with an extremely low OTV, will be responsible for the majority of odours produced. After all, waste treatment facilities mostly get their permits based on odour levels - not on total VOCs emitted.

4.1 Odour Testing Results: Lelystad and Erembodegem

The odour results will be presented for both locations. The experiments in Lelystad have been executed around June 2020, testing in Erembodegem took place in October 2020.

4.1.1 Small-Scale: Lelystad

First of all the setup as described in the Methodology section has been executed at the site in Lelystad, with a maximum air flow rate of 1000 m³/h. Although many more experiments have been conducted, the focus for this report lies on the scenarios where external odour measurements are executed. Even this data is too extensive to show, but a more detailed look in the measurement data can be found in Appendix C.2. Still, the data is reduced to increase readability.

The odour tests have been divided over three testing days. Eight scenarios, all executed in duplicate to decrease error margin of odour sampling, resulted in a total of sixteen tests. The results of all these three days have been sorted to the same type of experiment, which are: mixed air with ammonia scrubber and four lamps, tunnel air with scrubber and four lamps, tunnel air with scrubber and two lamps and several scenarios without ammonia scrubber. Results can be found in the table shown in Figure 4.1.

The first column in this figure tells the experiment details and setup, while the second and third column represent the total VOCs values and removal efficiencies per scenario, measured by the FID device. Lastly, the most important columns are the fourth and fifth column, showing the odour unit values and removal efficiencies measured by a licensed external company: Witteveen & Bos.

Experiment setup					FID signal in ppm (avg. of several per experiment)				FID removal efficiencies per stage				Odour results from W&B. Unit = [OUe/m ³]				Odour removal efficiencies per stage			
Test	Day	Air	Scrub	Lamps	L1	L2	L3	L6	Scrub	UV	AC	Total	L1	L2	L3	L6	Scrub	UV	AC	Total
1	Day 1	Tunnel	Yes	4	35	34	29	28	4%	15%	3%	20%	2057	1520	421	75	26%	72%	82%	96%
2	Day 1	Tunnel	Yes	4	41	40	31	28	3%	22%	9%	31%	1915	1083	458	120	43%	58%	74%	94%
3	Day 3	Tunnel	Yes	4	107	101	96	96	6%	5%	0%	11%	6550	5474	4041	1621	16%	26%	60%	75%
4	Day 3	Tunnel	Yes	4	61	57	50	48	6%	13%	5%	22%	5943	6257	2291	2070	-5%	63%	10%	67%
5	Day 1	Tunnel	Yes	2	42	40	31	27	5%	22%	14%	36%	2673	1767	1415	116	34%	20%	92%	96%
6	Day 1	Tunnel	Yes	2	39	40	30	28	-2%	24%	7%	29%	2763	1631	1114	156	41%	32%	86%	94%
7	Day 2	Tunnel	Yes	2	50	55	47	37	-11%	15%	22%	34%	6248	7209	4113		-15%	43%	n.a.	n.a.
8	Day 2	Tunnel	Yes	2	63	64	52	48	-2%	19%	9%	26%	5825	6055	4418		-4%	27%	n.a.	n.a.
9	Day 1	Tunnel	No	2	48		42	34	n.a.	13%	20%	30%			3133		n.a.	n.a.	n.a.	n.a.
10	Day 1	Tunnel	No	2	49		42	34	n.a.	14%	19%	31%			2130		n.a.	n.a.	n.a.	n.a.
11	Day 2	Mixed	No	4	72		65	39	n.a.	9%	41%	46%			15750		n.a.	n.a.	n.a.	n.a.
12	Day 2	Mixed	No	4	75		66	41	n.a.	11%	38%	45%			12688		n.a.	n.a.	n.a.	n.a.
13	Day 2	Mixed	Yes	4	54	49	36	33	9%	27%	8%	38%	6551	7597	4383		-16%	42%	n.a.	n.a.
14	Day 2	Mixed	Yes	4	37	34	27	21	6%	21%	23%	43%	5799	4779	9988	344	18%	-109%	97%	97%
15	Day 3	Mixed	Yes	4	79	61	58	36	23%	6%	37%	54%	11081	24089	11969	7555	-117%	50%	37%	69%
16	Day 3	Mixed	Yes	4	51	45	40	28	11%	12%	31%	46%	10232	26336	10310	6636	-157%	61%	36%	75%

Figure 4.1: Summarised results of Small-Scale odour scenario experiments in Lelystad. The colours represent the severity of odours and FID-signal respectively: green is the cleanest, while red is the worst.

Ozone concentrations are consistently lower for scenarios where the scrubber is being bypassed, compared to similar tests with scrubber. This can be explained by the fact that UV-radiation is required to destroy ammonia molecules, rather than radicalising oxygen atoms to ozone and destroying VOCs directly. In scenarios without scrubber, obviously no odour measurements have been done at L2. Although, in some other tests, no odour measurements have been conducted at L1 and L6 either, in order to save costs. In hindsight, this was a mistake as the FID values differ significantly from earlier tests on the same day. This makes it hardly possible to make any educated assumptions, significantly decreasing the value of the experiments.

In experiments 1 until 4, the results for tunnel air with four UV-lamps are shown. A correlation between odour units measured and the FID signal measured cannot be found. Relatively high UV-reactor removal efficiencies of 72, 58, 26 and 63% are reached in these experiments, which results in an average UV-reactor removal efficiency of 55%. The overall odour removal efficiency is 83% on average.

In experiments 4, 7 and 8 a strange effect is seen. The scrubber actually added odour units in these experiments executed with tunnel air. Several possible causes will be discussed in Chapter 6. In a larger-scale experiment, this is expected not be the case, since the small-scale scrubber used is not on the same engineering-level.

When looking at the same tunnel air flow with half of the UV-power, 2 lamps instead of 4 lamps, the efficiencies change accordingly. The UV-reactor efficiencies of experiments 5 until 8 are 20, 32, 43 and 27% respectively. This results in an average UV-reactor removal efficiency of 31%, compared to 55% for the 4-lamp scenarios. The average overall

removal efficiency is 95%, compared to 83% for the 4-lamp scenario, which is in line with expectations since a fresher active carbon filter is used in these experiments.

When looking at the experiments without scrubber, it becomes more complex, as the number of UV-lamps is not constant and only odour measurements at L3 have been conducted. Furthermore, the input air significantly fluctuates, concluding the FID-measurements. When looking at average inlet concentrations of day 1 and day 2, the UV-reactor seems to add odours in experiments 9 until 12. This is however a false assumption, as the FID values are much higher as well. Unfortunately, these results are rather useless.

Lastly the scenarios where a mixture of field composting air with hall air has been treated. Again the scrubber fulfilled its work of removing ammonia, but it is not supposed to add odours, as it did in experiments 13, 15 and 16. Besides, either a big operational change occurred during the second test, or a supposedly measuring mistake has been made in the second test, where the odour units doubled after the UV-reactor (in contrast to the FID values). An average of 51% UV-removal efficiency has been reached with this scenario, which is the average of 42, 50 and 61% (and therefore ignoring the value -109%).

4.1.2 Medium-Scale: Erembodegem

The small-scale experiment has been repeated on a larger scale, while using a similar design, similar research questions, similar measurement devices and a similar testing scheme. These experiments have been executing in October 2020, with an air flow rate of 10,000 m³/h, thus ten times larger than the small-scale testing in Lelystad. Again, both odour measurements as well as multiple GC-MS analysis have been conducted.

The odour results are presented in the table shown in Figure 4.2. A few remarkable facts can be discovered from the data. During the last measurement with 50 UV-lamps, something unexpected occurs between the scrubber and the UV-box, as odour units first stay the same and then even increase.

More generally speaking, the biofilter on its own usually performs a bit better in terms of removal efficiency compared to the UV-reactor standalone, as can be seen in the table of Figure 4.2. When the biofilter in combination with an acid scrubber is compared to an acid scrubber, UV-reactor and active carbon filter, the UV-installation as a whole just outperforms the biofilter. This will be treated in more detail in Section 4.1.3. In all scenarios except the first test with 40 lamps, the scrubber performs adequate and removes a bit of the odour (or stays similar). The main goal of a scrubber is to remove all ammonia, which it did, as can be seen in detail in Appendix C.

The concentration of ozone left after the UV-reactor, the rest-ozone, tend to decrease only a fairly bit when less UV-power is installed. Therefore the rest-ozone concentration is relatively independent of the amount of lamps, as seen in Appendix C. This is not in line with expectations, as a higher concentration was expected in scenarios with more UV-power. On the other hand, the pressures, temperatures and air flows are fairly constant, which improves the reliability of the results. The values can be found in the appendix.

Concluding, there is no clear relation between the amount of lamps and the removal efficiency. On average, the removal efficiencies turn out to be significantly better in Erembodegem, where the UV-reactor's designed air flow capacity of 10,000 m³/h was used. The comparison of a UV-reactor with a biofilter is treated in the next section.

Experiments	Amount of lamps	30		40		50	
Odour results from Olfascan Unit = [OUe/m ³]	Before scrubber	25912	11207	11219	14842	14384	10229
	After scrubber	17885	11223	19557	13484	11190	10222
	After UV-reactor	5428	5067	6543	8480	5109	12406
	After biofilter	1504	3225	7864	2588	5177	2488
Odour removal efficiencies per stage	Scrubber	31%	0%	-74%	9%	22%	0%
	UV-reactor	70%	55%	67%	37%	54%	-21%
	Biofilter	92%	71%	60%	81%	54%	76%
	TOTAL (with UV)	79%	55%	67%	43%	64%	-21%
	TOTAL (with bio)	94%	71%	60%	83%	64%	76%

Figure 4.2: Summarised results of Medium-Scale odour testing in Erembodegem. Red cells have a more severe odour than green cells.

Next to the chemical analysis conducted in both Lelystad and Erembodegem, also a sensory analysis has been executed. Odour units only tell a part of the story, as this describes the intensity of the odour, not the odour itself. A high strength but nice-smelling odour is much less of a problem than a rotten smell. These sensory measurements are executed by at least a 4-person panel gathered by the Belgian company Olfascan. For all scenarios with 30, 40 and 50 lamps the same sensory analysis is done at all locations, so before the scrubber, after scrubber treatment, after UV-reactor treatment and in parallel to the UV-reactor also after the biofilter. The results can be seen in Table 4.1.

Table 4.1: Sensory odour development for all scenarios in Erembodegem.

Location	Odour description (sensory)
30 UV-lamps	
Before scrubber	(green-)compost, ammonia, hay
After scrubber	organic waste, (green-)compost, dry manure
After UV-reactor	organic waste, hay, ozone (light)
After biofilter	tree bark, woodland
40 UV-lamps	
Before scrubber	(green-)compost, ammonia, hay
After scrubber	organic waste, (green-)compost
After UV-reactor	organic waste, potting soil, ozone (light)
After biofilter	tree bark, woodland
50 UV-lamps	
Before scrubber	(green-)compost, ammonia, hay
After scrubber	(green-)compost
After UV-reactor	vegetable cooking liquid, ozone (strong)
After biofilter	tree bark, woodland

Several remarks can be made about these results. First of all, a confirmation of the sensitivity of the analysis. As it is clear that all inlet air smells similar, based on independent measurements. Furthermore it is interesting that the acid scrubber does not change much about the smell itself, expect for ammonia removal, which it is supposed to do.

The UV-reactor does not change the "type of smell" in two scenarios either, for both 30 and 40 lamps (except the addition of a light ozone smell). In the 50-lamp scenario the actual odour changes from (green-)compost to vegetable cooking liquid and a strong ozone smell. The ozone smell will normally be caught by an active carbon filter, as this was not the case.

Lastly, it is known that biofilters can produce their own distinctive smell. It is usually described as a forest smell, which is in line with the description for all three scenarios: tree bark and woodland-smell. This smell is strongly dependent on the type of wood (chips) used in the biofilter, and the state of the wood as well. A monster has been taken in Erembodegem, and it became clear that this wood was already in the composting phase, therefore producing some odours as well.

4.1.3 Comparison: UV-installation and biofilter

A biofilter is usually the way to go for composting air treatment, as is also the case in Erembodegem. As already seen in the results in Figure 4.2, simultaneous parallel testing has been done on the biofilter installed in Erembodegem. Therefore a fair comparison can be made for a UV-installation and a biofilter. The results can be seen in Figure 4.3.

Since both techniques make use of the same inlet air flow, namely after scrubber treatment, the first two data points in Figure 4.3 are equal. The biofilter with acid scrubber has to be compared to the complete UV-installation for a fair comparison. This means a combination of an acid scrubber, UV-reactor and active carbon filter. Without one of these components, air treatment will not be sufficient. Since there was no active carbon filter present in Erembodegem, the mean removal efficiency has been extracted from the data of Lelystad. Therefore an active carbon odour removal efficiency of 70% is used. This is even expected to be a bit higher, since several oddly low measurements have been taken in Lelystad. Furthermore the average value of two measurements per light-setting (i.e. 30, 40 or 50) has been used to decrease the margin of error. All data is extracted from the table in Figure 4.2.

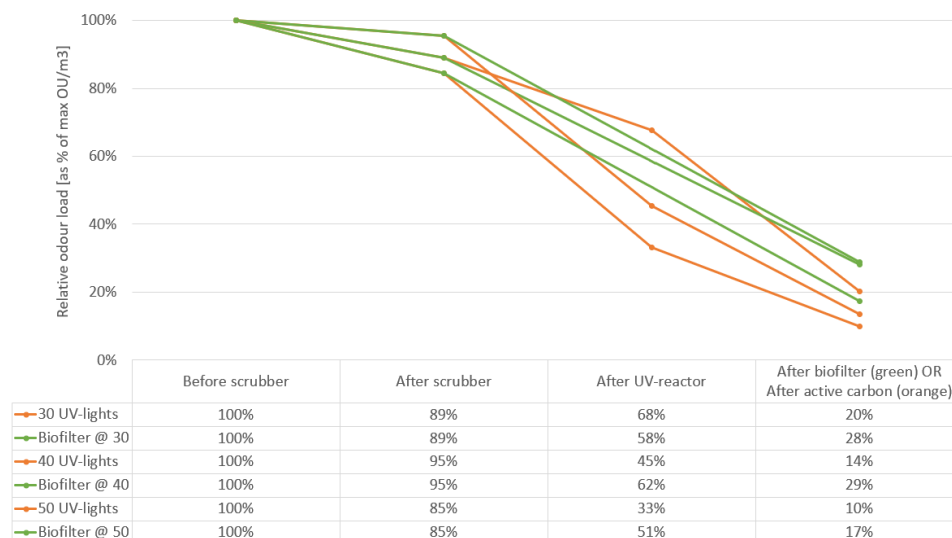


Figure 4.3: Odour removal efficiency comparison between complete UV-installation and biofilter on simultaneous sampled experiments.

To compare different inlet conditions in terms of odour units, a relative scale has been used. The highest odour units measured per experiment is assumed as 100%, which results in the following important assumption. If an increase of odour units over time has been measured, previous measurements are scaled such that the measure before was 100% of the maximum. The partial removal efficiencies of the scrubber and biofilter are relatively constant (shown as parallel, non-crossing lines), whereas the UV-reactor deviates more.

Most noticeable is that the UV-installation has a better total removal efficiency compared to the biofilter. For 30 lights, the odour remaining is 20% and 28% in favour of the UV-installation. With 40 lights this is 14% and 29% and for 50 lights this compares as 10% and 17% remaining odours.

Since the inlet air for both the biofilter system as well as the UV-installation is the air already treated by the acid scrubber, it might make more sense to use the odour values after the scrubber as index number. In Figure 4.4 a similar graph is shown with odour values after the scrubber shown as 100%. Now the real inlet air might have a value higher than 100%.

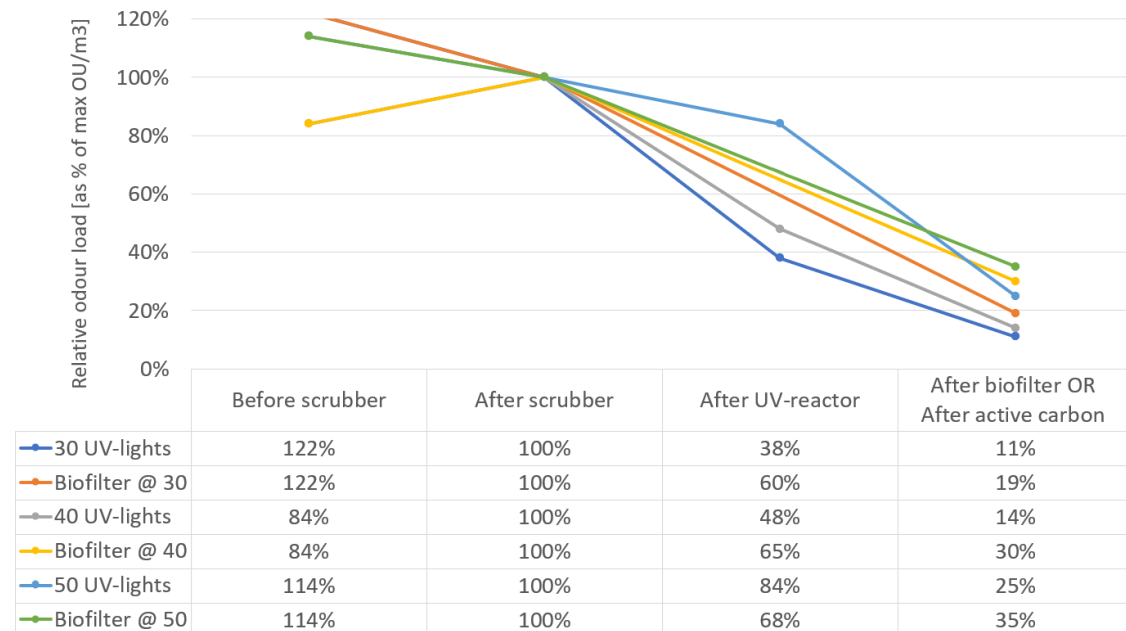


Figure 4.4: Odour removal efficiency comparison with "after scrubber" as index number (100%).

4.2 GC-MS Analysis Results

To make a fair comparison between Lelystad and Erembodegem, GC-MS analysis have been conducted at both locations. This should also help indicate the composting air composition. In Lelystad, four analysis have been conducted in total. All measurements are executed with inlet air, on different days. The first two are accredited measurements by the Dutch company Witteveen & Bos. The last two measurements are done with sorbent tubes, making them less sensible and reliable. In contrast to Lelystad's measurements, GC-MS analysis conducted in Erembodegem are executed simultaneously on different locations in the installation: before the scrubber, after the scrubber and after the UV-installation.

4.2.1 Small-Scale: Lelystad

Several GC-MS analysis have been conducted, in total finding 35 components from 10 different groups of components in Lelystad. The components can be found in white in Figure 4.5, while the groups are indicated in yellow in that same figure. Not all of these are equally important, mainly due to higher and lower Odour Threshold Values (OTV). This is the concentration above which a certain compound can be smelled, as explained in Section 2.1.2. Besides, not each component is equally treatable by either direct or indirect effects of UV: UV-radiation and ozone generated by UV-light.

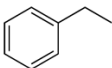
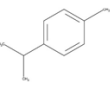
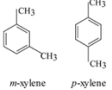
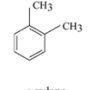
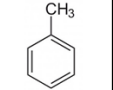
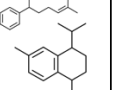
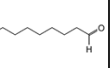
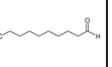
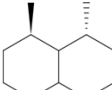
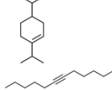
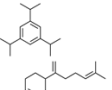
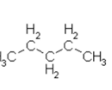
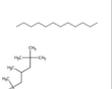
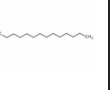
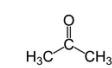
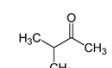
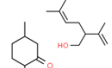
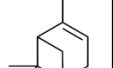
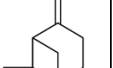
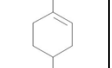
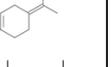
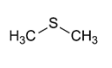
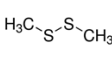
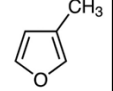
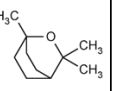
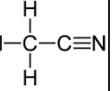
Aromatic carbohydrates							Aldehydes	
benzene	ethylbenzene	p-cymene	m,p-xylene	o-xylene	toluene	C15H22	nonanal	decanal
								
Cyclic carbohydrates				Alifatic carbohydrates				
dimethyl decahydronafta	C12H22	C15H24	C15H28	pentane	dodecane	tridecane	C14 alkanes	C15 alkanes
								
Alcohols		Ketones			Terpenes			
ethanol	acetone	2-butanone	C10H16O	C10H18O	alfa-pinene	beta-pinene	limonene	C10H16
								
Organic sulphuric compounds			Ethers				Organic nitrogen compounds	
dimethylsulfide	dimethyldisulfide	carbondsulfide	furan	2,3-dihydrofuran	3-methylfuran	eucalyptol	acetonitrile	
		$S=C=S$						

Figure 4.5: All thirty five components found while conducting GC-MS analysis on untreated air flows.

Actually, only 10 of these 35 components have a higher concentration than the odour threshold of that component. All the others cannot be smelled. This is shown in Figure 4.6. Unfortunately, there might be compounds with a threshold far below the actual lower measuring limit of the GC-MS analysis. This might result in several compounds contributing heavily to the odour, but not found in the analysis. An example are mercaptans, known for their OTV in the ppt's. The full GC-MS result, including all components under the odour threshold value, can be found in Appendix C.3. Furthermore, there are several compounds where the odour threshold value is unknown or has never been determined before. This means these are not taken into account in Figure 4.6. Possibly there are also interactions between several different compounds present in the air, which may either increase or decrease the odours present in the overall air. As mentioned in the literature research, based on previous literature it was expected that organic sulphuric compounds, terpenes and aldehydes would be the largest and most problematic contributors. Whether these ten largest contributors can be treated by either direct germicidal UV or ozone generated by UV-light molecules is described in Section 4.4.

Sample method	W&B	W&B	Sorbent	Sorbent	Molar	Odour	Odour Activity Value (conc. div. by threshold)				
Sampling date	28-4-2020	28-5-2020	5-6-2020	5-6-2020	mass	Treshold	Ratio of odour threshold divided by GC-MS result.				
Day	Tuesday	Thursday	Friday	Friday	per	per	This gives an indication of the odour "severity".				
Analysis date	7-5-2020	29-5-2020	29-6-2020	29-6-2020	compound	compound	A high number means a large contribution to the				
Type of air	Tunnel	Tunnel	Mixed	Tunnel			odours measured by Witteveen & Bos				
CAS number	Compound	$\mu\text{g}/\text{m}^3$ ⁽¹⁾	$\mu\text{g}/\text{m}^3$ ⁽¹⁾	$\mu\text{g}/\text{m}^3$	$\mu\text{g}/\text{m}^3$	g/mol	$\mu\text{g}/\text{m}^3$	First test	Second test	Third test	Fourth test
Ketones											
-	Σ C10H16O	0	297	0	0	152,23	16	0,00	18,35	0,00	0,00
	Total	0	297	0	0						
Aldehydes											
124-19-6	nonanal	59	0	0	0	142,24	2	29,70	0,00	0,00	0,00
112-31-2	decanal	44	0	0	0	156,2	3	17,06	0,00	0,00	0,00
	Total	102	0	0	0						
Organic sulphuric compounds											
75-18-3	dimethyl sulfide	455	823	0	160	62,14	13	35,84	64,80	0,00	12,59
624-92-0	dimethyl disulfide	0	33	0	0	94,19	8	0,00	3,87	0,00	0,00
75-15-0	carbon disulfide	2428	0	0	0	76,139	654	3,71	0,00	0,00	0,00
	Total	2883	856	0	160						
Ethers											
470-82-6	eucalyptol	0	132	0	0	154,25	7	0,00	19,43	0,00	0,00
	Total	0	132	0	0						
Terpenes											
80-56-8	alfa-pinene	48	198	430	200	136,23	100	0,48	1,97	4,29	1,99
5989-27-5	limonene	681	980	3500	210	136,23	212	3,21	4,63	16,53	0,99
-	Σ C10H16	103	297	0	0	136,23	156	0,66	1,90	0,00	0,00
	Total	832	1475	3930	410						
	Grand total	3817	2761	3930	570						

Figure 4.6: The "problematic" compounds found in the four GC-MS analysis conducted. All others have a concentration below the OTV (or unknown OAV).

4.2.2 Medium-Scale: Erembodegem

Similar GC-MS analysis have been conducted during the testing period in Erembodegem. The major difference with the analysis in Lelystad is that now the measurements are taken simultaneously at different locations in the installation (before scrubber, after scrubber, after UV-reactor). In Lelystad, only the inlet air before the scrubber has been analysed. This gives great insight in the development of VOCs and therefore their treatability. The results can be seen in Figure 4.7. Once again, only compounds with an odour activity value (OAV) above 1 are shown. In case the odour threshold value is unknown due to too little research, the compound is not shown either. If there's an interest in all measured compounds, these can be found in Figure C.4 in Appendix C.3.

When looking at the results, the first thing that comes to mind is the overlap between compounds compared to Lelystad. This makes the results more reliable, as the composition of composting air seems to be fairly constant. There are a few more compounds above the OTV in Erembodegem, for instance 3-methyl-1-butanol, 2,3-butadion and hexanal. From this GC-MS analysis can be concluded that some groups are removed efficiently by the UV-reactor, such as terpenes, organic sulphuric compounds and to a lesser extent ethers and ketones. Contrary, some groups increase over the UV-reactor, such as aldehydes and alcohols. A very similar appearance is seen for the scrubber. The acid scrubber removes ammonia efficiently, not shown in this figure, but known from previous sections. In this figure can be seen that nearly all compounds from alcohols, ketones, aldehydes, OSCs, ethers and terpenes increase over the course of the acid scrubber. Some compounds increase significantly, such as DMDS, limonene or eucalyptol. Others decrease or increase just a bit, such as alfa-pinene or DMS. It is important to keep in mind that the odour perception per compound varies extremely. The odour perception of individual important compounds can be found in Appendix C.1 in order to increase readability. For instance, aldehydes usually have a much more pleasant smell than sulphuric compounds.

Project Sampling date Description CAS number Compound	Erembodeg	Erembodeg	Erembodeg	Molar	Odor	Odor Activity Value (conc. div. by threshold)		
	15-10-2020	15-10-2020	15-10-2020	mass	Threshold	Ratio of odor threshold divided by GC-MS result		
	Inlet air	After scrubber	After UV	per compound	per compound	This gives an indication of the odour "severity"		
	$\mu\text{g}/\text{m}^3$	$\mu\text{g}/\text{m}^3$	$\mu\text{g}/\text{m}^3$	g/mol	$\mu\text{g}/\text{m}^3$	Inlet air	After scrubber	After UV
Alcohols								
64-17-5 ethanol	1413	3213	15003	46,07	980	1,44	3,28	15,31
3-methyl-1-butanol	11	58	52	88,148	6	1,83	9,67	8,67
Total	1424	3271	15055					
Ketones								
431-03-8 2,3-butadion	0	15	15	86,089	0,18	0,00	83,33	83,33
- $\Sigma \text{C}_{10}\text{H}_{16}\text{O}$	0	32	0	152,23	16	0,00	1,98	0,00
Total	0	47	15					
Aldehydes								
124-19-6 nonanal	9	0	386	142,24	2	4,55	0,00	195,15
112-31-2 decanal	8	0	12	156,2	3	3,13	0,00	4,70
2-methylpropanal	23	119	112	72,11	1	23,00	119,00	112,00
3-methylbutanal	50	265	197	86,13	0,36	138,89	736,11	547,22
hexanal	2	0	30	100,16	1	2,00	0,00	30,00
octanal	0	0	53	128,21	0,05	0,00	0,00	1060,00
Total	92	384	790					
Organic sulphuric compounds								
75-18-3 dimethyl sulfide (DMS)	118	259	178	62,14	13	9,29	20,38	14,01
624-92-0 dimethyl disulfide (DMDS)	8	55	8	94,19	8	0,94	6,49	0,94
Total	126	314	186					
Ethers								
470-82-6 eucalyptol	67	231	203	154,25	7	9,84	33,92	29,81
Total	67	231	203					
Terpenes								
80-56-8 alfa-pinene	124	363	27	136,23	100	1,24	3,62	0,27
127-91-3 beta-pinene	55	172	49	136,23	131	0,42	1,32	0,38
5989-27-5 limonene	1657	5073	5	136,23	212	7,83	23,96	0,02
- $\Sigma \text{C}_{10}\text{H}_{16}$	260	863	35	136,23	156	1,67	5,53	0,22
Total	2096	6471	116					
Grand total	3805	10718	16365					

Figure 4.7: Major compounds found in GC-MS analysis conducted in Erembodegem. Measured simultaneously at different locations in the installation.

4.3 Ozone Generation and Depletion

In order to gain insight in the systems' capabilities of ozone generation, experiments have been conducted in Lelystad with fresh hall air suction and different amount of UV-lamps turned on. For this test, the air velocity measured in 160 mm diameter duct-work turned out to be 10.2 m/s on average, corresponding to an air flow rate of 738 m³/h. Together with the molecular weight of ozone being 48 g/mole and assuming an ideal gas with the constant 24.45 L/mole for ideal gases, the ozone load can be calculated. The ozone generation levels, ozone load and energy can be found in Table 4.2. Each scenario has been repeated several times and is measured directly after the UV-reactor. Note that the bottom row is expected to be approximately constant, if the ozone generation measured in ppm is linear, which is approximately the case.

After the Ozone generation, it flows through the system and ends in the afterburner. To get insight in the decrease of ozone - and hopefully in FID signal as well, ozone and FID tests have been conducted in multiple afterburner locations as can be seen in Table 4.3. L1, L2, L3 and L6 refer to the explanation in figure 3.2, while 0, 4, 8 and 12 meters refer to the location in the afterburner.

Table 4.2: *Ozone generation levels with clean inlet air and a varying number of lamps turned on.*

Amount of (145W) lamps	unit	0	2	4	6	8	10
Ozone generation	[ppm]	0.0	1.2	1.8	2.7	4.2	4.8
Ozone generation	[mg/m ³]	0.0	2.4	3.5	5.3	8.2	9.4
Ozone load @ 738 m ³ /h	[mg/h]	0	1739	2608	3912	6085	6954
Ozone per energy	[g/kWh]	n.a.	5.99	4.50	4.50	5.25	4.80

Table 4.3: *Ozone depletion through the afterburner, including measured FID values, with four (4·145W) UV-lamps using tunnel air.*

Location	(a f t e r b u r n e r)							
	L1	L2	L3	0 m	4 m	8 m	12 m	L6
Ozone conc. (ppm)	0.00	0.00	1.44	1.26	1.10	1.00	0.98	0.00
FID signal (ppm)	62	59	48	48	46	44	42	24

4.4 Treatability of Composting Air Pollutants

As a result of the testing executed in both Lelystad and Erembodegem, a list of problematic contributors to the odour is known. It is important to know whether these components can be treated using either the ozone generated by the 185 nm wavelength UV or directly by the germicidal UV wavelength of 254 nm. Another option is biological treatment using a bio(trickling)filter as described in Section 2.3.2.

Table 4.4: *Treatability of the most severe (airborne) components: by UV-radiation, ozonization or biologically with a biofilter.*

Compound	Destructible by ...		
	direct UV-radiation	ozone (by UV)	biologically
nonanal	no	no [17, 26, 40]	yes [3]
decanal	no	no [17, 26, 40]	yes [3]
dimethyl sulfide	unknown	yes [15]	yes [4]
dimethyl disulfide	unknown	yes [43]	yes [4, 21]
carbon disulfide	yes [11]	no [11]	yes [4, 20]
alfa-pinene	yes [23, 50]	yes [50]	moderate [3]
limonene	yes [49]	yes [49]	moderate [3]

In Table 4.4, seven components can be seen which were found in the GC-MS analysis of Lelystad (More specific information in Figure 4.6 in Section 4.2.1) with a concentration at least as high as the OTV of that specific component. The first two compounds listed, the aldehydes nonanal and decanal, are special. It seems to be that these compounds are actually generated as products of the ozonation [17, 26, 40]. Although present with relatively high Odour Activity Values (OAV), these compounds do not have a severe smell and are often being used in some perfumes for instance. Dimethyl sulfide (DMS) and dimethyl disulfide (DMDS) are severe but easily treated with ozone, and therefore can be neutralised with this technology [15, 43]. Another organic sulphuric compound is carbon disulfide, which has a severe smell. According to other research, this compound is not treatable by either direct UV-radiation or ozone [11]. Luckily, this compound was only measured once, and with a relatively low OAV, while it has a high OTV. This means the

smell will fade away with a few dilutions in outside air by the definition of odour units. Then the terpenes alfa-pinene and limonene remain, which are both treatable by either direct UV-radiation or ozone reactions, making them easy to remove [23, 49, 50].

Biologically, so either by a bio-trickling filter or a traditional biofilter, most of the components are removable as well [3, 4, 20, 21]. Terpenes however are harder to remove. Next to that, as described in Section 2.3.2, bio(trickling)filters have difficulties with fluctuating air flows, temperatures and VOC concentrations.

Once again, many more compounds are possibly present in other air samples, requiring additional treatability research. One type of compound that has not been measured, but is known to be present with a low OTV in composting air, are mercaptans. Previous research shows that mercaptans in general have a high treatability of both direct UV-radiation as well as ozone treatment [53].

Chapter 5

Mathematical Reactor Modelling

Accurate modelling of photo-chemical reactors is extremely difficult due to complex reaction kinetics and light intensity gradients caused by light dispersion, reflection, absorption and shadowing. In this section two basic reactor-design models are described, where the focus lies on the removal of two major VOC-compounds.

Roughly seen there are these two earlier mentioned basic theoretical approaches to simple reactors. The Continuously Stirred Tank Reactor (CSTR) and the Plug Flow Reactor (PFR). Both are hard to be approached in real life, although they still give a representation of the approximate truth, which will be further elaborated later.

A Continuously Stirred Tank Reactor is an ideal reactor, simplified this means that everywhere inside the tank, the same concentration is assumed to be present. Therefore the outlet conditions are identical as the conditions inside the CSTR. It is assumed to be a steady state process. A Plug Flow Reactor on the other hand, assumes no mixing at all. It has an either increasing or decreasing concentration along the whole reactor. To make calculations, very thin slices with width dx are assumed to have the same concentration. The neighbour-slice on the left has a lower concentration, whereas the right-slice has a higher concentration. Especially the PFR will be explained in more detail in its corresponding Section 5.1, and the CSTR is treated in Appendix F. Both share similar main equations, and will be explained below. For schematic overviews, see Figures 5.1 and 5.2.

To make a theoretical reactor more suitable for this thesis' purpose, two major VOC-compounds regularly present in composting air are examined taking these reactors into consideration. These originate from two different compound-groups (organic sulphuric compounds and terpenes) and seem to be a fair representation of the major odour cause. Especially if the concentrations are scaled to the total measured concentrations. The advantage is that it is not necessary to model hundreds of compounds.

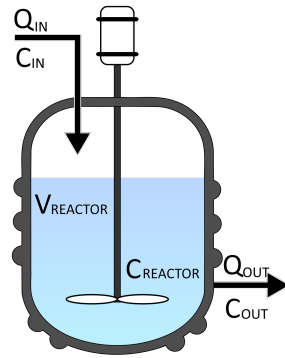


Figure 5.1:
Schematically shown CSTR.

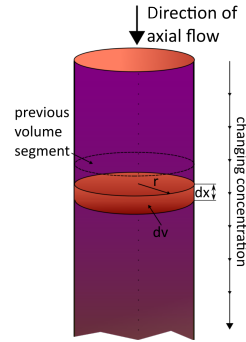


Figure 5.2:
Schematically shown Plug Flow Reactor.

The starting point of the derivation of these reactors is the Arrhenius equation, as shown in Eq. 5.1. In this equation, k is the rate constant, with unit dependent on reaction order, E_a is the activation energy, T is the temperature in K, R is the ideal-gas constant: $8.314 \frac{J}{\text{mol}\cdot K}$ and A is known as the frequency or pre-exponential factor [19]. The value for k is often also experimentally determined.

$$k = Ae^{\frac{-E_a}{RT}} \quad (5.1)$$

The reaction rate r is then defined using the power law expression as seen in Eq. 5.2.

$$r = \underbrace{Ae^{\frac{-E_a}{RT}}}_{\text{Kinetic factor}} \cdot \underbrace{\prod C_i^{\beta_i}}_{\text{Driving force}} \quad (5.2)$$

The overall molar balance can be seen in Eq. 5.3, although it is suitable for one component as well. Since the topic is a reactor, there will be production, i.e. $\text{PROD} \neq 0$. Furthermore, it is a steady-state process, and therefore accumulation is equal to zero: $\text{ACC} = 0$. All calculations start with this molar balance [27].

$$\text{accumulation} = \text{in} - \text{out} + \text{production} \quad (5.3)$$

A few often used quantities are described with their units: V is the volume with unit $[\text{m}^3]$, C is the concentration with unit $[\text{mol}/\text{m}^3]$, Q is the air flow rate with unit $[\text{m}^3/\text{s}]$ and τ is the residence time in seconds and can be calculated with the previous quantities: $\frac{V}{Q}$. The same is true for "in" and "out" of Eq. 5.3, since they can be calculated as $Q \cdot C$ with the unit $[\text{mol}/\text{s}]$. Lastly, the production is calculated as $V \cdot \nu \cdot r$ with the unit $[\text{m}^3 \cdot \text{mol}/(\text{m}^3 \cdot \text{s})]$ or $[\text{mol}/\text{s}]$.

The major characteristics as well as similarities and differences between the two types of reactors are shown in Table 5.1. The most important assumption both reactors share within this chapter is the constant-density-assumption. This is a realistic assumption for this case, generally there are little temperature and pressure changes after the UV-reactor. This assumption simplifies the calculations significantly.

Table 5.1: *Continuous Stirred Tank Reactor versus Plug Flow Reactor.*

	CSTR	PFR
Assume	Steady-state operation Equal conditions through reactor Outlet conditions are equal to reactor conditions	One-dimensional (axial) flow Flow is independent of r and φ No (back)mixing, stationary operation
Pros	Simplicity of the reactor Copes with two-phase reactions Easily controllable (e.g. temp, concentration, volume flow)	No moving parts, so extremely simple Accurate approach for gas-phase reactions Lower volume required for same conversion rate
Cons	Lowest conversion per unit volume Uneven concentration distribution Fluctuations in residence time	Limited transfer of heat Problematic in case of high viscosity/low velocity

5.1 Plug Flow Reactor

The reaction $A \rightarrow B$ is considered for the derivation of a plug flow reactor. Recall Equation 5.3, so $\text{ACC.} = \text{IN} - \text{OUT} + \text{PROD}$. The derivation for a plug flow reactor starts with the change of concentration through a very small slice of the reactor, dx as seen in Figure 5.2. Φ_V is the (constant) flow velocity, dV is the change of volume, r_A is the rate of compound A, defined as $r_A = \nu_A \cdot r$ and $C_{A,x}$ is the concentration of A at location x , where location 0 is the inlet concentration. The following equation is obtained.

$$\underbrace{\Phi_V C_{A,x} - \Phi_V C_{A,x+dx}}_{\Delta A \text{ from } x \text{ to } x+dx} + (r_A)dV = 0 \quad \Rightarrow \quad \Phi_V (C_{A,x+dx} - C_{A,x}) = (r_A) dV \quad (5.4)$$

Now τ is defined as $\frac{V_R}{\Phi_V}$, which is equal to dV and $\Phi_V d\tau$. This means the right side of Eq. 5.4 can be rewritten as $(r_A)dV = (r_A)\Phi_V d\tau$. This is equal to $(-r)\Phi_V d\tau$, since ν_A is -1 for the reaction $A \rightarrow B$. When rewriting the left-hand side as $\Phi_V(dC_A)$, equation 5.5 follows.

$$\Phi_V dC_A = (-r)\Phi_V d\tau \quad \rightarrow \quad \frac{dC_A}{-r} = d\tau \quad \rightarrow \quad \int_{C_{A,0}}^{C_A} \frac{dC_A}{-r} = \int_0^\tau d\tau \quad (5.5)$$

Then, from the definition of τ mentioned above, the following equation is obtained, where the time τ can be derived.

$$\tau = \frac{V_R}{\Phi_V} = \int_{C_{A,0}}^{C_A} \frac{dC_A}{-r} = \int_{C_{A,0}}^{C_A} \frac{dC_A}{r_A} \quad (5.6)$$

For a first order reaction, i.e. $r_A = -kC_A$, the final expression for τ can be seen in Eq. 5.7.

$$\tau = \int_{C_{A,0}}^{C_A} \frac{dC_A}{-kC_A} = \frac{-1}{k} \int_{C_{A,0}}^{C_A} \frac{dC_A}{C_A} = \frac{-1}{k} [\ln(C_A)]_{C_{A,0}}^{C_A} = \frac{1}{k} \ln\left(\frac{C_{A,0}}{C_A}\right) \quad (5.7)$$

For a second order reaction, i.e. $r_A = -kC_A^2$, a similar derivation is made. The result can be seen in Eq. 5.8.

$$\tau = \int_{C_{A,0}}^{C_A} \frac{dC_A}{-kC_A^2} \quad \rightarrow \quad \tau = \frac{1}{k} \int_{C_{A,0}}^{C_A} \frac{dC_A}{-C_A^2} = \frac{1}{k} \left[\frac{1}{C_A} \right]_{C_{A,0}}^{C_A} = \frac{1}{k} \left(\frac{1}{C_A} - \frac{1}{C_{A,0}} \right) \quad (5.8)$$

And lastly, the same can be done for a third order reaction in a plug flow reaction, where $r_A = -kC_A^3$. This actually yields for all further integer reaction orders, as shown in Table 5.2.

$$\tau = \frac{1}{k} \int_{C_{A,0}}^{C_A} \frac{dC_A}{-C_A^3} = \frac{1}{k} \int_{C_{A,0}}^{C_A} \frac{dC_A}{-C_A^3} = \frac{1}{2k} \left[\frac{1}{C_A^2} \right]_{C_{A,0}}^{C_A} = \frac{1}{2k} \left(\frac{1}{C_A^2} - \frac{1}{C_{A,0}^2} \right) \quad (5.9)$$

The results of the derivation of this section are summarised in Table 5.2. Similar CSTR derivations have been done and can be found in Appendix F, the results are shown in the table as well.

Table 5.2: Results of PFR and CSTR derivations for several reaction orders.

Reactor	1st order	2nd order	n-th order
CSTR	$C_{A,in} - C_{A,out} = k\tau C_{A,out}$	$C_{A,in} - C_{A,out} = k\tau C_{A,out}^2$	$C_{A,in} - C_{A,out} = k\tau C_{A,out}^n$
PFR	$\tau = \frac{1}{k} \ln \left(\frac{C_{A,0}}{C_A} \right)$	$\tau = \frac{1}{k} \left(\frac{1}{C_A} - \frac{1}{C_{A,0}} \right)$	$\tau = \frac{1}{n \cdot k} \left(\frac{1}{C_A^n} - \frac{1}{C_{A,0}^n} \right)$

5.2 Modelling the UV-technique

To make such a theoretical reactor type more suitable for the purpose of this thesis, two of the major VOC-compounds are chosen to model. These VOCs are dimethyl sulfide and alpha-pinene, they represent the two most important VOC-groups. They are regularly present in composting air and have a very different reaction speed. This is also the case for various other VOCs, which are not modelled specifically, but the initial concentration will be matched by a scaling-factor x to create a fair reflection of the reality. Both are examined taking the plug flow reactor into consideration. The main goal of this model is to be able to predict more accurately what will happen in case of for instance: a higher air flow, higher or lower initial conditions and/or in combination with more or less UV-lamps.

Depending on the scenario considered, the PFR or CSTR might be more suitable. If the UV-reactor operates on over-pressure, the piping or duct-work after the UV-reactor can accurately be simulated as a Plug Flow Reactor, since the both the concentration of ozone as well as the concentration of the VOC examined will drop over time with a certain reaction speed. On the other hand, in case the UV-reactor operates on under-pressure, this means there will be a fan placed behind it. This fan then causes extreme turbulence, which might be simulated by the CSTR-assumption that everything is mixed perfectly at $t = 0$. This is however a bit unrealistic, but its derivation can be seen in Appendix F.

For this chapter, a combination of two Plug Flow Reactors is considered. One for the UV-reactor, and one for the ductwork behind it. In the UV-reactor-PFR, first the oxygen radical concentration increases according to the PFR-reaction mechanism, followed by the ozone concentration. During this small period of time, also the VOC concentrations drop a little bit. This reaction rate will be relatively low, since it is a function of the ozone concentration. In the ductwork-PFR, similar equations occur, but the oxygen radical forming will stop, due to the absence of UV-power. The remaining oxygen radicals will react with oxygen molecules to form the final bit of ozone, while VOC concentrations will decrease according to the PFR-reaction mechanism derived earlier. A schematic overview can be seen in Figure 5.3. The reaction rates and kinetic pre-factors k_i of oxygen radicals, ozone and the VOCs can be conducted either from the experiments executed or found in literature. These values should match in the case of similar testing conditions.

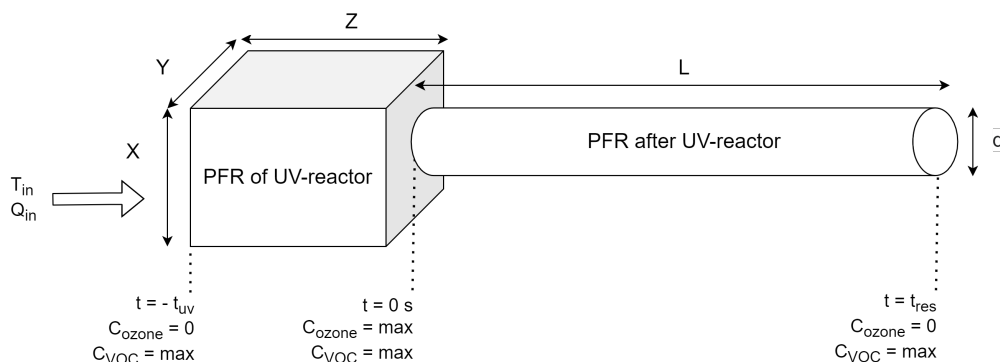


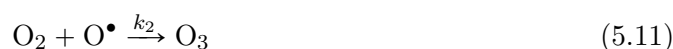
Figure 5.3: A combination of two PFR's to simulate the UV-installation.

The functions derived in Section 5.1 and Appendix F have the residence time τ as input, although τ is actually a function of the installation design. Therefore the final equation will be extended in the model. The input will be the reactor volume, a box with dimensions X [m], Y [m] and Z [m] for the UV reactor, and a straight pipe with length L [m] and diameter d [m]. When this is divided by the reactor air flow rate per second, the residence time τ is found accordingly: $\tau = \frac{V}{Q} = \frac{L \cdot (d/2)^2}{Q}$ or $\tau = \frac{X \cdot Y \cdot Z}{Q}$.

The chemical reactions used for this model, mentioned in the upcoming section, all have their own reaction orders and rates. The reaction orders and rates can be found the National Institute of Standards and Technology (NIST) database [1]. This reaction rate is influenced by two characteristics, also shown in Eq. 5.2. The first is the constant kinetic pre-factor k_i with a unit based on the reaction order. This k_i does not change and determines the reaction rate with the driving force of a reaction: the compound concentrations before on the left-hand side of the equations. Depending on the reaction order, these concentrations might be to the power 2, 3, etc. Since the concentrations are changing throughout the reaction, this means also the reaction rate changes. Therefore the calculation has to be done over and over again for a certain number of steps. It becomes an Ordinary Differential Equation (ODE), which is being solved by the ODE45-command in the program MatLab. The model itself is treated in much more detail in Appendix G, where all steps are explained.

5.2.1 Ozone Generation Modelling

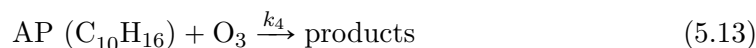
The formation of ozone in the UV-reactor occurs in two steps, according to Equations 5.10 and 5.11, which are second and third order reactions respectively. The principle of ozone generation is already explained earlier in Section 2.3.3, and the amount of ozone generation is calculated in Section 4.3 based on measurements and corresponding retention times executed with clean air. In Appendix G this is further extended. Oxygen molecules split into two atomic oxygen radicals. Then these radicals combine with another oxygen molecule to form ozone, as shown in the equations below.



The oxygen concentration in air is high compared to the concentrations of oxygen radicals and ozone that are generated. The pre-kinetic factor k_1 is determined empirically, just as k_2 . The first equation will develop rather linear, since the kinetic pre-factor and the reaction rate are constant, due to the constant driving force (C_{O_2}). The second reaction rate however, will be determined by both the constant oxygen concentration as well as the increasing radical concentration, and therefore increase over time until it reaches $t = 0$. Then the remaining oxygen radical concentration will react to ozone. In the UV-reactor, from $-t_{UV}$ to $t = 0$, the oxygen concentration will drop quickly, after leaving the UV-reactor it will still decrease due to reaction 5.11, but much slower. In the ductwork, ozone will see its concentration decreasing due to the reactions with VOCs, as is explained in the coming section.

5.2.2 VOC and Ozone Depletion Modelling

Then the second plug flow reactor, representing the ductwork behind the UV-reactor. The initial concentrations for this PFR are the final concentrations of the UV-PFR. This means there will be oxygen radicals present, which can form with oxygen to ozone according to reaction 5.11. Overall ozone concentration will however decrease over time, since it will react with all kinds of VOCs, amongst which dimethyl sulfide and alpha-pinene as shown in Equations 5.12 and 5.13, both second order reactions. The products are not of interest for the modelling, as the reaction rate is only determined by concentrations left of the arrow. This yields under the assumption that it is a one-way reaction. When considering odour reduction, the actual product can be of interest though. Pre-kinetic factors k_3 and k_4 are determined experimentally, and are the driving forces together with the AP-, DMS- and O_3 -concentrations.



As both reactions are second order reactions, the course of the graph will be comparable. One graph might be steeper due to a higher reaction rate, caused by a higher kinetic pre-factor or higher initial compound concentrations. The initial concentrations will be scaled by a factor x in the model, to represent the amount of total VOCs present in the air. This is of course assuming that the reaction of Eq. 5.12 and 5.13 are representative for the total VOC composition. This scaling is done on a molar basis. As an example, the molar mass of the total VOCs from Erembodegen's GC-MS analysis after the scrubber is 17.5 times higher than the sum of molar masses of DMS and AP. This will be the scaling-factor x in this case.

5.3 Modelling Examples: Several Scenarios

The whole model is explained in more detail in Appendix G, in this section, only the methodology and results are discussed. The model can be used for an infinite number of cases, of course. For the sake of getting insight, three cases are featured in this section. First the 50-lamp scenario in Erembodegem is modelled, also to verify and calibrate the pre-kinetic factors. Also a case with a higher air flow is considered, which could be used for future use of WTT in large-scale installation. Furthermore a case where the initial concentrations are a factor higher than in the first two cases. Results are described in the corresponding sections.

5.3.1 Erembodegem Case

To begin with, the model has been put into use for a well-known case, in the first place for calibration of the kinetic pre-factors k_i . The Erembodegem experiments had an air flow of 10,000 m³/h, with the standard UV-reactor dimensions X, Y and Z of 1.50, 0.65 and 0.85 meter respectively (referring to Figure 5.3). The first two will remain constant, but the Z-dimension depends on the amount of lamps installed, n . The air will be in the UV-reactor for about 0.3 seconds, exposed to 50 UV-lamps. A fair retention time τ of 6.87 in the ductwork is reached with a diameter of Ø900 mm and a length of 30 meters. The initial molar VOC concentrations are 17.5 times as high as the molar concentrations of alpha-pinene and dimethyl sulfide together. This is all summarised in Table 5.3.

Table 5.3: Model input of the "standard" case, dimensions refer to Figure 5.3.

Residence time		Dimensions			Model characteristics		
UV-reactor [s]	Ductwork [s]	Z [m]	d [m]	L [m]	n [#]	x [-]	Q [m ³ /h]
0.298	6.87	0.85	0.90	30	50	17.50	10,000

The results of the "standard" case in Erembodegem with 50 lamps can be seen in Figure 5.4. The right plots in the figure show the full picture: UV-reactor and ductwork. The top shows oxygen radicals and ozone molecules. The bottom shows VOC concentrations. The left part in the plot presents a detailed view on all concentrations in the UV-reactor. As can be seen in the figure, the results are fairly perfect, since the rest-ozone concentration is very little at the end of the ductwork. The DMS-concentration is less than a quarter at the end, compared to the inlet concentration. Terpenes are completely removed already after 2 seconds.

Recall that the initial concentrations of these compounds are much higher than in reality, they are scaled to represent the whole spectrum of VOCs. If this would not have been done, the ozone concentration is much too high for the removal capacity it requires, and a lot of rest-ozone would remain.

All these concentrations along the whole time-spectrum can be seen in Figure 5.6 to be able to compare actual concentrations. Besides, the conversion rate of all compounds is shown in Figure 5.5. The terpenes are around 1 (or 100%) rather quickly, but the DMS conversion is caught up by the ozone conversion, meaning there is just a bit too little ozone present to remove everything in the ductwork.

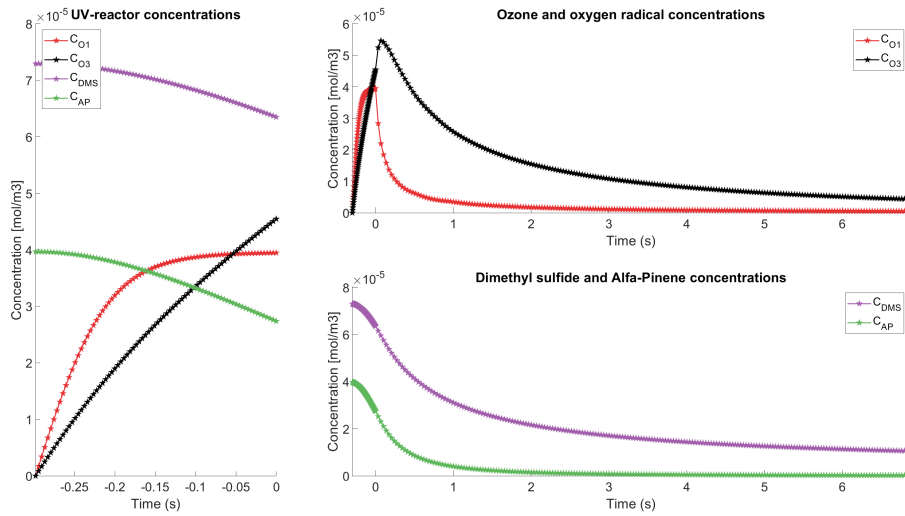


Figure 5.4: Concentrations of multiple compounds for the first case.

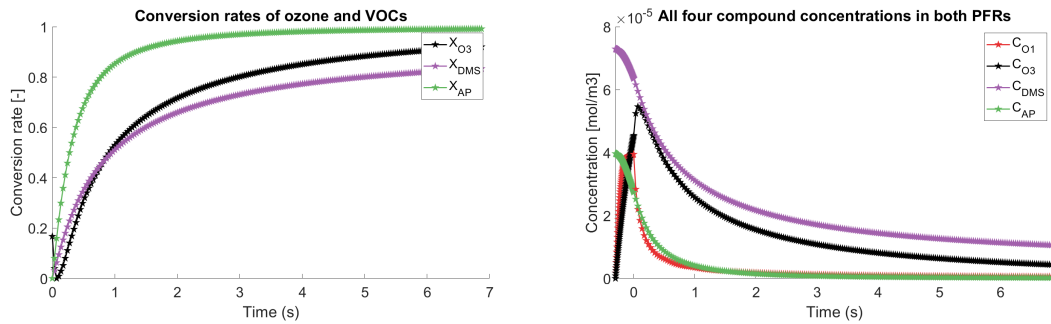


Figure 5.5: Conversion rates for the first case.

Figure 5.6: All plots of Figure 5.4 into one figure.

5.3.2 High Initial Concentrations Case

In order to show the effect of changing air inlet, a case can be imagined where the inlet concentrations are 2.5 times as high as the concentrations earlier. This means the value of x changes from 17.5 to 44. The rest is kept similar, so the retention times do not change, since the dimensions of both the UV-reactor as well as ductwork do not change. This makes sense, since the amount of lamps and also the air flow are kept similar at 50 lamps for 10,000 m³/h.

Table 5.4: Model characteristics of the high inlet concentration case.

Residence time		Dimensions			Model characteristics		
UV-reactor [s]	Ductwork [s]	Z [m]	d [m]	L [m]	n [#]	x [-]	Q [m ³ /h]
0.298	6.87	0.85	0.90	30	50	44.00	10,000

The layout of figures is similar to the case earlier, so a split plot per compound and a detailed view on the UV-reactor is given in Figure 5.7. The results of the Figure nearly speak for itself. The initial drop of VOC concentrations is actually fairly similar to those seen in Figure 5.4, but this decrease stagnates after only half a second or so. This is

definitely caused by the fact that the ozone concentration is insufficient to react with all VOCs. It can also clearly be seen that after $t = 0$, the remaining oxygen radical concentration is completely used to form ozone. After this concentration reached 0 as well, no more ozone is produced.

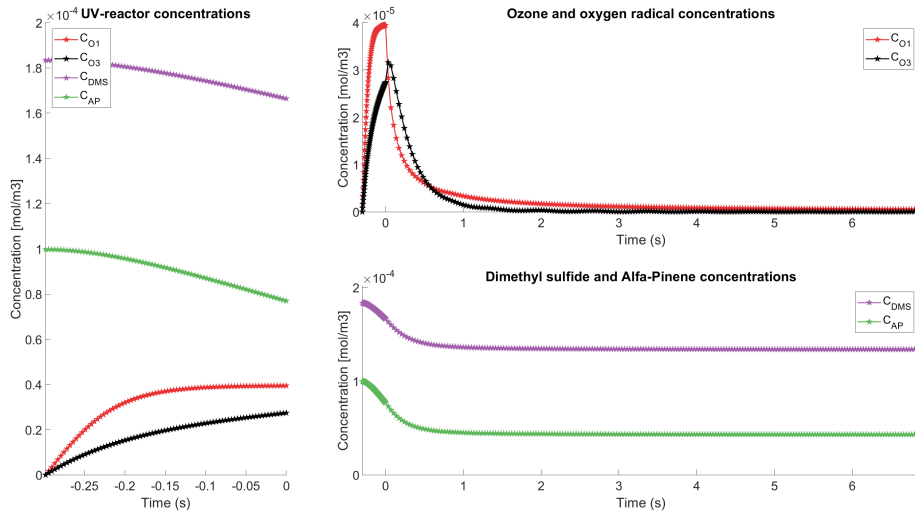


Figure 5.7: Concentrations of multiple compounds for the high load case.

A similar phenomenon can be concluded from Figure 5.8, where the conversion rates are shown. The ozone concentrations reach 100% conversion in a way too early stage, causing the conversion of alpha pinene and dimethyl sulfide to stagnate a bit above 40% and a bit below 20% respectively. From Figure 5.9 can be concluded that the the representative VOC concentrations are factors higher than either oxygen radicals or ozone concentrations.

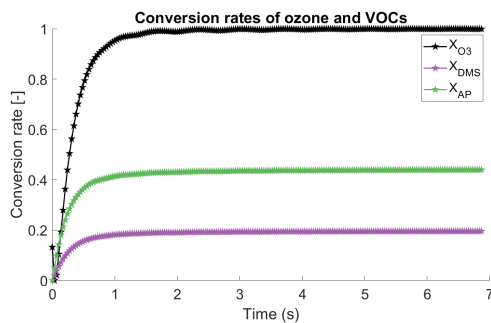


Figure 5.8: Conversion rates for the high load case.

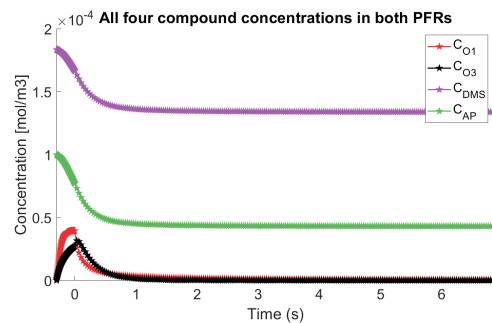


Figure 5.9: All plots of Figure 5.7 into one figure.

5.3.3 Higher Air Flow Case

To show the versatility of the model, a case for possible future use is shown with a higher air flow. Of course, many other options are possible. For this specific case, an air flow of $50,000 \text{ m}^3/\text{h}$ is considered, that is five times as high as the two previous cases. Therefore also the length and diameter of the ductwork had to be adapted, and these are now 50 meters with a diameter of 1.5 meter. The VOC concentration at inlet however, is chosen to be half the initial concentration of the "standard" case. Therefore the value of scaling-factor x is now 8.75 in stead of 17.50. To be sure that this air flow can be treated, a margin to be on the safe side has been used for the UV lamps. This means there is now three times the power, 150 lamps in stead of 50.

Table 5.5: Model characteristics of the high air flow case.

Residence time		Dimensions			Model characteristics		
UV-reactor [s]	Ductwork [s]	Z [m]	d [m]	L [m]	n [#]	x [-]	Q [m^3/h]
0.181	6.36	2.55	1.5	50	150	8.75	50,000

The effect of a bit of over-power can directly be seen in the right-top plot of Figure 5.10, since the rest-ozone concentration remains approximately $2.5\text{E-}05 \text{ mol}/\text{m}^3$. This is caused by the fact that terpenes (represented by alpha-pinene) is removed after around two seconds, while the organic sulphuric compounds (represented by dimethyl sulfide) are also almost completely vanished after the residence time in the ductwork. All oxygen radicals are used up by that time as well, therefore the ozone concentration does not increase anymore.

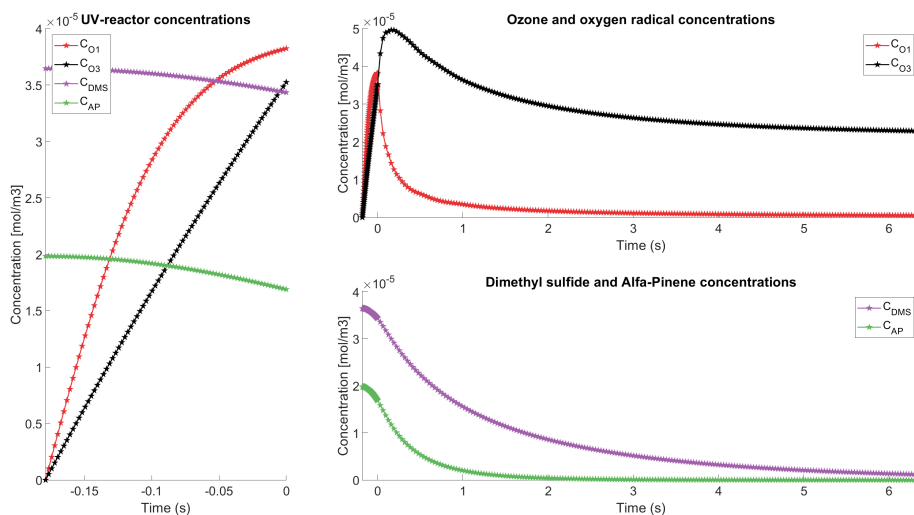


Figure 5.10: Concentrations of multiple compounds for the high air flow case.

A very similar story can be concluded from Figure 5.11 as well. The conversion rates of the VOCs both approach 1 after a certain amount of time. Only half of the ozone is converted at the end of the ductwork, since there are insufficient VOCs to react with. This conversion corresponds to approximately $2.5\text{E-}05 \text{ mol}/\text{m}^3$ at the end of the ductwork, as seen in Figure 5.12.

As mentioned earlier in Section 2.3.3, this rest-ozone will decay after a certain amount of time, in the order of magnitude of seconds to minutes maximum. This rest-ozone concentration is however not unimportant. Only one ppm of ozone has an odour value of around 600 OU/m^3 . This value might differ a bit on the literature it is found in. To remain in the units of the figures, 1 ppm of ozone is approximately $4.1\text{E-}05 \text{ mol/m}^3$, which is approximately 1.6 times as high as the rest-ozone concentration in this case. If even more rest-ozone is caused by a more over-powered installation, this might seriously influence odour measurements. Luckily it can relatively easily be solved by an active carbon filter, absorbing ozone molecules (or thereby reaction with earlier caught VOCs, as explained in Section 2.3.4).

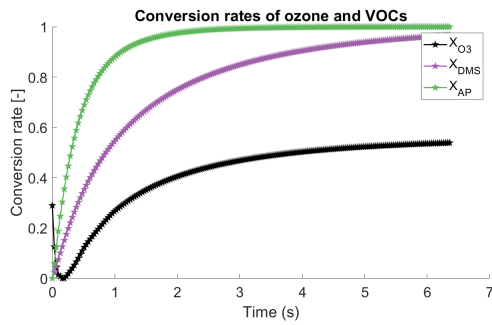


Figure 5.11: Conversion rates for high air flow case.

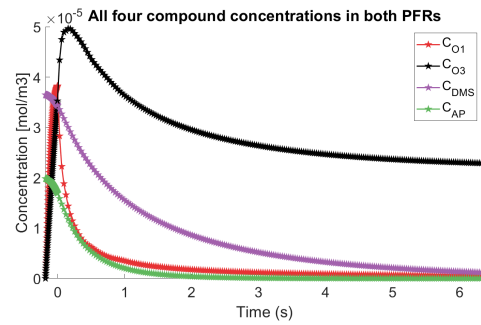


Figure 5.12: All plots of Figure 5.10 into one figure.

Chapter 6

Discussion

6.1 General Remarks on the Experimental Results

Generally speaking about the experimental results, the testing in Lelystad achieved odour removal efficiencies of between 30% and 60% for the UV-reactor alone, with a few exceptions on both lower and upper side of the spectrum. The tests in Erembodegem turned out to have higher removal efficiencies, between 40% and 70% for the UV-reactor alone. In Lelystad, the scrubber was under-designed for its purpose, and showed some strange results, as elaborated further. General performance of the installation as a whole, so acid scrubber with UV-reactor and active carbon-filter, is expected to reach odour removal efficiencies of 90% and above in full-scale setup.

The decrease in both total VOCs as well as odour units might partly be caused by several other factors than reacting with UV or ozone. An example is false air suction at the underpressure side of the installation or condensation of the humid air, where dissolved VOCs are now in the liquid-phase. The effect of condensation is investigated and is discussed in Section 6.4.

Due to operational changes, for instance changes in fan capacity or cooling valves (partly or fully) opening during testing, there might be enormous fluctuations in air flow and VOC concentrations in the inlet air. Although this should ideally be evened out as all odour samples are taken simultaneously at all locations, small timing differences might cause uncertainties.

There might be unknown components with an OTV in the order of magnitude of ppb's or even ppt's. such as mecaptans. This means that an enormous amount of dilutions is required to not smell these components anymore, possibly even with concentrations too low to be found in the GC-MS analysis.

6.2 Mismatch in Measured VOCs: FID and GC-MS

A remarkable gap can be noticed between two measurement methods, in the basis measuring the same quantity: total VOCs. The completely different working principles of both are already shortly explained in Sections 3.4 and 3.5.

The FID's output unit is propane-ppm-eq. with its own corresponding response factors to other gases. Although still after converting the mg/m³ unit as a result of a GC-MS anal-

ysis to ppm, the mismatch is too large. Most probably this gap is caused by gases such as methane, ethane, propane, etc. whereas methane will be the largest contributor. In contrast to anaerobic composting processes, where the main goal is to produce methane biogas, aerobic composting processes theoretically does not produce any biogas. Still, there are always anaerobic spots in the waste where methane might be produced, and since gases like these are too volatile to be measured by a GC-MS analysis, but are being burnt (and therefore measured) in the FID-device. This might be the cause of uneven quantities of total VOCs measured. On the complete opposite, extremely large strings of carbohydrates are difficult to measure in an FID-device as well.

This also explains why the VOC reduction percentages are remarkably less than the odour reduction percentages. Assume a simplified gas mixture existing of methane and dimethylsulfide. Methane gases flow unaffected through the scrubber, UV-reactor and active carbon, while being measured as VOCs and carrying very little smell. On the other hand, smelly mercaptans such as dimethylsulfide are effectively destroyed in the UV or adsorbed in the active carbon, which is being measured as both decreasing VOCs and odour. When combining these, the odour has a larger reduction compared to the total VOCs, which has been seen in the measurements as well.

To make things even more complicated, the concentration of VOCs measured is often not even representative for the odour removal. This has been investigated by the supplier of the UV-reactor, Centriair, and the results can be seen in Figure 6.1. From this figure it can be concluded that the reduction in relative odour strength is almost always stronger than the reduction of the relative measured concentration of volatile organic compounds in the air.

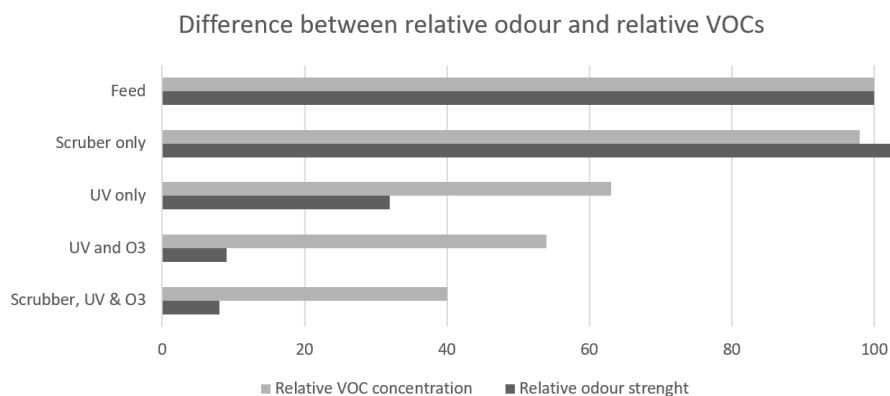


Figure 6.1: Visual representation of the difference between VOCs and odour strength.

6.3 Increase of Odour Level in Ammonia Scrubber

Already mentioned several times in Chapter 4 is the strange odour increase in the ammonia scrubber. In every experiment the ammonia is successfully removed, as seen in Appendices C.2 and C. However, the odour level increased through the acid scrubber in more than 50% of the experiments conducted. There are several hypothesis about the cause, for which additional testing is required to confirm them.

The first possibility is that during experiments with air on elevated temperatures, a certain amount of VOCs is dissolved in the warmed circulating diluted sulphuric acid mixture. If experiments on lower temperatures are conducted directly after, the temperature of the acid also decreases, causing the VOC saturation limit to decrease as well, releasing more VOCs in the air than actually entered the scrubber.

Another hypothesis is based on previous experience of WTT colleagues, namely that the not-so-smelly ammonia actually covers for the more smelly VOCs. So when the ammonia is being removed, the VOCs suddenly can be smelled.

Lastly, another potential option is the pH of the ammonia scrubber being too low in several experiments, at around 2.5 in Lelystad. This is contradictory in the first place, as with a lower pH the ammonia removal is expected to be larger. However, since sulphuric acid has an enormous odour itself, it might be possible that the air smells like the acid used to remove the ammonia, since there's no drip catcher present in the scrubber.

6.4 VOC loss in condensate disposal

As mentioned in Section B, a continuous decrease in FID signal can be seen without UV-lamps, this is in the order of magnitude of 8%. Leakage air is expected to be negligible after hermetically sealing the pilot. There is an hypothesis that certain VOCs get lost in condensate, since the air is very humid and water condensates in the installation. The solubility in water of individual compounds is stated in the table of Appendix C.1. Test have been conducted to measure the Chemical Oxygen Demand (COD) values in the condensate. The results can be seen in Table 6.1.

Table 6.1: Results of the condensate test on both types of air, in order to get insight in VOC losses in the UV-reactor.

#	Air type	Time	Duration	Volume	COD conc.	COD per hour
-	[M/T]	[hh:mm]	[min]	[L]	[mg/L]	[mg/hr]
1	Mixed	15:15	10 min	0.03	378	68
2	Mixed	16:37	10 min	0.04	650	156
3	Tunnel	10:36	10 min	0.19	320	365
4	Tunnel	13:07	10 min	0.18	377	407

Especially when looking at the tunnel air, more than a liter of condensate escapes each hour, corresponding to approximately 400 mgCOD/h which is lost from air into condensate. With an airflow of around 750 m³/h, this corresponds to a VOC decrease of 0.53 mgCOD/m³ tunnel air. From Appendix C.3 can be concluded that on average of four analysis 4.5 mg/m³ VOCs are found. This means the VOCs dissolved in the condensate as COD contributes about 10% to the decrease of VOCs.

6.5 Scalability Issues to a Full-Scale Installation

As can be seen from the average UV-reactor odour removal efficiencies mentioned in the results of Lelystad in Figure 4.1, the system seems to scale relatively linear. Four scenarios on tunnel air with two lamps resulted in an average odour removal efficiency of 30%, while seven other scenarios with double the number of lamps on both types of air resulted in respectively 55% and 51%, almost twice the efficiency. An important question is whether the results of a small-scale pilot installation can be extrapolated to a full-scale waste processing installation. The expectation is that the air distribution over the UV-reactor is much better, as a result of less sharp bends and dedicated duct-work. This should theoretically result in a minor efficiency increase. This is partially confirmed, with odour removal efficiencies of between 40% and 70% in the medium-scale experiments in Erembodegem.

6.6 Extension of the Mathematical Model

Assuming that the concentration reduction of VOCs is correlated to the odour reduction, the model seems to predict the reduction in concentration of major VOCs well compared to the odour reduction measured in both Lelystad and Erembodegem, when linked to the calculated retention times after the UV-reactor. This is of course assuming that the combination of these VOCs is a representation of the total air composition treated in these facilities.

Concluding the assumptions mentioned above, the mathematical model needs extension to be sufficiently reliable. Further research should be done in the following directions:

- An important notice is that the decrease of odours is usually larger than the decrease of VOCs, as is discussed at the end of Section 6.2 as well. The model can be improved by finding the correlation between VOC concentration reduction and odour reduction, as seen in Figure 6.1.
- Extend the model with more VOCs measured in the GC-MS analysis of both -or possibly even more- installations, to increase accuracy of the air composition. There are definitely many more reactants in the air, which on their turn decrease ozone concentrations and therefore decrease the reaction rate of VOC components treated in the current model. This can be limited to a representative group of VOCs, but by increasing the number, accuracy will increase.
- Execute more experiments where the reaction rates of the VOCs is measured more often and more accurate. Currently very little research has been done on reaction rates of specific VOCs.
- Execute more measurements to verify the scalability of the model, for instance with 50,000 m³/h. This also incorporates the stability and robustness of the model. If the robustness increases, the model can be extended to more exceptional cases.

Chapter 7

Financial Feasibility Analysis

The financial aspect of a new emerging technique is always important. Scalability from lab-scale to pilot-scale turned out to be hard to estimate, and even pilot-scale to medium-scale was not completely predictable. Therefore existing plants will be analysed both on their functioning as well as the financial aspect in this section.

First the traditional biofilter will be compared to the UV-technique with an active carbon section. This is done for a composting facility with an air flow of 53000 m³/h and an odour concentration of approximately 10000 OU/m³ in Section 7.1. Furthermore the old and less environmental-friendly catalytic combustion technique will also be compared to the UV-technique with an active carbon section behind it in Section 7.2.

Most of the data used was relatively complete, although some information was missing. Educated guesses and additional assumptions were made to complete this analysis, combining mostly readily available data from previous installations of WTT. To make a fair comparison of the annual costs, the investment costs have been translated to an annual cost using an annuity percentage assumption.

7.1 Biofilter Compared To UV-Technique

As mentioned before in this report, the UV-technique's biggest competitor is the biofilter, therefore this has been analysed for the financial comparison first. The data has been based on an average relatively small composting facility, as typical air flows can reach values as high as 150,000 m³/h. The air will be treated either by a biofilter or by the UV-reactor with an active carbon filter positioned behind it.

The results of this analysis can be found in Table 7.1. A few assumptions worth mentioning are that in no case the foundation and building costs are implemented in the investment costs, the ground area required is without taking into account the scrubber and storage area, but this will be similar for both cases. Furthermore the annual maintenance costs of the UV-lamps is based on an exchange every 1.5 years, the active carbon grains will be replaced after 4 years in this overview and the biofilter material lasts for 5 years. Other assumptions, elaborations and calculations which have been made to make this financial comparison can be found in Appendix H.

Table 7.1: UV-technique compared to the traditional biofilter technique.

	Unit	UV-reactor	Biofilter
Technical data air flows			
<u>Inlet characteristics</u>			
Temperature range	[deg C]	0 - 40	10 - 35
Average air flow	[m3/h]	53000	53000
Average odour concentration	[OU/m3]	10000	10000
Ammonia concentration	[ppm]	≤ 30	≤ 30
<u>Outlet characteristics</u>			
Average odour concentration	[OU/m3]	≤ 500	≤ 500
Ammonia concentration	[mg/m3]	≤ 5	≤ 5
Ground area required	[m2]	65	352
Investment costs			
UV-reactor or biofilter itself	[€]	€295,000	€400,000
Chemical acid scrubber	[€]	€86,000	€86,000
Stack for air outlet	[€]	€15,000	-
Piping and connection	[€]	€70,000	€70,000
Total investment costs	[€]	€466,000	€556,000
Capital costs (20% annuity)	[€/yr]	€93,200	€111,200
Maintenance costs			
<u>UV-reactor</u>			
Exchange of UV-lamps	[€/yr]	€17,500	-
Exchange of AC grains	[€/yr]	€16,500	-
Exchange of other spare parts	[€/yr]	€6,000	-
<u>Biofilter</u>			
Exchange of biofilter material	[€/yr]	-	€10,000
Exchange of other spare parts	[€/yr]	-	€4,000
Total maintenance costs	[€/yr]	€40,000	€14,000
Operational costs			
Electricity	[€/yr]	€24,000	€30,000
Fresh water supply	[€/yr]	€15	€1,200
Sulphuric acid and disposal	[€/yr]	n.a.**	n.a.**
Total operational costs	[€/yr]	€24,015	€31,200
Annual totals			
Total annual costs	[€/yr]	€157,215	€156,400

* based on an annuity of 20%.

** costs depend on unknown details, but equal for both techniques.

The first thing that comes to mind is the very similar removal results, both techniques score very similar in terms of removal efficiency. Also in terms of costs there is no winner between the two treatment solutions, as it is very similar. Some remarkable differences however are the fact that the ground area required for the UV-reactor is more than five times as small. Besides, the investment costs and operational costs are in favour of the UV-reactor. The biofilter will be cheaper in terms of maintenance costs, especially because of the expensive exchange of components for the active carbon and UV-reactor. Also, the UV-reactor requires a stack of at least 20 meter height, in order to be sure that no unreacted ozone molecules will be within the reach of humans, this expensive component is not required for biofilters.

Not taken into account in this comparison is the fact that biofilters have a very specific operation window, especially the maximum temperature turns out to be a difficult task from previous experience with exothermic composting air. The biofilters' biology of the microorganisms is currently relatively poorly understood.

7.2 Catalytic Combustion Compared To UV with AC-filter

The following financial analysis has been constructed from various different researches done previously, mostly in Sweden and Norway. It has been based on a number of assumptions specified up next. The removal efficiencies estimated on previous experience are 96% for catalytic combustion, 87% for the combination of UV-technology with an active carbon filter and 79% for the active carbon filter working standalone. Besides, to compare the different techniques, not only the investment costs nor operational costs are of importance. Therefore, to integrate the investment costs into the yearly costs, an annuity of 20% per year is assumed, as can be seen in the tables in this section. Besides, the costs of the foundation and building and so forth are not considered, as these will be comparable and probably readily built.

There are three treatment methods considered, traditionally most often used is catalytic combustion, which is simply said burning the air with a catalyst. This is the most environmentally-unfriendly and not very cost-effective. The second technique is the throughout this report explained UV-technique, which is as cost-effective as the biofilter, as seen in the previous section. Lastly there is the active carbon technique, with an extremely high efficiency. However, if not well-maintained this technique requires regular replacement of the active carbon grains.

The case considered has an air flow of 11000 m³/h, with an average VOC concentration of 140 mg/m³, which is in the same order of magnitude as the experiments done in Lelystad en Erembodegem, with an air flow similar to Erembodegem. Depending on the treatment methods chosen, the efficiency lies between 79% and 96%. The results can be found in Table 7.2. Remarkable is the fact that only using catalytic combustion is very expensive to treat this specific type of air, compared to the other techniques. This does not even take into account the difficulties of keeping the catalyst in perfect operating condition.

Another noticeable difference is the fact that active carbon has relatively low investment costs, but the operational costs increases significantly when this technique is applied standalone. That is not even taking into account the downtime of replacing the active carbon grains and fact that condensation becomes a possible problem.

Table 7.2: Comparison of catalytic combustion, UV-technique with active carbon and standalone active carbon.

	Unit	All CC	All UV+AC	All AC
Technical data inlet air flow				
Average air flow	[m ³ /h]	11000	11000	11000
Average VOC concentration	[mg/m ³]	140	140	140
Removal efficiency	[%]	96%	87%	79%
Investment costs				
Combustor or UV-installation itself	[€]	€100,000	€30,000	€54,500
Chemical acid scrubber	[€]	-	€15,000	€15,000
Stack for air outlet	[€]	€10,000	€10,000	€10,000
Piping and connection	[€]	€8,000	€8,000	€8,000
Total investment costs	[€]	€118,000	€63,000	€87,500
Capital costs (20% annuity)	[€/yr]	€23,600	€12,600	€17,500
Maintenance costs				
UV-lamp replacement costs	[€/yr]	-	€4,000	-
AC grains costs	[€/yr]	-	€7,000	€21,800
Other spare parts	[€/yr]	€1,000	€2,000	€1,000
Total maintenance costs	[€/yr]	€1,000	€13,000	€22,800
Operational costs				
LPG costs for combustion	[€/yr]	€120,000	-	-
Electricity costs UV-lamps	[€/yr]	-	€6,000	-
Electricity costs AC fan	[€/yr]	-	€2,300	€4,000
Total operating costs	[€/yr]	€120,000	€8,300	€4,000
Annual totals				
Total costs per year	[€/yr]	€144,600	€33,900	€44,300
Total VOC removed annually	[kg/yr]	12931	11764	10694
Total VOC treated annually	[kg/yr]	13490	13490	13490
Costs per kg VOC				
Cost per kg VOC removed	[€/kg]	€11.18	€2.88	€4.14
Cost per kg VOC treated	[€/kg]	€10.72	€2.51	€3.28

Chapter 8

Conclusion

The main goal of this research is to find the influence of ozone generated by UV-light on the removal of odour in a large-scale composting installation. This is caused by the removal of certain pollutants, mostly VOCs. It turns out that the relation between pollutant removal and odour removal is not linear. Relatively more odour is removed when compared to the decrease in pollutant concentrations. This is possibly caused by the cutting of long carbohydrates, therefore concentrations do not decrease as much. The longer chains are but to shorter less-smelling molecules, decreasing odours. Furthermore, the removal of odour is not limited to ozone only. Apart from direct destroying double bonds, also other radicals such as hydroxyls are generated by the UV-lamps. These achieve a similar result as ozone.

The removal efficiencies and external conditions influencing this efficiency are investigated, and extensive experimenting has been done. Examples of external conditions influencing the removal efficiency are the reaction temperature, relative humidity and light intensity. Generally speaking, the higher the temperature, the higher the reaction rate. However above 80 degrees Celsius is undesirable, as the activation energy becomes negative. The relative humidity has an influence very dependent on the compound, for example alcohols are very prone to RH changes, whereas alkanes do not respond that much. Last example is the light intensity, which of course changes by adding more UV-lamps, but is also influenced by dust formation on the glass. For optimal efficiencies, regular cleaning of the lamps is important.

The exact efficiencies per section of the installation are dependent on a lot of things. From the experiments can be concluded that the scrubber for instance generally does not remove odour units, but does remove nearly all ammonia. The UV-reactor stand-alone generally removes between 40% and 70% of the odour units, but this is dependent on inlet concentrations, amount of lamps installed and the ratio of power per cubic meter. An active carbon filter removes $\geq 90\%$ of the remaining odours, but is expensive to operate. Another important function is to remove rest-ozone, functioning as a safety net. This also answers the question whether the UV-reactor could operate stand-alone: it cannot. The UV-reactor requires an acid scrubber because it cannot cope with the extremely high ammonia concentrations, and therefore releasing NO_x into the atmosphere. Furthermore it requires an active carbon filter to cope with fluctuating inlet concentrations and to catch any possible rest-ozone. The system as a whole typically removes 95% of both odours and ammonia. In comparison a well-functioning acid scrubber and biofilter typically remove between 70% and 90% of the odours, although the biofilter is relatively difficult to maintain in perfect condition in terms of temperature, humidity, air flow and pressure drop.

A mathematical prediction model is made to further increase insight in the odour-removal process. It has been based around the equations of two plug flow reactors attached in series. To simplify the model and still be accurate, two representative VOC groups have been analysed. These have their own reaction rates and initial concentrations, influencing concentration development. In the first plug flow reactor, oxygen radicals are generated by the UV-lamps, resulting in increased ozone concentrations and decreasing VOC concentrations. The second plug flow reactor generally has a much higher retention time, where no new radicals are formed and therefore both ozone and VOC concentrations drop. This model can be used to estimate outlet conditions and concentration development while using such a system.

The final question concerns the financial aspect. Traditionally the UV-reactor competes against catalytic combustion or a biofilter. Both share the same major drawback: it is difficult to maintain perfect conditions for either the catalyst or the biofilter packing material. Since the major competitor is the biofilter, this will be used as comparison reference in a case with 53,000 m³/h and 10,000 OU/m³. Both the investment costs as well as the operational costs of a biofilter are about 20% higher than the UV-installation (as a whole). However, the maintenance costs are significantly lower, with only a third or the UV-reactor's costs. The overall annual costs to treat the total air flow are in the same order of magnitude, around €157,000. The main advantages of the UV-reactor are its ability to cope with fluctuating inlet conditions and the total ground surface area required, which is approximately a fifth.

The final choice might come down on exact details of the installation, such as available ground area, air composition, removal demands and availability of suitable wood species for a biofilter. Price-wise they are extremely evenly matched, which also yields for the removal efficiencies. The UV-reactor requires significantly less ground area, is less prone to fluctuations in temperature and inlet concentration since it does not require perfect micro-biology, probably demands less man-hours for maintenance, but is not often applied yet.

8.1 Recommendations

To improve this research, additional work could be executed. The major improvement points of the author are discussed in this chapter. First and most important is the scalability, to verify the measurements taken, an even larger scale experiment could be done, for instance with an air flow of 50,000 m³/h. Furthermore, the relation between odour units and VOC concentrations could be further elaborated. It is currently known that this is far from linear, but the exact reasoning and understanding is unknown. This is especially important for the improvement of the prediction model, which is currently based around concentration reduction, while most permits are given with an odour unit reduction. The model itself can be extended as well, since it currently only exists of two major VOC compounds. Next to that, additional reaction rate experiments could be executed to improve the accuracy of compound-specific reaction rates.

Bibliography

- [1] National Institute of Standards and Technology: Chemical Kinetics Database. URL <https://kinetics.nist.gov/kinetics/index.jsp>.
- [2] Yuval Alfiya, Eran Friedler, Janin Westphal, Oliver Olsson, and Yael Dubowski. Photodegradation of micropollutants using V-UV/UV-C processes; Triclosan as a model compound. *Science of the Total Environment*, 601-602:397–404, 2017. ISSN 18791026. doi: 10.1016/j.scitotenv.2017.05.172.
- [3] Daniel Almarcha, Manuel Almarcha, Sílvia Nadal, and Arne Poulssen. Assessment of odour and VOC depuration efficiency of advanced biofilters in rendering, sludge composting and waste water treatment plants. *Chemical Engineering Transactions*, 40(Special Issue):223–228, 2014. ISSN 22839216. doi: 10.3303/CET1440038.
- [4] Luis Arellano-García, Sylvie Le Borgne, and Sergio Revah. Simultaneous treatment of dimethyl disulfide and hydrogen sulfide in an alkaline biotrickling filter. *Chemosphere*, 191:809–816, 2018. ISSN 18791298. doi: 10.1016/j.chemosphere.2017.10.096. URL <https://doi.org/10.1016/j.chemosphere.2017.10.096>.
- [5] P.W. Atkins. *Physical Chemistry*. W H Freeman & Co, 1998. ISBN 978-0716731689.
- [6] A. J. Bard and Larry R. Faulkner. *Electrochemical Methods: Fundamentals and Applications, 2nd Edition*. Wiley, 2 edition, 2000. ISBN 978-0-471-04372-0.
- [7] A. Beeldens. Air purification by road materials: Results of the test project in Antwerp. Proceedings International RILEM Symposium on Photocatalysis. *Environment and Construction Materials*, pages 187–194, 2007.
- [8] Jennifer C. Brookes, A. P. Horsfield, and A. M. Stoneham. Odour character differences for enantiomers correlate with molecular flexibility. *Journal of the Royal Society Interface*, 6(30):75–86, 1 2009. ISSN 17425662. doi: 10.1098/rsif.2008.0165. URL [/pmc/articles/PMC2610320/?report=abstract](https://www.ncbi.nlm.nih.gov/pmc/articles/PMC2610320/?report=abstract) <https://www.ncbi.nlm.nih.gov/pmc/articles/PMC2610320/>.
- [9] Lixin Cao, Aimin Huang, Franz Josef Spiess, and Steven L. Suib. Gas-phase oxidation of 1-butene using nanoscale TiO₂ photocatalysts. *Journal of Catalysis*, 188(1):48–57, 1999. ISSN 00219517. doi: 10.1006/jcat.1999.2596.
- [10] Robert M Clark and Jeffrey Q Adams. EPA’s Drinking Water and Groundwater Remediation Evaluation: Granular Activated Carbon - Design, Operation and Cost. Technical Report March 1991, Lewis Publishers, 1991.
- [11] Jonah J. Colman and William C. Trogler. The long-wavelength photochemistry of carbon disulfide. *Journal of Geophysical Research Atmospheres*, 102(15):19029–19041, 1997. ISSN 01480227. doi: 10.1029/97jd00401.

- [12] Leitrim County Council, P J Tobin, Consulting Engineers, Hynes Building, and Augustine Street. Sewerage Improvement Scheme - Environmental Impact Statement. *Leitrim Country Council*, pages 122–138, 2003.
- [13] Nele Defoer, Inge De Bo, Herman Van Langenhove, Jo Dewulf, and Toon Van Elst. Gas chromatography-mass spectrometry as a tool for estimating odour concentrations of biofilter effluents at aerobic composting and rendering plants. *Journal of Chromatography A*, 970(1-2):259–273, 2002. ISSN 00219673. doi: 10.1016/S0021-9673(02)00654-4.
- [14] P. J.L. Derikx, H. J.M. Op den Camp, C. Van der Drift, L. J.L.D. Van Griensven, and G. D. Vogels. Odorous sulfur compounds emitted during production of compost used as a substrate in mushroom cultivation. *Applied and Environmental Microbiology*, 56(1):176–180, 1990. ISSN 00992240. doi: 10.1128/aem.56.1.176-180.1990.
- [15] Venu Gopal Devulapelli and Endalkachew Sahle-Demessie. Catalytic oxidation of dimethyl sulfide with ozone: Effects of promoter and physico-chemical properties of metal oxide catalysts. *Applied Catalysis A: General*, 348(1):86–93, 2008. ISSN 0926860X. doi: 10.1016/j.apcata.2008.06.038.
- [16] Mary Dimambro. Literature review : Compost stability – impact and assessment. Technical Report November, Cambridge University, 2016.
- [17] F. M. Farrell, Thomas M. Fitch, and Merlin K.L. Bicking. Analysis of Chemical and Physical Effects of Ultraviolet Bulbs on Cooking Emissions. *Journal of the Air and Waste Management Association*, 61(10):1005–1014, 2011. ISSN 10473289. doi: 10.1080/10473289.2011.599271.
- [18] L. S. Hadlocon, R. B. Manuzon, and L. Y. Zhao. Optimization of ammonia absorption using acid spray wet scrubbers. *Transactions of the ASABE*, 57(2):647–659, 2014. ISSN 21510032. doi: 10.13031/trans.57.10481.
- [19] Louis Van Der Ham. Introduction Reactors Basics for Process Simulation, 2020.
- [20] Walter Hugler, Craso Acosta, and Sergio Revah. Biological removal of carbon disulfide from waste air streams. *Environmental Progress*, 18(3):173–177, 1999. ISSN 02784491. doi: 10.1002/ep.670180313.
- [21] Reza Iranpour, Huub H.J. Cox, Marc A. Deshusses, and Edward D. Schroeder. Literature review of air pollution control biofilters and biotrickling filters for odor and volatile organic compound removal. *Environmental Progress*, 24(3):254–267, 2005. ISSN 02784491. doi: 10.1002/ep.10077.
- [22] Björn Klotz, Ian Barnes, and K. H. Becker. New results on the atmospheric photooxidation of simple alkylbenzenes. *Chemical Physics*, 231(2-3):289–301, 1998. ISSN 03010104. doi: 10.1016/S0301-0104(98)00024-X.
- [23] Loo Hwa Koh, David C.S. Kuhn, Madjid Mohseni, and D. Grant Allen. Utilizing ultraviolet photooxidation as a pre-treatment of volatile organic compounds upstream of a biological gas cleaning operation. *Journal of Chemical Technology and Biotechnology*, 79(6):619–625, 2004. ISSN 02682575. doi: 10.1002/jctb.1030.
- [24] B Krohn. Defining moments in movies: The greatest films, stars, scenes, and events that made movie magic. *Cineaste*, 33(4):70–72, 2008. doi: 10.1021/ES980299.

- [25] M. Kruza, A. C. Lewis, G. C. Morrison, and N. Carslaw. Impact of surface ozone interactions on indoor air chemistry: A modeling study. *Indoor Air*, 27(5):1001–1011, 2017. ISSN 16000668. doi: 10.1111/ina.12381.
- [26] Bruno Langlais, David A. Reckhow, and Deborah R Brink. *Ozone in Water Treatment - Application and Engineering*. CRC Press, 1991.
- [27] Octave Levenspiel. *Chemical reaction engineering*, volume 38. John Wiley & Sons, 1999. ISBN 047125424X. doi: 10.1021/ie990488g.
- [28] Lin Lin, Yuchao Chai, Bin Zhao, Wei Wei, Dannong He, Belin He, and Qunwei Tang. Photocatalytic oxidation for degradation of VOCs. *Open Journal of Inorganic Chemistry*, 03(01):14–25, 2013. ISSN 2161-7406. doi: 10.4236/ojic.2013.31003.
- [29] E. Magnus Johansson, Magnus Berg, Johan Kjellström, and Sven G. Järås. Catalytic combustion of gasified biomass: Poisoning by sulphur in the feed. *Applied Catalysis B: Environmental*, 20(4):319–332, 1999. ISSN 09263373. doi: 10.1016/S0926-3373(99)00004-1.
- [30] Dennis McNevin and John Barford. Biofiltration as an odour abatement strategy. *Biochemical Engineering Journal*, 5(3):231–242, 2000. ISSN 1369703X. doi: 10.1016/S1369-703X(00)00064-4.
- [31] Francesco Montecchio. Process Optimization of UV- Based Advanced Oxidation Processes in VOC Removal Applications. *KTH Royal Institute of Technology*, 2018.
- [32] Yoshio Nagata. Measurement of Odor Threshold by Triangle Odor Bag Method. *Odor Measurement Review*, pages 118–127, 2003.
- [33] Timothy N. Obee and Steve O. Hay. Effects of moisture and temperature on the photooxidation of ethylene on titania. *Environmental Science and Technology*, 31(7):2034–2038, 1997. ISSN 0013936X. doi: 10.1021/es960827m.
- [34] Satu Ojala, Satu Pitkäaho, Tiina Laitinen, Niina Niskala Koivikko, Rachid Brahmi, Jana Gaálová, Lenka Matejova, Alexei Kucherov, Sanna Päivärinta, Christian Hirschmann, Tuomas Nevanperä, Markus Riihimäki, Minna Pirilä, and Riitta L. Keiski. Catalysis in VOC abatement. *Topics in Catalysis*, 54(16-18):1224–1256, 2011. ISSN 10225528. doi: 10.1007/s11244-011-9747-1.
- [35] A. O’Malley and B. K. Hodnett. The influence of volatile organic compound structure on conditions required for total oxidation. *Catalysis Today*, 54(1):31–38, 1999. ISSN 09205861. doi: 10.1016/S0920-5861(99)00166-2.
- [36] Michel Ondarts, Cécile Hort, Vincent Platel, and Sabine Sochard. Indoor air purification by compost packed biofilter. *International Journal of Chemical Reactor Engineering*, 8(June), 2010. ISSN 15426580. doi: 10.2202/1542-6580.2176.
- [37] OrgaworldNL. Lelystad Composterij Locatie Zeeasterweg, 2018. URL orgaworld.nl/meer-over-ons-bedrijf/onze-locaties/lelystad-zeeasterweg.
- [38] V. N. Parmon, A. D. Simonov, V. A. Sadykov, and S. F. Tikhov. Catalytic combustion: Achievements and problems. *Combustion, Explosion and Shock Waves*, 51(2): 143–150, 2015. ISSN 15738345. doi: 10.1134/S001050821502001X.

- [39] Madhumita Bhowmick Ray. Photodegradation of the volatile organic compounds in the gas phase: a review. *Developments in Chemical Engineering and Mineral Processing*, 8(5-6):405–439, 2000. ISSN 09691855. doi: 10.1002/apj.5500080502.
- [40] Alfredo Santos, Xavier Guimerà, Antonio David Dorado, Xavier Gamisans, and David Gabriel. Conversion of chemical scrubbers to biotrickling filters for VOCs and H₂S treatment at low contact times. *Applied Microbiology and Biotechnology*, 99(1):67–76, 2015. ISSN 14320614. doi: 10.1007/s00253-014-5796-2.
- [41] Paula Schulze, Johan Holstein, Ria de Haan, and Harm Vlap. Rapport: Terpenenverwijdering uit Biogas. *DNV Kema Energy & Sustainability*, 1(1):5–6, 2013.
- [42] Sonil Nanda. Microbial biofiltration technology for odour abatement: An introductory review. *Journal of Soil Science and Environmental Management*, 3(2):28–35, 2012. doi: 10.5897/jssem11.090.
- [43] Graduate Student Theses and Lawrence Roman Schmitz. Aqueous phase ozonation of methanethiol and dimethyl disulfide. *The University of Montana*, 1973.
- [44] Kåre Tjus and Mats Ek. Utvärdering och utveckling av reningsteknik för VOC från lackering och oljedimma Pilotstudie med aktivt kol och. *IVL Svenska Miljöinstitutet*, 2006.
- [45] Outi K. Tolvanen, Kari I. Hänninen, Anja Veijanen, and Kirsi Villberg. Occupational hygiene in biowaste composting. *Waste Management and Research*, 16(6):525–540, 1998. ISSN 0734242X. doi: 10.1177/0734242X9801600604.
- [46] Yizhak Tzvi and Yaron Paz. Highly efficient method for oxidation of dissolved hydrogen sulfide in water, utilizing a combination of UVC light and dissolved oxygen. *Journal of Photochemistry and Photobiology A: Chemistry*, 372(July 2018): 63–70, 2019. ISSN 10106030. doi: 10.1016/j.jphotochem.2018.12.005. URL <https://doi.org/10.1016/j.jphotochem.2018.12.005>.
- [47] Robin Vaessen. Luchtreiniging door middel van Ozon - Afstudeerverslag WTT. Technical report, Fontys Technische Hogeschool te Venlo (FTHV), 2006.
- [48] Valerie Vranova, Klement Rejsek, and Pavel Formanek. Aliphatic, cyclic, and aromatic organic acids, vitamins, and carbohydrates in soil: A review. *The Scientific World Journal*, 2013(November 2014), 2013. ISSN 1537744X. doi: 10.1155/2013/524239.
- [49] Kuo Pin Yu, Grace Whei May Lee, and Guo Hao Huang. The effect of ozone on the removal effectiveness of photocatalysis on indoor gaseous biogenic volatile organic compounds. *Journal of the Air and Waste Management Association*, 60(7):820–829, 2010. ISSN 21622906. doi: 10.3155/1047-3289.60.7.820.
- [50] Kuo Pin Yu, Grace Whei May Lee, and An Jie Hung. Removal of indoor α -pinene with a fiber optic illuminated honeycomb monolith photocatalytic reactor. *Journal of Environmental Science and Health - Part A Toxic/Hazardous Substances and Environmental Engineering*, 49(10):1110–1115, 2014. ISSN 15324117. doi: 10.1080/10934529.2014.897146.

- [51] Hongyu Zhang, Frank Schuchardt, Guoxue Li, Jinbing Yang, and Qingyuan Yang. Emission of volatile sulfur compounds during composting of municipal solid waste (MSW). *Waste Management*, 33(4):957–963, 2013. ISSN 0956053X. doi: 10.1016/j.wasman.2012.11.008. URL <http://dx.doi.org/10.1016/j.wasman.2012.11.008>.
- [52] Yuefeng Zhao, Yurong Zhang, Jing Gao, Xu Wang, Hui Li, Yanqi Wang, and Mengjun Duan. VOC Monitoring and Ozone Generation Potential Analysis Based on a Single-Photon Ionization Time-of-Flight Mass Spectrometer. *MDPI*, 2020.
- [53] Kristin Zoschke, Norman Dietrich, Hilmar Börnick, and Eckhard Worch. UV-based advanced oxidation processes for the treatment of odour compounds: Efficiency and by-product formation. *Water Research*, 46(16):5365–5373, 2012. ISSN 18792448. doi: 10.1016/j.watres.2012.07.012.
- [54] Kristin Zoschke, Hilmar Börnick, and Eckhard Worch. Vacuum-UV radiation at 185nm in water treatment - A review. *Water Research*, 52:131–145, 2014. ISSN 18792448. doi: 10.1016/j.watres.2013.12.034.

Appendices

Appendix A

Measurement Devices Used

In order to determine efficiency of the system and its individual parts, a series of measurement instruments is required, which is described in this section. Multiple temperature probes with an expected range between 20°C and 60°C to indicate characteristics of influent air, functioning status of the ammonia-scrubber and possible leakages/false air suction. To determine over- and underpressure caused by the fan, a pressure difference device is required. The expected range is between -2000 Pa and +2000 Pa. This might indicate a congestion in the scrubber or incorrect settings or installation elsewhere. Air velocity devices are necessary to map air flows through the installation, which can be calculated in combination with the inner diameter of the section. Such devices require the most laminar flow as possible, so a straight section of pipe before the measurement location is advised. The velocity range is between 0 and 15 m/s. Electrical conductivity (EC) and pH devices are required to control the IBC functioning as acid storage for the ammonia-scrubber. The electrical conductivity may not exceed 200 mS/cm, indicating that the water is too saturated with salts, mostly caused by the high ammonia concentration. At the same time, the pH must be kept between 3 and 5 for optimum ammonium removal performance.

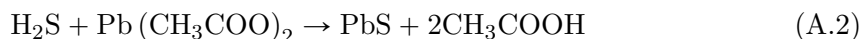
A.1 Kitagawa Pump Explanation of Working Principle

Furthermore, a Kitagawa pump is required in combination with ozone and ammonia Kitagawa-tubes to determine their concentrations. Ozone concentrations indicate the functioning of the UV-lamps and active carbon section, where concentrations are expected between 0 and 5 ppm. Ammonia concentrations are an indication of the ammonia-scrubber's functioning, the required range of untreated air is as high as 300 ppm, although a more precise tube might be necessary to determine concentrations after the scrubber. Alternatively, a Dräger-pump and corresponding tubes function perfectly as well.

These Kitagawa, GASTEC or Draäger tubes all rely on the same working principle. The tubes are colour-changing. For ammonia the reaction is as follows: ammonia present in the air reacts with sulphuric acid inside the tube, while ammonium sulphate is being formed. This yields a pH-shift. The tube consist of Cresol-red, making it possible to observe the pH-shift. Possibly other reactions occur as well, resulting in false results, although the chances are minor. The reaction is shown in Eq. A.1. The lower detection-limit lies around 0.2 ppm.



Something similar occurs for hydrogen sulfide, H_2S . The major difference is that there is no pH-shift, but a colourful compound is formed. Hydrogen sulfide present in the air reacts with lead acetate in the reactor tube, under the formation of lead sulfide. The latter results in a brownish colour, making the concentration visible in the tube. Possibly other reactions occur as well, resulting in false results, although the chances are minor again. The reaction is shown in Eq. A.2. The lower detection-limit is 0.05 ppm, which is often not even the case in composting air.



Finally ozone reacts according to a similar reaction, shown in Eq. A.3. Ozone reacts with the indigo-dye (blueish) to piperonyl nitrile. This has a white colour, so a shift from blue to white is visible, indicating the concentration of ozone. Also for the reaction shown in Eq. A.3, false results can be obtained due to other reactions, but this is expected to only have a very minor effect. The lower detection-limit is 0.05 ppm.



A.2 Measuring VOCs: Photoionisation-/Flame Ionisation Detector

So far the devices are all straightforward and often used measurement devices, it becomes more complex when determining the amount of VOCs, being one of the most important objective measurements to indicate odourous compounds. A Photoionisation Detector (PID) or Flame Ionization Detector (FID)-device is required. Both devices produce a signal in ppm's by ionization (expected range between 0 and 150 ppm), but the devices differ significantly in working principle as well as operating conditions, which is explained below.

A FID-device requires H_2 -gas to burn (mostly organic) components coming through the gas chromatography column. This causes the release of an ion, which is caught between two electrodes. This ion current is amplified and converted to parts per million by a digital meter. Since the FID is being calibrated with 80 ppm propane gas, these ppm's are actually a ppm-equivalent to propane. Each gas has their own response factor, but for the sake of simplicity, this factor is assumed to be 1. Therefore, it is safer to use this number only for relative use, and not absolute comparisons with other methods.

On the other side, a PID-device ionizes both organic and inorganic molecules using ultraviolet (UV)-light, causing the molecules to release an electron, detected by electrodes. This device is calibrated using isobutylene, and the same applies for this technique: each gas has their own response factor, which is assumed to be 1. The PID-device is much smaller compared to a FID, which means it can be used portable. Since PID devices cannot cope well with humid air, this makes them less suited for this application. An ammonia-correction must be done for each individual measurement, due to the mixed (in)organic signal measured, requiring a simultaneous Kitagawa-ammonia measurement.

The advantage of a FID-device is that inorganic compounds such as nitrogen or ammonia are lost as a background noise signal, meaning that they do not appear in the number of ppm's. This is confirmed by pouring the device in a bottle of cleaning ammonia and reading a value of 0 ppm. Disadvantages are the size, weight, mobility and costs of such a device.

Appendix B

Testing Conditions Separated Per Day

Each day has their own characteristics. In order to achieve as similar air characteristics as possible, all tests have been done at the end of the working week, as is explained in Section 3.2.1. Still there were some major differences, described in the coming sections.

Testing Day 1: Lelystad - May 28th, 2020

The day after the first testing day, it became apparent that there was a VOC removal over the UV-reactor according to the FID-device, although all UV-lamps were off. The conclusion is that there was additional air diluted into the system, influencing the results. Based on observations the next day, this leakage air flow was in the order of magnitude of 10-15%. Besides, the inlet air had a relatively low average value of $2352 \text{ OU}_E/\text{m}^3$.

Due to only using one cassette in a UV-reactor designed for five alternating UV-cassettes, there were gaps where air could pass untreated, decreasing the results. This effect is expected to cancel out against the leakage air flow by estimations made on site. Based on the findings of May the 28th modification was made on the experimental test setup to compensate for measuring errors and dilutions factors.

Testing Day 2: Lelystad - June 4th, 2020

The large air dilutions of testing day one have been blocked. However, still a small continuous decrease of FID-signal of a few percent was found with the UV-lamps turned off. It might be caused by several factors, such as VOCs dissolved in the UV-reactor's condensate (see Section 6.4), dust collection and maybe a bit of leakage air.

The second measurement of this day shows a doubling of the odour units though the UV-reactor (mixed air, 4 lamps). Although Witteveen & Bos claims no mistakes were made, this is expected to be a measurement mistake. Another explanation could be that during testing some of the in-vessel reactor settings were changed which might resulted in a big change in odour concentration. All other tests showed a decrease though the UV-reactor.

Testing Day 3: Lelystad - June 19th, 2020

Since the active carbon was completely unsaturated on the first day of testing, the outlet air had concentrations below $200 \text{ U}_E/\text{m}^3$. Especially the last two measurements of this day were completely the opposite, with concentrations as high as $7555 \text{ OU}_E/\text{m}^3$. The first hypothesis was condensate water in the active carbon box, although this one is denied as there was no condensate present when dismantling. The current hypothesis is that the carbon itself is saturated, probably caused by hours of running without scrubber and UV-lamps, as the raw air has up to 300 ppm of ammonia and 100 ppm of VOC.

Testing Day 4: Erembodegem - October 15th, 2020

During this testing day, all previous experience was taken into account and no real problems occurred. Besides, the UV-reactor was now installed with its design capacity: $10,000 \text{ m}^3$ per hour. The only minor improvement could be to use permanent duct-work in stead of flexible air-conditioning piping, which were a bit permeable for steam when entering cold air.

Appendix C

Extensive Experimental Results

On the upcoming pages more extensive data of the odour experiments, GC-MS analysis and odour perceptions of often-found compounds is shown. This data is still reduced to make it more insightful. The full data sheets can be requested, please contact the author of this thesis.

C.1 Odour Perception of Regularly Found Compounds

The odour perception, chemical formulas, odour threshold values (OTVs) and solubility in water are stated for most of the regularly-found compounds in composting air. These values and descriptions can all be found in Table C.1.

Table C.1: *Odour perception, OTVs and solubility in water of the most prominent compounds found in composting air.*

Group	Compound	Formula	Odour perception	OTV	Water solubility
Alcohols	ethanol	C ₂ H ₅ OH	Sharp acrid smell	980 ppm	high
Ketones	2,3-butanedione	C ₄ H ₆ O ₂	Chlorine-like swimming-pool smell	180 ppb	high
	nonanal	C ₉ H ₁₈ O	Fresh waxy rose and orange smell	2000 ppb	very poor
Aldehydes	2-methylpropanal	C ₄ H ₈ O	Sharp pungent smell	1000 ppb	fair
	3-methylbutanal	C ₅ H ₁₀ O	Nutty, chocolate, coffee	360 ppb	slightly
	octanal	C ₈ H ₁₆ O	Citrus oils, fruity smell	50 ppb	slightly
(Organic) Sulphuric Compounds	dimethyl-sulfide	C ₂ H ₆ S	At low concentrations: cabbage, broccoli. At medium concentrations: seaside	3 ppb	fair
	dimethyl-disulfide	C ₂ H ₆ S ₂	At high concentrations: garlic At very high concentrations: dead animals	2.2 ppb	very poor
Esters	carbon-disulfide	CS ₂	Sweetish aromatic smell	210 ppb	very poor
	eucalyptol	C ₁₀ H ₁₈ O	Pleasant minty smell	7000 ppb	fair
Terpenes	alfa-pinene	C ₁₀ H ₁₆	Pine or fir trees	18 ppb	very poor
	beta-pinene	C ₁₀ H ₁₆		33 ppb	very poor
	limonene	C ₁₀ H ₁₆	Orange or lemon smell	38 ppb	very poor
(Organic) Nitrogenous Compounds	ammonia	NH ₃	Unmistakable ammonia smell	1500 ppb	high
Mercaptans	methane thiol	CH ₄ S	Rotten cabbage, sewer smell	0.07 ppb	high

C.2 Odour Testing Results: Lelystad and Erembodegem

Parameter	Unit	Expected range	Description, device, location	ODOUR day 1: four lamps	ODOUR day 1: four lamps	ODOUR day 1: two lamps	ODOUR day 1: two lamps	ODOUR day 1: no scrubber	ODOUR day 1: no scrubber	
Air flow	Hz	0-1000	frequency	45	45	45	45	38	38	
Type of air	...123	...123	connection	1 (tunnel)	1 (tunnel)	1 (tunnel)	1 (tunnel)	1 (tunnel)	1 (tunnel)	
acid scrubber	on/off	...01	on/off	on	on	on	on	bypassed	bypassed	
UV-#lamps	#	0-20	amount of lam	4	4	2	2	2	2	
Active Carbon	on/off	...01	on/off	on	on	on	on	on	on	
Time	hh:mm:d d:mm	2020	clock	-	28 May @ 12:45	28 May @ 14:20	28 May @ 14:55	28 May @ 15:47	28 May @ 16:57	28 May @ 17:30
Temp	Celcius	... 0-60	thermom eter	L1		43	43	44	42	41
				L2	43	41	41	41		
				L3	44	43	42	42	42	42
				L6	43	42	40	40	41	43
Pressure	kPa w.r.t 1 atm	... -1000 tot +1000	pressure meter	L1				-0,50	-0,58	-0,59
				L2	-1,56	-1,51	-1,59	-1,59		
				L3	0,82	0,82	0,83	0,85	1,02	1,06
				L6	0,13	0,10	0,06	0,10	0,14	0,14
Air flow	m/s in PVC tube	... 0-1000	flow meter	L1					9,5	
				L6						9,5
O3	ppm	... 0-3	Kitagawa tubes	L3	1,7	0,7	0,7	0,7	0,5	0,5
				L5	0,1	0,0	0,0	0,0	0,1	0,0
Ammonia	ppm	... 0-500	Kitagawa tubes	L1	210	200	180	190	165	145
				L2	0	0	0	0		
				L3	0	0	0	0	150	140
				L5	0	0	0	0		
				L6	0	0	0	0	105	120
FID signal	-	... 0-50	FID device	L1	32,1	41,9	44,0	37,5	47,0	49,1
				L2	27,9	40,0	41,9	39,7		
				L3	23,7	31,7	31,7	30,4	42,0	43,4
				L6	22,7	28,1	28,1	28,1	33,6	34,0
FID signal (2nd round)	-	... 0-50	FID device	L1	37,5	39,5	40,0	39,9	48,6	48,6
				L2	39,1	39,0	38,0	39,5		
				L3	33,4	29,6	31,0	30,0	41,4	40,8
				L6	32,8	27,9	26,0	27,8	33,4	33,9
Odour	OU	...0-10 ⁶	external	L1	2057	1915	2673	2763		
				L2	1520	1083	1767	1631		
				L3	421	458	1415	1114	3133	2130
				L6	75	120	116	156		
Elec. Conduc.	mS/cm	...0-200	EC meter	IBC	25,7	25,1	24,9	24,8	n.a.	n.a.
Acid scrubber	-	...2-9	pH meter	IBC	2,29	2,32	2,32	2,34	n.a.	n.a.

Figure C.1: More extensive testing data of Lelystad experiments day 1.

Parameter	Unit	Expected range	Description, device, location	ODOUR: 4 lamps, mixed air	ODOUR: duplo test 41	ODOUR: no scrub, mixed air	ODOUR: duplo test 44	ODOUR: 2 lamps, tunnelair	ODOUR: duplo test 45	
Air flow	Hz	0-1000	frequency	45	45	33	33	45	45	
Type of air	...123	...123	connection	2 (mixed)	2 (mixed)	2 (mixed)	2 (mixed)	1 (tunnel)	1 (tunnel)	
acid scrubber	on/off	...01	on/off	on	on	bypassed	bypassed	on	on	
UV-#lamps	#	0-20	amount of lamp	4	4	4	4	2	2	
Active Carbon	on/off	...01	on/off	on	on	on	on	on	on	
Time	hh:mm:d d:mm	2020	clock	-	4 jun @ 10:45	4 jun @ 12:40	4 jun @ 13:57	4 jun @ 14:30	4 jun @ 15:40	4 jun @ 16:24
Temp	Celcius	... 0-60	thermom eter	L1	30	29	31	31	44	41?
				L2	30	28			36	40
				L3	34	33,5	33	33	39	40
				L6		31,5	32	32	35	35
Pressure	kPa w.r.t 1 atm	... -1000 tot +1000	pressure meter	L1	-0,19	-0,20	-0,25	-0,20	-0,50	-0,55
				L2	-1,50	-1,51			-1,67	-1,66
				L3	0,90	0,88	0,96	1,00	0,75	0,70
				L6	0,08	0,10	0,08	0,10	0,05	0,07
Air flow	m/s in PVC tube	... 0-1000	flow meter	L1	10,0	10,0	10,0	10,0	7,8	7,3
				L3	n.a.	n.a.	n.a.			
				L6	7,6	8,0	8,3	8,5	7,2	7,3
O3	ppm	... 0-3	Kitagawa tubes	L3	0,6	0,5	0,2	0,2	0,3	0,3
				L6	0,0	0,0	0,0	0,0	0,0	0,0
Ammonia	ppm	... 0-500	Kitagawa tubes	L1	32	32	35	32	300	240
				L3	0	0	30	28	0	0
				L6	0	0	15	20	0	0
FID signal	-	... 0-50	TigerLT (later FID)	L1	52-57	35-38	68-71	73-75	50-52	62-64
				L2	45-48	33-34			56-58	65-67
				L3	36-38	27-28	61-64	65-69	50 steady	53 steady
				L6	29-30	20-21	38-39	40-42	36-38	48 steady
FID signal (2nd round)	-	... 0-50	FID unit	L1	51-54	35-38	73-75	74-76	48-49	63-64
				L2	50-52	34-36			52-54	62-63
				L3	33-36	26-27	66-71	64-66	43-44	51-52
				L6	36-37	21-22	38-39	40-42	36 steady	47 steady
Odour	OU	...0-10 ⁶	external	L1	6551	5799			6248	5825
				L2	7597	4779			7209	6055
				L3	4383	9988	15750	12688	4113	4418
				L6		344				
Elec. Conduc.	mS/cm	...0-200	EC meter	IBC	25,9	25,9			24,6	22,6
Acid scrubber	-	...2-9	pH meter	IBC	2,32	2,34			2,43	2,51

More extensive testing data of Lelystad experiments day 2.

Parameter	Unit	Expected range	Description, device, location	ODOUR: tunnel 4 lamps	ODOUR: duplo test 55	ODOUR: mixed 4 lamps	ODOUR: duplo test 59	
Air flow	Hz	0-1000	frequency	42	42	42	42	
Type of air	...123	...123	connection	1 (tunnel)	1 (tunnel)	2 (mixed)	2 (mixed)	
acid scrubber	on/off	...01	on/off	on	on	on	on	
UV-#lamps	#	0-20	amount of lam	4	4	4	4	
Active Carbon	on/off	...01	on/off	on	on	on	on	
Time	hh:mm:d d:mm	2020	clock	-	19 jun @ 12:00	19 jun @ 12:45	19 jun @ 15:30	19 jun @ 16:30
Temp	Celcius	... 0-60	thermom eter	L1	49,5	49,5	38	33
				L2	48,5	48	36,5	35
				L3	49,5	50	40	39
				L6	45	45	36	35
Pressure	kPa w.r.t 1 atm	... -1000 tot +1000	pressure meter	L1	-0,53	-0,3	-0,16	-0,16
				L2	-1,42	-1,39	-1,32	-1,34
				L3	0,57	0,6	0,77	0,76
				L6	0,08	0,07	0,09	0,08
Air flow	m/s in PVC tube	... 0-1000	flow meter	L1	8,5	8,5	9,2	9,5
				L6	7,2	6,7	6,8	7,3
O3	ppm	... 0-3	Kitagawa tubes	L3	1	1,35	0,25	0,27
				L6	0,05	0	0	0
Ammonia	ppm	... 0-500	Kitagawa tubes	L1	330	320	43	32
				L2	0	0	0	0
				L3	0	0	0	0
				L6	0	0	0	0
FID signal	-	... 0-50	TigerLT (later FID)	L1	102-105	60-63	63-64	51-52
				L2	99-100	59-61	31-53	44-45
				L3	94-97	51-53	47-50	40-41
				L6	95-97	50 (steady)	35-37	27-28
FID signal (2nd round)	-	... 0-50	FID unit	L1	110-112	59-62	93-95	49-51
				L2	101-104	53-56	79-81	45-47
				L3	96-97	47-48	66-67	39-40
				L6	95-96	45 (steady)	35-37	27-28
Odour	OU	...0-10 ⁶	external	L1	6550	5943	11081	10232
				L2	5474	6257	24089	26336
				L3	4041	2291	11969	10310
				L6	1621	2070	7555	6636
Elec. Conduc.	mS/cm	...0-200	EC meter	IBC	9,5	12,9	11,6	12,5
Acid scrubber	-	...2-9	pH meter	IBC	2,94	2,70	2,62	2,62
Acid temp	degrees Celsius	...20-50	pH meter		48,4	48,4	36,6	35,4

More extensive testing data of Lelystad experiments day 3.

OPERATIONAL PARAMETERS	Phase	Measurements								
	Description [-]	Fifty lamps Duplicate (day 4)	Forty lamps Duplicate (day 4)	Thirty lamps Duplicate (day 4)	Percolate recirculation OFF Duplicate (day 4)					
Day	[-]	1	2	3	4	5	6	7	8	
Scenario	[#]	10000	10000	10000	10000	10000	10000	120000	120000	
Air flow	[m3/h]	48	48	40	40	30	30	0	0	
Amount o	[#]									
MEASUREMENTAL PARAMETERS	Air flow [m3/h]	L1								
		L2	12114	12114	12623	11503	12216	11299	11299	13030
		L3	9874	10180	9874	9671	10689	9772		
		L4								
	Temp [C]	L1	38.5	38.6	38.6	39.4	39.7	42.2	40.1	42.0
		L2	34.7	36.8	37.5	37.0	38.0	38.2	39.7	39.0
		L3	34.0	36.6	37.3	37.5	37.6	38.7		
		L4			34.1	34.1	34.1	34.2	34.1	
	Pressure [mbar]	L1								
		L2	2.5	2.7	3.0	2.6	3.1	2.7		
		L3	1.0	1.0	1.2	0.9	1.5	0.8		
		L4								
	Ammonia [ppm]	L1	140	170	178	220	260	180	180.0	160
		L2	8.0	9.5	10.5	10.0	10.5	9.0	6.0	6.0
		L3	7.0	9.0	9.5	9.5	9.5	9.0		
		L4	6.0	6.0	6.0	6.0	6.0	6.1	4.0	8.0
	Ozone [ppm]	L1								
		L2								
		L3	0.20	0.15	0.12	0.15	0.13	0.13		
		L4								
Odour [OU/m3]	L1	14384	10229	11219	14842	25912	11207	38828	41353	
	L2	11190	10222	19557	13484	17885	11223	14804	16260	
	L3	5109	12406	6543	8480	5428	5067			
	L4	5177	2488	7864	2588	1504	3225	8480	7103	

Figure C.2: More extensive testing data of Erembodegem experiments, day "4".

C.3 GC-MS Results: Lelystad and Erembodegem

On the next page several GC-MS analysis conducted for the experiments in Lelystad and Erembodegem are shown. Also the odour threshold values per compound are shown, as well as the odour activity value (defined as the ratio of OTV divided by the concentration measured in the GC-MS analysis).

Sample method Sampling date Day Analysis date Type of air	W&B	W&B	Sorbent	Sorbent	Molar	Odour	Odour Activity Value (conc. div. by threshold)				
	28-4-2020	28-5-2020	5-6-2020	5-6-2020	mass	Threshold	Ratio of odour threshold divided by GC-MS result.				
CAS number	Compound	$\mu\text{g}/\text{m}^3$ ⁽¹⁾	$\mu\text{g}/\text{m}^3$ ⁽¹⁾	$\mu\text{g}/\text{m}^3$	$\mu\text{g}/\text{m}^3$	g/mol	$\mu\text{g}/\text{m}^3$	First test	Second test	Third test	Fourth test
Aromatic carbohydrates											
71-43-2	benzene	43	30	0	0	78,11	8626	0,01	0,00	0,00	0,00
100-41-4	ethylbenzene	3	0	0	0	106,17	738	0,00	0,00	0,00	0,00
99-87-6	p-cymene	281	79	0	0	123,22	287	0,98	0,28	0,00	0,00
108-38-3 / 106-42-3	m,p-xylene	14	0	0	0	106,16	178	0,08	0,00	0,00	0,00
95-47-6	o-xylene	5	0	0	0	106,16	1650	0,00	0,00	0,00	0,00
108-88-3	toluene	77	178	730	0	92,14	603	0,13	0,30	1,21	0,00
-	Σ C15H22	0	30	0	0	202,33	n.a.	n.a.	n.a.	n.a.	n.a.
-	Total	423	317	730	0						
Cyclic carbohydrates											
3604-14-6	dimethyl decahydronaftalene (C12H22)	39	0	0	0	166,3	n.a.	n.a.	n.a.	n.a.	n.a.
-	Σ C12H22	0	46	0	0	166,31	n.a.	n.a.	n.a.	n.a.	n.a.
-	Σ C15H24	0	932	0	0	204,35	n.a.	n.a.	n.a.	n.a.	n.a.
-	Σ C15H28	0	159	0	0	208,38	n.a.	n.a.	n.a.	n.a.	n.a.
-	Total	39	1136	0	0						
Alifatic carbohydrates											
109-66-0	pentane (C5H12)	124	139	0	0	72,15	4131	0,03	0,03	0,00	0,00
112-40-3	dodecane (C12H26)	13	0	0	0	170,33	766	0,02	0,00	0,00	0,00
629-50-5	tridecane (C13H28)	33	30	0	0	184,37	39	0,85	0,76	0,00	0,00
629-59-4	Σ C14 alkane (tetradecane)	0	30	0	0	198,39	4667	0,00	0,01	0,00	0,00
629-62-9	Σ C15 alkane (pentadecane)	0	158	0	0	212,41	n.a.	n.a.	n.a.	n.a.	n.a.
-	Total	170	356	0	0						
Alcohols											
64-17-5	ethanol	0	307	0	0	46,07	980	0,00	0,31	0,00	0,00
-	Total	0	307	0	0						
Ketones											
67-64-1	acetone	106	812	390	340	58,08	99770	0,00	0,01	0,00	0,00
78-93-3	2-butanone	0	109	700	130	72,11	1298	0,00	0,08	0,54	0,10
-	Σ C10H16O	0	297	0	0	152,23	16	0,00	18,35	0,00	0,00
-	Σ C10H18O	0	20	0	0	154,25	n.a.	n.a.	n.a.	n.a.	n.a.
-	Total	106	1238	1090	470						
Aldehydes											
124-19-6	nonanal	59	0	0	0	142,24	2	29,70	0,00	0,00	0,00
112-31-2	decanal	44	0	0	0	156,2	3	17,06	0,00	0,00	0,00
-	Total	102	0	0	0						
Organic sulphuric compounds											
75-18-3	dimethyl sulfide	455	823	0	160	62,14	13	35,84	64,80	0,00	12,59
624-92-0	dimethyl disulfide	0	33	0	0	94,19	8	0,00	3,87	0,00	0,00
75-15-0	carbon disulfide	2428	0	0	0	76,139	654	3,71	0,00	0,00	0,00
-	Total	2883	856	0	160						
Ethers											
110-00-9	furan	110	347	0	0	68,07	27562	0,00	0,01	0,00	0,00
1191-99-7	2,3-dihydrofuran	169	0	0	0	70,09	n.a.	n.a.	n.a.	n.a.	n.a.
930-27-8	3-methylfuran	0	80	0	0	82,1	n.a.	n.a.	n.a.	n.a.	n.a.
470-82-6	eucalyptol	0	132	0	0	154,25	7	0,00	19,43	0,00	0,00
-	Total	279	559	0	0						
Terpenes											
80-56-8	alfa-pinene	48	198	430	200	136,23	100	0,48	1,97	4,29	1,99
127-91-3	beta-pinene	0	59	0	0	136,23	131	0,00	0,45	0,00	0,00
5989-27-5	limonene	681	980	3500	210	136,23	212	3,21	4,63	16,53	0,99
-	Σ C10H16	103	297	0	0	136,23	156	0,66	1,90	0,00	0,00
-	Total	832	1535	3930	410						
Organic nitrogenous compounds											
75-05-8	acetonitrile	0	20	0	0	41,05	21826	0,00	0,00	0,00	0,00
-	Total	0	20	0	0						
-	Grand total	4834	6323	5750	1040						

Figure C.3: GC-MS data Lelystad: OTVs, OAVs & measured concentrations.

Figure C.4: GC-MS data Erembodegem: OTVs, OAVs & measurements.

Project Sampling date Description	Erembodeg	Erembodeg	Erembodeg	Molar	Odor	Odor Activity Value (conc. div. by threshold)		
	15-okt	15-okt	15-okt	mass	Treshold	Ratio of odor threshold divided by GC-MS result		
CAS numbe Compound	Inlet air	After scrubber	After UV	per compound	per compound	This gives an indication of the odour "severity"		
	µg/m ³	µg/m ³	µg/m ³	g/mol	µg/m ³	Inlet air	After scrub	After UV
Aromatic carbohydrates								
71-43-2 benzene	3	4	4	78,11	8626	0,00	0,00	0,00
100-41-4 ethylbenzene	1	1	1	106,17	738	0,00	0,00	0,00
99-87-6 p-cymene	0	0	0	123,22	287	0,00	0,00	0,00
108-38-3 / m,p-xylene	3	3	2	106,16	178	0,02	0,02	0,01
95-47-6 o-xylene	0	2	2	106,16	1650	0,00	0,00	0,00
108-88-3 toluene	4	12	8	92,14	603	0,01	0,02	0,01
- Σ C15H22	0	12	4	202,33	n.a.	n.a.	n.a.	n.a.
Total	11	34	21					
Cyclic carbohydrates								
3604-14-6 dimethyl decahydronaftalene (C12H22)	0	0	0	166,3	n.a.	n.a.	n.a.	n.a.
- Σ C12H22	0	0	0	166,31	n.a.	n.a.	n.a.	n.a.
- Σ C15H24	59	531	16	204,35	n.a.	n.a.	n.a.	n.a.
- Σ C15H28	0	0	0	208,38	n.a.	n.a.	n.a.	n.a.
Total	59	531	16					
Alifatic carbohydrates								
109-66-0 pentane (C5H12)	15	77	73	72,15	4131	0,00	0,02	0,02
112-40-3 dodecane (C12H26)	0	5	4	170,33	766	0,00	0,01	0,01
629-50-5 tridecane (C13H28)	2	5	4	184,37	39	0,05	0,13	0,10
629-59-4 Σ C14 alkane (tetradecane)	0	0	0	198,39	4667	0,00	0,00	0,00
629-62-9 Σ C15 alkane (pentadecane)	0	0	0	212,41	n.a.	n.a.	n.a.	n.a.
Total	17	87	81					
Alcohols								
64-17-5 ethanol	1413	3213	15003	46,07	980	1,44	3,28	15,31
3-methyl-1-butanol	11	58	52	88,148	6	1,83	9,67	8,67
Total	1424	3271	15055					
Ketones								
67-64-1 acetone	590	2283	2793	58,08	99770	0,01	0,02	0,03
78-93-3 2-butanone	191	641	749	72,11	1298	0,15	0,49	0,58
431-03-8 2,3-butadion	0	15	15	86,089	0,18	0,00	83,33	83,33
- Σ C10H16O	0	32	0	152,23	16	0,00	1,98	0,00
- Σ C10H18O	0	0	0	154,25	n.a.	n.a.	n.a.	n.a.
Total	781	2971	3557					
Aldehydes								
124-19-6 nonanal	9	0	386	142,24	2	4,55	0,00	195,15
112-31-2 decanal	8	0	12	156,2	3	3,13	0,00	4,70
2-methylpropanal	23	119	112		1	23,00	119,00	112,00
3-methylbutanal	50	265	197		0,36	138,89	736,11	547,22
hexanal	2	0	30		1	2,00	0,00	30,00
octanal	0	0	53		0,05	0,00	0,00	1060,00
Total	92	384	790					
Organic sulphuric compounds								
75-18-3 dimethyl sulfide	118	259	178	62,14	13	9,29	20,38	14,01
624-92-0 dimethyl disulfide	8	55	8	94,19	8	0,94	6,49	0,94
75-15-0 carbon disulfide	31	0	81	76,139	654	0,05	0,00	0,12
Total	157	314	267					
Ethers								
110-00-9 furan	0	0	0	68,07	27562	0,00	0,00	0,00
1191-99-7 2,3-dihydrofuran	0	0	0	70,09	n.a.	n.a.	n.a.	n.a.
930-27-8 3-methylfuran	0	43	0	82,1	n.a.	n.a.	n.a.	n.a.
470-82-6 eucalyptol	67	231	203	154,25	7	9,84	33,92	29,81
Total	67	274	203					
Terpenes								
80-56-8 alfa-pinene	124	363	27	136,23	100	1,24	3,62	0,27
127-91-3 beta-pinene	55	172	49	136,23	131	0,42	1,32	0,38
5989-27-5 limonene	1657	5073	5	136,23	212	7,83	23,96	0,02
- Σ C10H16	260	863	35	136,23	156	1,67	5,53	0,22
Total	2096	6471	116					
Organic nitrogenous compounds								
75-05-8 acetoneitrile	24	0	47	41,05	21826	0,00	0,00	0,00
Total	24	0	47					
Grand total	4728	14337	20153					

Appendix D

FID Development Over Time

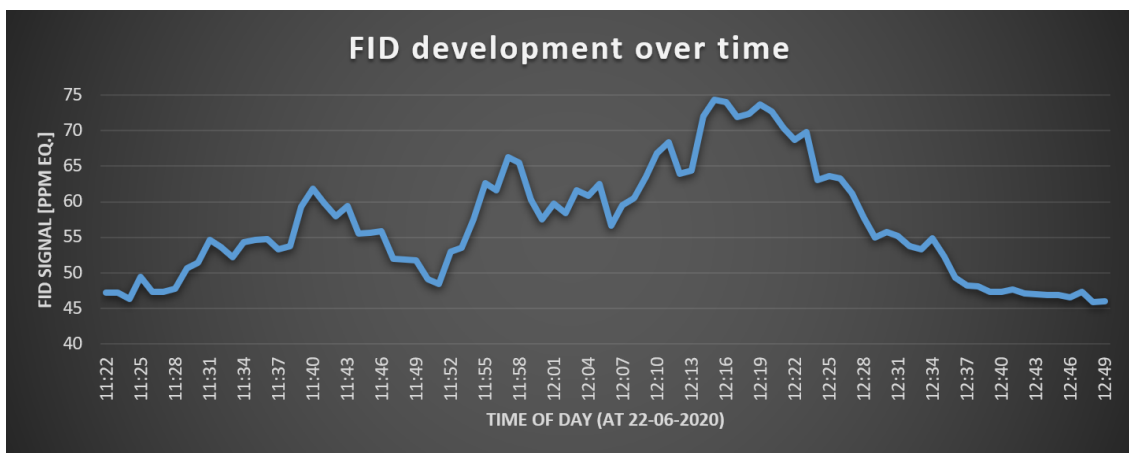


Figure D.1: *The development of the FID signal in a randomly chosen 90 minutes period of time continuously measured in Lelystad, the difference can be called significant.*

Appendix E

Photos of experiments



*UV-reactor with reducers,
not connected in Erem-
bodegem.*



*Industrial acid scrubber for
full 120,000 m³/h in Erem-
bodegem.*



*Ø600 mm air outlet with
10,000 m³/h in Erem-
bodegem.*



*Ø600 mm air outlet discon-
nected in Erembodegem.*



UV-reactor with activated lamps, top view in Lelystad.



UV-reactor from the inside, no lamp-cassettes mounted.



Front of Lelystad installation: acid, scrubber, UV-reactor.



End of Lelystad installation: active carbon and after-burner.



Acid scrubber for 700 m³/h as installed in Lelystad.



UV-lamp cassette. These slide in the empty UV-reactor.

Appendix F

Modelling: Derivation CSTR

The aim is to derive an expression for several series of orders. It is most logical to start with a first order. Again, the starting point is the following formula explained in Eq. 5.3, describing a certain compound in a reactor: ACC. = IN - OUT + PROD. Let's assume there's an interest in the concentration is compound A, following from the reaction $A \rightarrow B$. The stoichiometric value ν is -1, as compound A is a reactant, this would have been +1 if it was the product. The following equation is obtained for a first order CSTR:

$$0 = Q_{in}C_{A,in} - Q_{out}C_{A,out} + V\nu r_A, \quad \text{where } r_A = k \cdot C_{A,reactor} \text{ and } \nu = -1 \quad (\text{F.1})$$

Since the CSTR-assumption yields that the conditions of A and B in the reactor are equal to the outlet conditions, e.g. the same concentration, this means $C_{A,reactor} = C_{A,out}$. Furthermore, also $Q_{in} = Q_{out} = Q$ as this follows from the total mass balance: there are no density and phase changes. This yields the following equation.

$$0 = Q_{in}C_{A,in} - Q_{out}C_{A,out} - V k C_{A,out} \quad \Rightarrow \quad 0 = \frac{Q}{V}C_{A,in} - \frac{Q}{V}C_{A,out} - kC_{A,out} \quad (\text{F.2})$$

Lastly, recall the residence time is defined as follows: $\tau = \frac{V}{Q}$, rephrasing the equation to

$$0 = C_{A,in} - C_{A,out} - k\tau C_{A,out} \quad \Rightarrow \quad C_{A,out} = \frac{C_{A,in}}{1 + k\tau} \quad (\text{F.3})$$

The conversion of A, ζ_A , is then calculated as in Eq. F.4

$$\zeta_A = 1 - \frac{C_{A,out}}{C_{A,in}} = 1 - \frac{1}{1 + k\tau} = \frac{k\tau}{1 + k\tau} \quad (\text{F.4})$$

For a second and third order reaction mechanism, r_A is not equal to $k \cdot C_{A,reactor}$, but $r_A = -k \cdot C_{A,reactor}^2$. Then a similar derivation occurs, as seen in the equation below. This could be solved for $C_{A,out}$ and then ζ_A as well, although this required "trial and error", i.e. numerical computation [19].

$$C_{A,in} - C_{A,out} = k\tau C_{A,out}^2 \quad (\text{2nd order}) \quad \text{and} \quad C_{A,in} - C_{A,out} = k\tau C_{A,out}^3 \quad (\text{3rd order}) \quad (\text{F.5})$$

Appendix G

Modelling and MatLab files

First of all, the ozone measurements from Lelystad are examined thoroughly. They are already mentioned in Section 4.3. but repeated and extended in Table G.1. The measurements are converted to grams per Joule. This is done by converting the measured ppm's to moles, converting the known amount of lamps to wattage and with the use of the measured air flow during that test. Since this resulted in a fairly linear relation between ozone concentration and amount of power installed, this means the grams per Joule measurement is a constant and turned out to be around 1.96 $\mu\text{g}/\text{J}$.

Table G.1: *Ozone measurements in Lelystad, using fresh air with an air flow of $Q=738 \text{ m}^3/\text{h} \equiv 0.2969 \text{ m}^3/\text{s}$.*

lamps [#]	power [W]	O ₃ concentration		O ₃ load [g/s]	O ₃ generation	
		[ppm]	[g/m ³]		[g/J]	[$\mu\text{g}/\text{J}$]
2	290	1.1	0.0022	0.000641	0.00000221	2.21
4	580	2.1	0.0040	0.001197	0.00000206	2.06
6	870	2.7	0.0052	0.001539	0.00000177	1.77
8	1160	3.9	0.0075	0.002221	0.00000192	1.92
10	1450	4.7	0.0089	0.002650	0.00000183	1.83

Since the ozone generation is fairly constant, this can reliably be extrapolated to the case in Erembodegem. The design air flow is 10,000 m^3/h . The intended amount of lamps to treat this amount of air is 30, 40 or 50 lamps. Since the model will have an output with the unit mol/m^3 , all values are converted to this unit in Table G.2. These numbers can then be used to calibrate the model with the ozone measurements taken.

Table G.2: *Calculated ozone generation for fresh air with an air flow of $Q=10,000 \text{ m}^3/\text{h} \equiv 2.778 \text{ m}^3/\text{s}$ and 30, 40 or 50 lamps.*

lamps [#]	power [W]	O ₃ load [g/s]	O ₃ concentration		
			[g/m ³]	[ppm]	[mol/m ³]
30	4350	0.008516	0.0031	1.42	6.39E-05
40	5800	0.011355	0.0041	1.89	8.52E-05
50	7250	0.014193	0.0051	2.37	1.07E-04

Now the calibration can be done, it is time for the actual modelling. The choice has been made to choose two compounds that are representative for the actual air-composition. A terpene called alpha-pinene together with a Sulphuric Organic Compound called dimethyl sulfide are chosen. Alpha-pinene reacts much faster with ozone compared to dimethyl sulfide.

The model starts with the most important input characteristics. These can be tweaked in order to change parameters. First and most obvious are the amount of UV-lamps and the amount of air flow that must be treated. Furthermore the dimensions of the ductwork can be tweaked. The UV-reactor has fixed dimensions, but the "depth" is tweaked automatically by the amount of UV-lamps, to increase the residence time, as will be explained later. Lastly, a factor x can be used to play with the amount of initial VOCs. This is multiplied by the concentrations of alpha-pinene and dimethyl sulfide. The number 17.49 in the example below is chosen as reference, since this is the amount of total VOCs (based on moles) divided by the sum of moles of alfa-pinene and dimethyl sulfide as measured in the GC-MS in Erembodegem.

```

1 clear all, clc
2 global k1 k2 k3 k4
3
4 %% INPUT OF THE MODEL - air/UV characteristics and ductwork dimensions
5 n = 50;      % amount of UV-lamps (factor used to tweak ozone generation)
6 x = 17.49;  % amount of times of initial AP- & DMS-concentration (factor ...
              % used to tweak initial VOC-concentration)
7 Q = 10000;  % total air flow rate [m^3/h]
8 d = 0.900;  % diameter of the ductwork [m]
9 L = 30;     % length of the ductwork [m]

```

Then some general calculations and calculation-constants are stated. As mentioned before, the UV-reactor has fixed dimensions, but the depth Z is tweaked by the amount of lamps to increase the retention time in the UV-reactor. All other calculations speak for itself. Intervals `tspan` and `tspan2` are used later as input for the ODE-solver.

```

1 %% General calculations and calculation-constants
2 X = 1.50;      % height of the UV-reactor [m]
3 Y = 0.65;     % width of the UV-reactor [m]
4 Z = 0.85*(n/50); % depth of the UV-reactor [m]
5 Qo = Q/3600;  % total air flow rate per second [m^3/s]
6 C_O2=0.21;   % percentage [%] of oxygen present in the air ...
              % of 45 deg C.
7 A_UV = X*Y;  % area of the UV-reactor [m2]
8 v_UV = Qo/A_UV; % velocity in the UV-reactor [m/s]
9 t_UV = Z/v_UV; % residence time in the UV-reactor [s]
10 A_duct = pi*(d/2)^2; % area of the ductwork [m2]
11 v_duct = Qo/A_duct; % velocity in the ductwork [m/s]
12 t_duct = L/v_duct; % residence time in the ductwork [s]
13 tspan = [-t_UV 0]; % time interval for the reaction in the ...
              % UV-reactor [s]
14 tspan2 = [0 t_duct]; % time interval for the reaction in the ductwork[s]

```

In the following section the reactions are described, together with their reaction order and a simplified version with compounds A, B, C, D, E and (reaction) P(roducs). Next up are empirically determined kinetic pre-factors, dependent on the reactions. The first two are also dependent on the amount of UV-lamps, as mentioned earlier. The square

root has to do with the reaction order (third instead of second) and the unit of k_i , which will be much clearer after the ODE-solver code. The initial compound concentration of oxygen is calculated with some estimation, but will remain relatively (roughly) unchanged throughout the reaction. The initial concentrations of alpha-pinene and dimethyl sulfide are extracted from the GC-MS data in Erembodegem.

```

1 %% Modelling of ozone formation in the UV-reactor
2 % the reactions considered are the following:
3 % O2 --> 2 O1 (A --> 2*B) === SECOND ORDER
4 % O2 + O1 --> O3 (A + B --> C) === THIRD ORDER
5 % (CH3)2S + O3 --> products (D + C --> P) === SECOND ORDER
6 % alfa-pinene + O3 --> products (E + C --> P) === SECOND ORDER
7
8 % Reaction rate constants and other characteristics
9 k1=0.000000612*n; % kinetic factor O1 (second order), so [m^3/mol*s]
10 k2=37565/sqrt(n); % kinetic factor O3 (third order), so [m^6/mol^2*s]
11 k3=18240; % kinetic factor DMS(second order), so [m^3/mol*s]
12 k4=48780; % kinetic factor AP (second order), so [m^3/mol*s]
13
14 C1o=C_O2*1121/(2*15.99); % [mol/m^3] (estimation of 45 deg C air with ...
    rho = 1.121 kg/m3. Divided by molar mass of molecular oxygen (O2))
15
16 %% UV-REACTOR PLUG FLOW REACTOR
17 Fo(1)=C1o; % initial molecular oxygen (O2) concentration [mol/m3]
18 Fo(2)=0; % initial atomic oxygen (O1) concentration [mol/m3]
19 Fo(3)=0; % initial ozone (O3) concentration [mol/m3]
20 Fo(4)=x*4.168e-06; % initial dimethylsulfide (DMS) concentration [mol/m3]
21 Fo(5)=x*2.267e-06; % initial alfa-pinene (AP) concentration [mol/m3]
22
23 FTot = Fo(1)+Fo(2)+Fo(3)+Fo(4)+Fo(5); % total initial molar concentration

```

Everything is set for the ODE-solver (ordinary differential equation), which is necessary because the reaction rate is a function of the previously calculated concentrations of a certain reaction. The standard MatLab-function "ode45" is used. The ODE-solver is called according to the following code. The result is a matrix of concentrations for all compounds separated per unit time. This matrix is split into vectors with concentrations separated per compound.

```

1 % Call ODE-function
2 [tUV,FUV]=ode45('ode2.PFR_UV',tspan,Fo); % solves for the concentration ...
    per compound, based on concentration and time
3 F_O2 =FUV(:,1); F_O1 =FUV(:,2); F_O3 =FUV(:,3); F_DMS=FUV(:,4); F_AP ...
    =FUV(:,5); % concentrations of all compounds [mol/m3]

```

The actual ODE-solver for the UV-reactor is modelled as follows. Now the effect of the higher order reaction can clearly be seen in the second reaction rate r_2 . Based on stoichiometry the change in concentration is calculated accordingly per unit time.

Another similar script is written for the ductwork, but then without the first equation as no new oxygen radicals are formed. The remaining oxygen radicals can and will still react with oxygen to form ozone in the ductwork (second equation).

```

1 function dF_dt=ode2.PFR_UV(t,F)
2 global k1 k2 k3 k4
3
4 r1=k1*F(1); % reaction rate of 1st reaction: (A-->2*B) [m^3/mol*s]

```

```

5  r2=k2*F(1)^2*F(2)^2; % reaction rate of 2nd reaction: (A+B-->C) ...
    [m^6/mol^2*s]
6  r3=k3*F(4)*F(3);      % reaction rate of 3rd reaction: (D+C-->P) [m^3/mol*s]
7  r4=k4*F(5)*F(3);      % reaction rate of 4th reaction: (E+C-->P) [m^3/mol*s]
8
9  % based on stoichiometry
10 dF_dt(1)= (-r1-r2);    % dF_dtA for molecular oxygen (O2)
11 dF_dt(2)= (2*r1-r2);   % dF_dtB for atomic oxygen (O1)
12 dF_dt(3)= (r1-r3-r4); % dF_dtC for ozone (O3)
13 dF_dt(4)= (-r3);      % dF_dtD for dimethylsulfide (DMS)
14 dF_dt(5)= (-r4);      % dF_dtE for alfa-pinene (AP)
15
16 dF_dt=dF_dt';         % summation of the three above

```

The final concentrations of the UV-reactor PFR are calculated as being the last number in the vector mentioned earlier. Then these values are used as initial concentration for the second PFR of the ductwork behind it, to ensure a smooth transition.

```

1  % Concentrations at end of UV-reactor (equal to inlet concentrations ...
    ductwork)
2  O3_final = F_O3(length(F_O3)); % final ozone concentration [mol/m3]
3  DMS_final = F_DMS(length(F_DMS)); % final DMS concentration [mol/m3]
4  AP_final = F_AP(length(F_AP)); % final AP concentration [mol/m3]
5  O2_final = F_O2(length(F_O2)); % final oxygen concentration [mol/m3]
6  O1_final = F_O1(length(F_O1)); % final oxygen radical (O1) ...
    concentration [mol/m3]
7
8  %% DUCTWORK PLUG FLOW REACTOR INITIAL CONDITIONS
9  Foo(1)=O2_final; % initial molecular oxygen (O2) concentration [mol/m3]
10 Foo(2)=O1_final; % initial oxygen radical (O1) concentration [mol/m3]
11 Foo(3)=O3_final; % initial ozone (O3) concentration [mol/m3]
12 Foo(4)=DMS_final; % initial dimethylsulfide (DMS) concentration [mol/m3]
13 Foo(5)=AP_final; % initial alfa-pinene (AP) concentration [mol/m3]

```

Finally a similar ODE-solver is used to calculate the compound-concentrations and their conversion rates in the ductwork behind the UV-reactor accordingly. Very similar to that before, but now also the conversion rates X_i of ozone, dimethyl sulfide and alpha pinene are incorporated as well.

```

1 % Call ODE-function for the ductwork
2 [tduct,Fduct]=ode45('ode2_PFR.duct',tspan2,Foo); % solves for the ...
   concentration per compound, based on concentration and time
3 F2_O2 =Fduct(:,1); F2_O1 =Fduct(:,2); F2_O3 =Fduct(:,3); ...
   F2_DMS=Fduct(:,4); F2_AP =Fduct(:,5); % similar as before
4
5 % calculate conversion rates as a function of time
6 X_O3 = (max(F2_O3)-F2_O3)/max(F2_O3); % calculates conversion rate ...
   of ozone
7 X_DMS= (max(F2_DMS)-F2_DMS)/max(F2_DMS); % calculates conversion rate ...
   of DMS
8 X_AP = (max(F2_AP)-F2_AP)/max(F2_AP); % calculates conversion rate ...
   of AP

```

Now that all data is gathered, figures can be made in order to make the data more insightful. This can be done in many different ways, according to personal preference. For this thesis, the following figures have been made.

```

1 % making of TOTAL figure with zoom of [-t 0] sec
2 figure(1), clf(1), hold on
3 subplot(2,3,[1 4]); hold on
4 plot(tUV,F_O1,'-rp', tUV,F_O3,'-kp',tUV,F_DMS,'-gp', tUV,F_AP,'-cp')
5 legend('F_O-1','F_O-3','F-D.M.S','F-A-P','Location','NorthWest'), ...
   title('UV-reactor concentrations')
6 xlabel('Time (s)'),ylabel('Concentration [mol/m3]'),xlim([-t_UV ...
   0]),hold off
7 subplot(2,3,[2 3]); hold on
8 plot(tUV,F_O1,'-rp', tUV,F_O3,'-kp', tduct,F2_O1,'-rp', tduct,F2_O3,'-kp')
9 legend('F_O-1','F_O-3'), title('Ozone and oxygen radical concentrations')
10 xlabel('Time (s)'), ylabel('Concentration [mol/m3]'), xlim([-t_UV ...
   t_duct]), hold off
11 subplot(2,3,[5 6]); hold on
12 plot(tUV,F_DMS,'-gp',tUV,F_AP,'-cp', tduct,F2_DMS,'-gp', tduct,F2_AP,'-cp')
13 legend('F-D.M.S','F-A-P'), title('Dimethyl sulfide and Alfa-Pinene ...
   concentrations')
14 xlabel('Time (s)'), ylabel('Concentration [mol/m3]'), xlim([-t_UV ...
   t_duct]), hold off, hold off
15 % making of "conversion rate" figure
16 figure(2),clf(2),hold on
17 plot(tduct, X_O3, '-k'), plot(tduct, X_DMS, '-g'), plot(tduct, X_AP, '-c')
18 legend('X_O-3','X-D.M.S','X-A.P'), title('Conversion rates of ozone and ...
   VOCs')
19 xlabel('Time (s)'), ylabel('Conversion rate [-]'), hold off
20 % making of DMS and AP figure
21 figure(3),clf(3),hold on
22 plot(tUV,F_O1,'-rp', tUV,F_O3,'-kp',tUV,F_DMS,'-gp', ...
   tUV,F_AP,'-cp',tduct,F2_O1,'-rp',tduct,F2_O3,'-kp',tduct,F2_DMS,'-gp', ...
   tduct,F2_AP,'-cp')
23 legend('F_O-1','F_O-3','F-D.M.S','F-A-P'), title('All four compound ...
   concentrations in both PFRs')
24 xlabel('Time (s)'), ylabel('Concentration [mol/m3]'), xlim([-t_UV ...
   t_duct]), hold off
25 % making of O2-plot as a check to see concentration drops
26 figure(4),clf(4), hold on
27 plot(tUV,F_O2,'-kp',tduct,F2_O2,'-kp')
28 legend('F_O-2'),title('O2 concentration [check]')
29 xlabel('Time (s)'), ylabel('Concentration [mol/m3]'), hold off

```

Appendix H

Financial Analysis

H.1 General Assumptions and Explanation

Although a lot of information is known from the suppliers, the authors of both cases, experience of WTT and other sources on the internet, still a set of assumptions had to be made for the financial comparisons. Below is given an explanation of Tables 7.1 and 7.2.

- The air flows used in the comparisons, as well as the average VOC concentrations, average odour concentrations, ammonia levels and temperature ranges and ground area required were presented in the financial cases of Centriair which have been used as a basis for the comparisons.
- In general, all costs have been rounded up to their nearest thousand or five-hundred
- The equipment prices are including the catalyst for the combustor, and are provided by the authors of the cases.
- The catalyst for catalytic combustion lasts for 20 years and does not need replacement, assuming operation conditions are managed well.
- The price of the 53,000 m³/h scrubber was known to be €86,200. Based on comparable inlet ammonia concentrations, the price for the 11,000 m³/h was estimated.
- Price estimations for the air outlet stacks have been based on knowledge from WTT on previous installations. The same is true for simple piping and connection of both financial comparisons, so based on previous knowledge.
- The annuity-percentage is based on one of the cases, and kept unchanged for the other.
- For the 11000 m³/h case a UV-capacity of 55 lamps is estimated, where the 53000 m³/h case requires 265 lamps.
- The UV-lamps have a lifetime of 12,000 hours on average. Running full-time, this is equivalent to approximately 1.5 years until replacement. With a price of €100 per UV-lamp, the UV-lamp replacement costs have been calculated.
- The costs for a kilogram of active carbon grains is assumed to be €3, based on the procurement for the Lelystad experiments.

- The annual mass of active carbon grains that has to be replaced as well as the biofilter material replacement costs and the "other spare parts" has been provided in the cases used.
- The LPG costs for combustion have been calculated simplistically using several assumptions and the formula $Q = c \cdot m \cdot \Delta T$. Although the value of the specific heat changes with the temperature change, an average of $800 \text{ J/kg} \cdot \text{K}$ has been used with a temperature difference of approximately 750 degrees to achieve the required temperature. The density of air varies between 0.45 and 1.20 kg/m^3 between this temperature range, so a mean of 0.85 kg/m^3 has been used. With a LPG-price of €0.071 per kWh, the total LPG costs for catalytic combustion has been calculated.
- The electricity costs of the biofilter have been based on the provided pressure drop. Electricity costs for the AC fans are given in the cases and the electricity costs for the UV-lamps can simply be calculated with an average industrial electricity price of €0.095 per kWh in the Netherlands and the fact that the UV-lamps are 145W each.
- Labour costs are not taken into account, as the variance is too large. Therefore it is assumed to be similar for the different treatment techniques, although in reality a biofilter probably has a higher share of labour costs compared to both catalytic combustion and the UV-technique.